Key comparison

EURAMET.PR-K2.a.2011

Spectral responsivity in the range of 900 nm to 1600 nm

Final Report

20 May 2020

Dutch Metrology Institute

VSL

Thijsseweg 11

2629 JA Delft

Postbus 654

2600 AR Delft

Nederland

Prepared by: Paul Dekker and Steven van den Berg

Table of contents

1 Introduction

Under the Mutual Recognition Arrangement (MRA)[1] the metrological equivalence of national measurement standards will be determined by a set of key comparisons chosen and organized by the Consultative Committees of the CIPM working closely with the Regional Metrology Organizations (RMOs). At its meeting in March 1997, the Consultative Committee for Photometry and Radiometry, CCPR, identified several key comparisons in the field of optical radiation metrology, one of which is spectral responsivity. A working group in charge of planning these key comparisons decided to split this task into three distinct comparisons: K2.a: IR (900 nm – 1600 nm), K2.b: VIS (300 nm – 1000 nm) and K2.c: UV (200 nm – 400 nm). For the IR wavelength range the CCPR key comparison CCPR-k2.a-2003 on spectral responsivity has been carried out, piloted by NIST, with the final report published in 2010 [1].

The Euramet.PR-K2.a comparison on responsivity for the wavelength range 900 nm to 1600 nm, as described in this report, was carried out to establish the degree of equivalence for the participating European laboratories with respect to the Key Comparison Reference Value (KCRV) of the CCPR-K2.a-2003 comparison. VSL (Netherlands) is the pilot of this comparison. Both VSL and NPL (UK) act as link laboratories to the CCPR-K2.a-2003 comparison. The Technical protocol of the Euramet.PR-K2.a comparison was prepared in 2010 and approved and uploaded to KCDB in 2011. Measurements have started in 2011. In 2018 the pre-draft A process was completed (verification of reported results, review of uncertainty budgets and review of relative data).

The Draft A1 report was delivered to the participants in May 2019. Based on the comments to the Draft A1 report, the report has been updated to a Draft A2 version, which was distributed in January 2020. No further comments to the Draft A2 report, except minor editorial ones, were received from the participants. The Draft B report was approved by CCPR WG-KC and by CCPR in May 2020.

This report provides an overview of the comparison, a description of the characterization of the reference detectors, the data-analysis, participant results and the degree of equivalence of participating laboratories with CCPR KCRV. The full Technical Reports of the participants are included in the Appendix. In the Appendix also the changes to the participant reports resulting from the Pre-Draft A phase and the Draft A1 report have been listed.

[1] MRA, Mutual Recognition Arrangement, BIPM, 1999.

2 Organization of the Key Comparison

In this Key Comparison 7 laboratories, including the pilot laboratory, participated. An overview of participating laboratories is given in Table 1. METAS withdrew from the comparison in 2014. The comparison was performed in a three group star scheme (Figure 1).

The comparison was carried out through the calibration of a group of single Germanium (Ge) photodiodes (labeled DGTx, with x an integer). A schematic outline of the detectors is shown in Figure 2. The measurement artefacts are single element photodiodes of type GM10HS (square 10x10 mm), purchased from GPD Optoelectronics Corp. The photodiode is separated from the working aperture (6 mm) by a Schott RG FGL715 glass filter. The filter is used as a transmission window between 750 nm and 2000 nm, and to prevent fatigue effects in the Ge photodiode. The detectors are mechanically robust but sensitive to dust and pollution. Precautions have been taken to avoid pollution, as described in the Technical protocol of the comparison. The detector DGT2 has been replaced by DGT12 because DGT2 was damaged during transport. All participants have measured the spectral responsivity of a set of 3 detectors and reported their results to the pilot laboratory.

Table 1. List of participants

Institute	**Contact Person**
VSL (pilot and link to CCPR)	Steven van den Berg Paul Dekker
NPL (link to CCPR)	Subrena Harris Teresa Goodman
CMI	Marek Šmíd
GUM	Grzegorz Szajna
JV	Jarle Gran
SP, now RISE[2]	Anne Andersson Stefan Kallberg
UME	Özcan BAZKIR Seval MERIC

[2] SP has changed its name to RISE during the comparison. The name ‘SP’ will be used throughout the report.

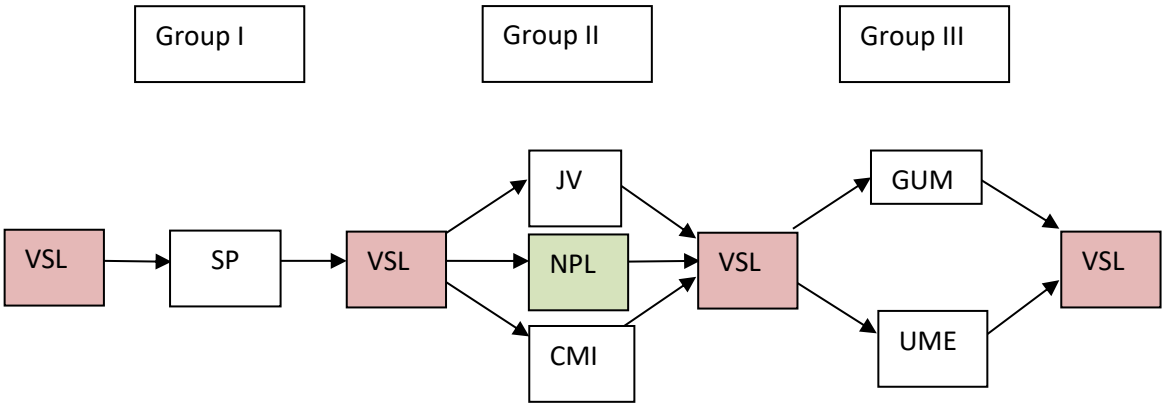

Figure 1. Star comparison with 3-groups : VSL is the link pilot laboratory, NPL is the link participant laboratory.

The table below shows the distribution of DGTx detectors over the participants.

Table 2. Overview of the detectors as measured by the participants

	Group I	Group II	Group III
SP	DGT6, DGT7, DGT8		
JV		DGT9, DGT10 DGT11	
NPL		DGT6, DGT7, DGT8	
CMI		DGT1, DGT3, DGT12	
GUM			DGT1, DGT3, DGT12
UME			DGT9, DGT10 DGT11

The detector housing is shown in Figure 2. Each detector is fitted with a BNC connector for the photodiode signal (current) and a 4-pin LEMO connector for the 4-wire PT100 resistance thermometer.

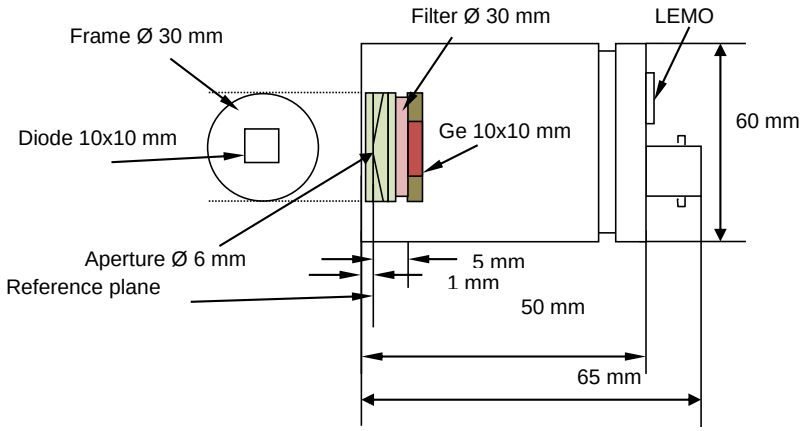

Figure 2. Schematic and dimensions of the Ge transfer detector.

3 Characterization of transfer detectors

3.1 Description of the VSL Spectral Responsivity Calibration Facility

The transfer detectors are calibrated with the spectral responsivity calibration facility. The facility is designed for both primary scale realization with a cryogenic radiometer and for spectral responsivity measurements at secondary level by calibrating a detector against a reference detector. The facility covers a wavelength range from 200 nm to 1600 nm. Figure 3 shows the layout of the spectral calibration facility. For this comparison the cryogenic radiometer is not used. The transfer detectors and reference detector are mounted on the 'secondary transfer unit' for the calibration of the transfer standards. A radiation source can be selected for the required wavelength range. For this comparison a 100 W quartz-tungsten-halogen lamp (QTH) is used. The current through the filament is stabilized within 10^{-5} by means of a Heinzinger power supply.

When the facility is operated the radiation from the QTH-lamp the light is imaged onto the entrance slit of the double-grating monochromator with a quartz lens. The radiation from the source is dispersed by a monochromator, which is used in double-subtractive mode for 200 nm to 1600 nm.

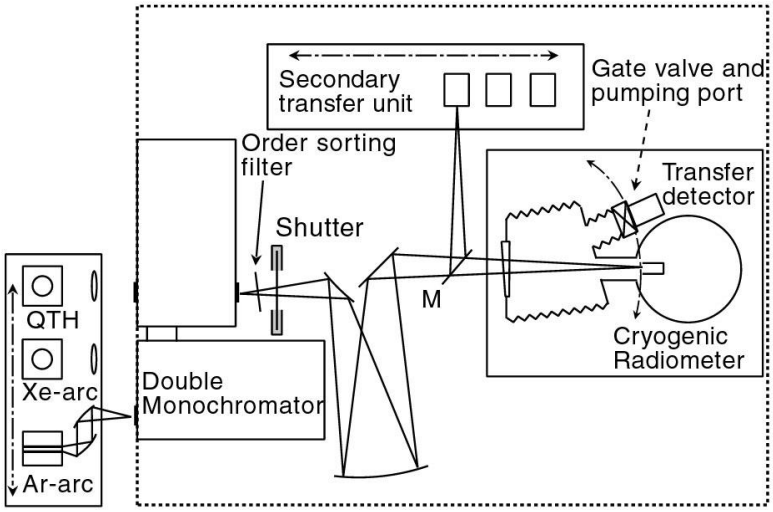

Figure 3. Layout of the spectral responsivity calibration facility for primary and secondary spectral responsivity calibration. For this comparison the QTH lamp is used. Both reference and transfer detector are mounted to the secondary transfer unit and illuminated via mirror M.

The radiation emerging from the monochromator first passes an order-sorting filter and shutter and is then imaged onto the secondary transfer unit by a set of two spherical and two folding mirrors. The order-sorting filters are bandpass filters that are used to suppress higher order wavelengths.

3.2 Spectral responsivity measurements by VSL

VSL has measured the responsivity of all DGTx detectors prior and after the measurement by the participants. The results of each detector are shown in Section 5, along with the participant results.

3.3 Uncertainty of DGTx calibration

The uncertainty on the spectral responsivity calibration of the DGTx detectors is based on the following uncertainty contributions:

- Temperature sensitivity
- Uniformity
- Angular alignment
- Wavelength
- Bandwidth
- Stray light
- Current measurement
- Nonlinearity
- Repeatability
- Uncertainty of reference detector

3.4 Temperature sensitivity

VSL has measured the temperature dependence of a subset of the DGT photodiodes used in the comparison. A special mount has been developed to vary the temperature of the photodiode. By measuring the responsivity as a function of temperature, the (wavelength-dependent) sensitivity of the responsivity for temperature has been determined for 4 transfer standards (DGT4, DGT5, DGT6, DGT9). For these measurements the temperature has been varied from 20 °C to 27 °C. The temperature is measured with a Pt100 sensor.

The temperature dependence of the resistance of the temperature sensors in the DGT detectors scales according to:

$$\mathrm{R_t} = \mathrm{R_0}\,(1 + 3.90802 \times 10^{-3}\mathrm{t} - 5.802 \times 10^{-7}\mathrm{t}^2), \tag{1}$$

which is based on the DIN/IEC 751 standard for Pt100 sensors. Here $\mathrm{R_0} = 100\,\Omega$ and t the temperature (in °C). The resistance corresponding to a temperature of 23 °C, is $R^{23} = 109.18\,\Omega$. The sensitivity coefficient c_R (unit: $\mathrm{AW^{-1}\Omega^{-1}}$) is the slope of the responsivity versus Pt100 resistance measurement, averaged for the 4 detectors. The uncertainty on the sensitivity coefficient $\mathrm{u_{C_R}}$ is based on the standard deviation of the results obtained with the 4 detectors.

The temperature dependence of the responsivity is used to obtain the responsivity at 23 °C for all laboratories. The uncertainty contribution associated with this correction is based on the uncertainty of the temperature sensitivity coefficient (see Section 4.1).

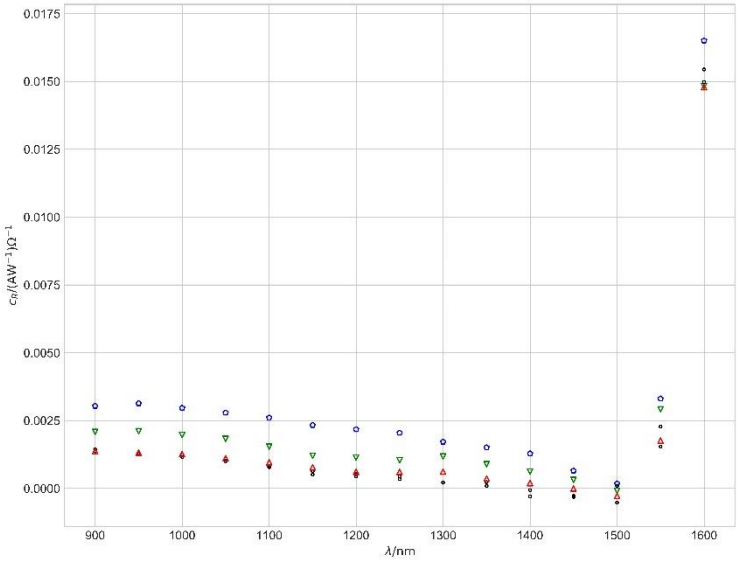

Figure 4. Temperature sensitivity of DGT4 (blue), DGT5 (green), DGT6 (black) and DGT9 (red).

Table 3. Temperature sensitivity and its standard deviation of the DGT detectors

λ/nm	$c_R/(AW^{-1})\Omega^{-1}$	$\sigma(c_R)/(AW^{-1})\Omega^{-1}$
900	0.001859	0.000725
950	0.001827	0.000810
1000	0.001722	0.000768
1050	0.001565	0.000759
1100	0.001344	0.000769
1150	0.001093	0.000740
1200	0.000979	0.000722
1250	0.000896	0.000697
1300	0.000787	0.000653
1350	0.000617	0.000584
1400	0.000348	0.000624
1450	0.000075	0.000408
1500	-0.000123	0.000286
1550	0.002360	0.000748
1600	0.015310	0.000718

3.5 Uniformity of spectral responsivity

The uncertainty due to inhomogeneity of the detector has been determined by measuring the detector responsivity at various positions for a subset of the DGT detectors. For the uncertainty budget we use the measurement data of DGT12 that has been characterized in most detail, by scanning the detector in the plane of the photodiode both horizontally and vertically over a range of 6 mm in steps of 0.2 mm. The spot is circular with a diameter of 4 mm. For DGT12 this measurement has been done for the wavelength range from 900 nm to 1600 nm in steps of 100 nm. A typical measurement is shown in Figure 5.

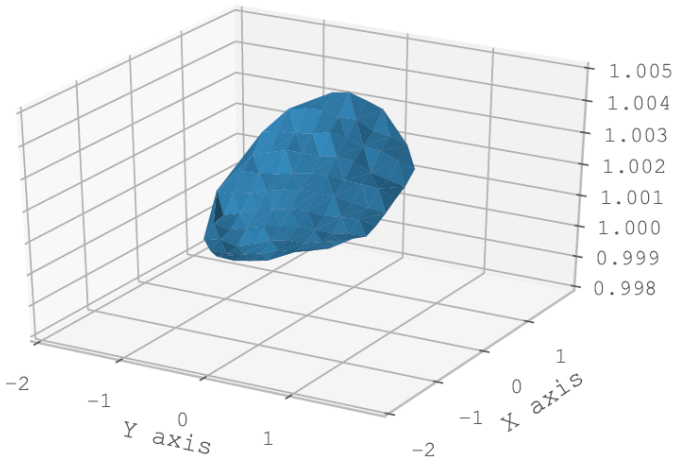

Figure 5. Typical measurement of inhomogeneity of the response of DGT12 (example taken at 1300 nm).

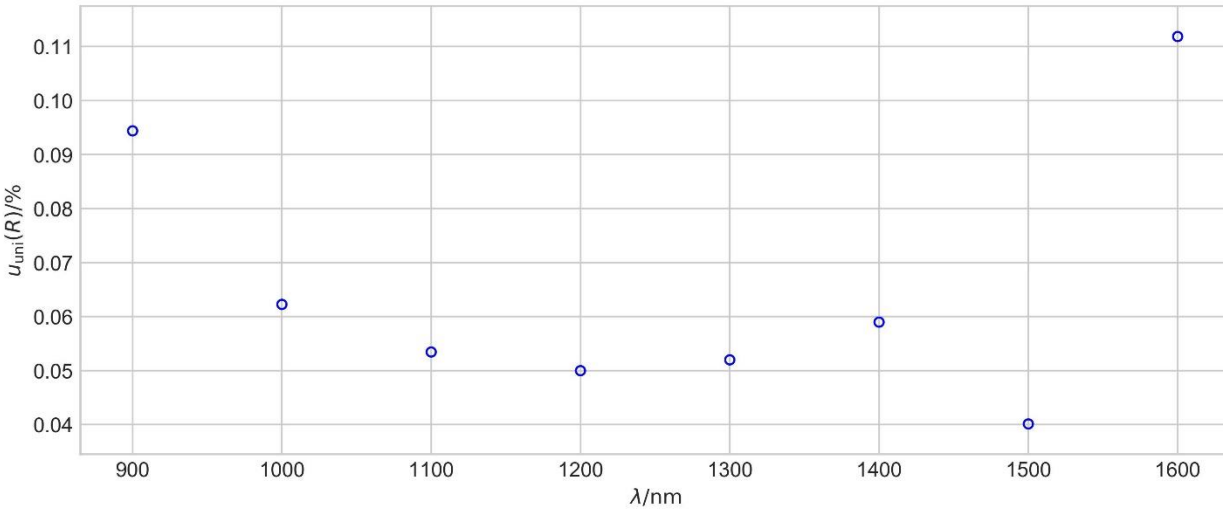

Figure 6. Uncertainty due to detector inhomogeneity for a DGT detector for a 4 mm spotsize and an alignment uncertainty of 0.4 mm.

Table 4. Uncertainty on uniformity for 4 mm spot size

λ/nm	$u_{uni}(R)$/%
900	0.094
1000	0.062
1100	0.053
1200	0.050
1300	0.052
1400	0.059
1500	0.040
1600	0.112

3.6 Angular alignment

The uncertainty on the responsivity due to uncertainty on the angular alignment has been investigated by positioning the DGT at various angles. The nominal angle of incidence is 2°. The detector responsivity has been measured for a range of +/- 4° around this value as a function of wavelength.

It is assumed that detector can be positioned within an uncertainty of 2°. The standard uncertainty on the responsivity due to the uncertainty on angular positioning then has a rectangular distribution and is then given by:

$$u(\alpha) = \frac{\mathrm{MAX}\left[\left(R(\alpha_0) - R(\alpha_0 + 2°)\right), \left(R(\alpha_0) - R(\alpha_0 - 2°)\right)\right]}{\sqrt{3}}, \quad (2)$$

which is a slight overestimate by taking the maximum deviation of the responsivity for a maximum angular deviation.

The uncertainty due to angular dependence of the responsivity has been measured for a subset of the DGT detectors (DGT6, DGT7, DGT8), showing similar behavior. The uncertainty due to angular alignment is based on the average angular dependence of these detectors and is shown in Figure 7. The reference detector is also aligned

with an angular uncertainty of 2°, so an additional uncertainty contribution for the reference detector is taken into account.

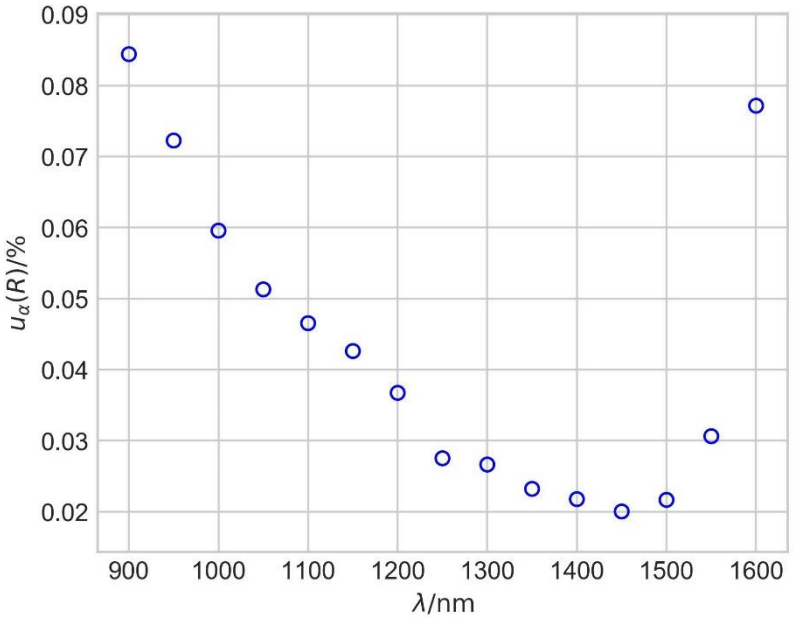

Figure 7. Measurement uncertainty as a function of wavelength due to uncertainty on angular alignment.

3.7 Wavelength

The sensitivity on responsivity resulting from wavelength uncertainty is given by:

$$u_\lambda\big(R(\lambda)\big) = u(\lambda)\frac{\partial R(\lambda)}{\partial \lambda}, \tag{3}$$

where $u(\lambda)$ is the wavelength uncertainty, which is 0.2 nm. The sensitivity coefficient $\frac{\partial R(\lambda)}{\partial \lambda}$ is directly derived from the measured responsivity data.

3.8 Bandwidth

This contribution accounts for the fact that the spectral width of the light offered during calibration has a finite bandwidth, i.e. is not a delta-function. The spectral width for the VSL double monochromator system is triangular with a full width of 10 nm.

In second order approximation the average responsivity over the triangular bandwidth can be described as:

$$\bar{R}(\lambda_0) = R(\lambda_0) + \frac{\Delta^2}{12}\frac{\partial^2 R(\lambda)}{\partial \lambda^2}, \tag{4}$$

The effect second derivative is based on the measurement data using 3 measurement points: λ_0 and the neighbouring measurement points at wavelength λ_{-1} and λ_1:

$$\frac{\partial^2 R(\lambda)}{\partial \lambda^2} \approx \frac{2R(\lambda_0) - R(\lambda_{-1}) - R(\lambda_1)}{\delta \lambda^2}, \quad (5)$$

where δλ is the wavelength step between neighboring wavelengths. When considering the deviation due to bandwidth as uncertainty (i.e. not correcting for bandwidth effect), one finds:

$$u_{bp}(R) = \frac{2R(\lambda_0) - R(\lambda_{-1}) - R(\lambda_1)}{\delta \lambda^2} \times \frac{\Delta^2}{12} \quad (6)$$

3.9 Other contributions

The linearity of the Ge detectors has not been measured. However, based on literature and given that the measurements by the participants have been performed at comparable and low flux levels, it is assumed the uncertainty due to nonlinearity <0.05 %.

The uncertainty on current measurement is estimated to be 0.05 %. The uncertainty due to stray light is estimated to be 0.017 %. This value is estimated by comparing spectral responsivity data in the middle of the measurement range (1250 nm – 1300 nm), as measured with and without order selection filter inserted, respectively.

3.10 Reference detector

All measurements of the transfer standards have taken place against the reference standard GT3, which has been calibrated against the absolute cryogenic radiometer. The uncertainty of the reference standard consists of the following components:

- Power measurement by the cryogenic radiometer (ACR)
- Current measurement
- Repeatability
- Wavelength calibration monochromator
- Bandwidth
- Temperature sensitivity and resistance measurement
- Drift/ageing
- Linearity
- Uniformity
- Stray light

The contributions related to polarization sensitivity is considered negligible. The uncertainty budget is very similar to the DGTx uncertainty budget. A summary of all uncertainty contributions to the calibration of the GT3 detector is given in Table 5.

Table 5. Uncertainty budget of the GT3 reference detector

Wavelength	Responsivity	Repeat-ability	Aging, Drift	Wavelength	Bandwidth	Temperature coefficient	Temperature resistance	Non-unformity	Stray light	ACR	Current	Linearity	Combined std. uncert.
nm	A/W	%	%	%	%	%	%	%	%	%	%	%	%
900	0.3967	0.048	0.022	0.058	0.004	0.109	0.008	0.058	0.017	0.030	0.050	0.050	0.17
925	0.4253	0.005	0.006	0.054	0.000	0.101	0.008	0.055	0.017	0.030	0.050	0.050	0.15
950	0.4539	0.006	0.001	0.050	0.001	0.094	0.007	0.053	0.017	0.030	0.050	0.050	0.14
975	0.4820	0.018	0.046	0.044	0.004	0.088	0.007	0.051	0.017	0.030	0.050	0.050	0.14
1000	0.5089	0.028	-0.036	0.043	-0.002	0.083	0.007	0.048	0.017	0.030	0.050	0.050	0.14
1025	0.5359	0.016	0.101	0.038	0.006	0.079	0.006	0.048	0.017	0.030	0.050	0.050	0.16
1050	0.5611	0.040	0.070	0.036	0.000	0.075	0.006	0.048	0.017	0.030	0.050	0.050	0.15
1075	0.5860	0.042	0.151	0.033	0.002	0.071	0.005	0.048	0.017	0.030	0.050	0.050	0.20
1100	0.6105	0.014	0.130	0.032	0.000	0.068	0.005	0.048	0.017	0.030	0.050	0.050	0.18
1125	0.6349	0.006	0.125	0.031	0.000	0.065	0.004	0.049	0.017	0.030	0.050	0.050	0.17
1150	0.6593	0.030	0.127	0.027	0.004	0.063	0.004	0.051	0.017	0.030	0.050	0.050	0.17
1175	0.6821	0.039	0.036	0.024	0.004	0.061	0.004	0.052	0.017	0.030	0.050	0.050	0.13
1200	0.7023	0.011	0.069	0.021	0.004	0.059	0.003	0.054	0.017	0.030	0.050	0.050	0.13
1225	0.7207	0.007	0.060	0.020	0.001	0.057	0.003	0.055	0.017	0.030	0.050	0.050	0.13
1250	0.7383	0.010	0.066	0.018	0.002	0.055	0.003	0.056	0.017	0.030	0.050	0.050	0.13
1275	0.7553	0.043	-0.050	0.017	0.000	0.054	0.003	0.058	0.017	0.030	0.050	0.050	0.13
1300	0.7715	0.010	-0.050	0.016	0.002	0.053	0.003	0.059	0.017	0.030	0.050	0.050	0.12
1325	0.7868	0.020	-0.083	0.015	0.000	0.052	0.002	0.058	0.017	0.030	0.050	0.050	0.14
1350	0.8017	0.006	-0.062	0.014	0.001	0.051	0.002	0.058	0.017	0.030	0.050	0.050	0.13
1375	0.8169	0.008	-0.171	0.013	0.003	0.050	0.002	0.058	0.017	0.030	0.050	0.050	0.20
1400	0.8293	0.007	-0.104	0.014	-0.002	0.049	0.002	0.057	0.017	0.030	0.050	0.050	0.15
1425	0.8434	0.003	-0.081	0.016	-0.003	0.048	0.001	0.056	0.017	0.030	0.050	0.050	0.14
1450	0.8602	0.007	-0.139	0.015	0.000	0.047	0.001	0.054	0.017	0.030	0.050	0.050	0.18
1475	0.8767	0.002	-0.139	0.015	-0.001	0.047	0.001	0.053	0.017	0.030	0.050	0.050	0.18
1500	0.8938	0.005	-0.174	0.014	0.001	0.046	0.000	0.051	0.017	0.030	0.050	0.050	0.20
1525	0.9097	0.002	-0.152	-0.001	0.026	0.045	0.000	0.152	0.017	0.030	0.050	0.050	0.23
1550	0.9086	0.007	-0.166	-0.095	0.157	0.044	0.005	0.252	0.017	0.030	0.050	0.050	0.36
1575	0.8017	0.009	-0.420	-0.178	0.115	0.044	0.024	0.352	0.017	0.030	0.050	0.050	0.60
1600	0.6229	0.003	-0.257	-0.135	-0.155	0.050	0.024	0.453	0.017	0.030	0.050	0.050	0.57

Drift/aging

Within the period of the Key comparison the GT3 reference detector has been calibrated twice against the cryogenic radiometer (2012 and 2014). The reference responsivity value of GT3 is based on the average of these realizations. An uncertainty associated to drift is based on the maximum difference between the two realization, scaled with time:

$$u_{\mathrm{drift}}\big(R(\lambda)\big) = \frac{39}{18} \times \frac{R_{2014}(\lambda) - R_{2012}(\lambda)}{2\sqrt{3}} \tag{7}$$

The factor 39/18 comes from the fact that the recalibration interval was 18 months, whereas the total duration of the comparison was 39 months. This is based on a linear extrapolation of drift.

3.11 Uncertainty transfer detectors

The combined measurement uncertainty of the contributions above has been summarized in the table below for one of the DGT transfer detectors.

Table 6. Typical uncertainty budget for a DGT transfer detector.

Wavelength /nm	Uni. \%	Angle ref. /%	Angle DGTx \%	Std. /%	Temp. corr. /%	Ref. det /%	Curr. /%	Bandwidth $ /%	Nonlin. /%	Stray light /%	Wavelength /%	u(comb) /%
900	0.09	0.080	0.080	0.013	0.096	0.17	0.050	0.004	0.050	0.017	0.058	0.26
950	0.07	0.070	0.070	0.009	0.096	0.14	0.050	0.001	0.050	0.017	0.050	0.23
1000	0.06	0.058	0.058	0.009	0.083	0.14	0.050	-0.002	0.050	0.017	0.043	0.21
1050	0.06	0.051	0.051	0.006	0.076	0.15	0.050	0.000	0.050	0.017	0.036	0.21
1100	0.05	0.047	0.047	0.008	0.073	0.18	0.050	0.000	0.050	0.017	0.032	0.22
1150	0.05	0.043	0.043	0.013	0.066	0.18	0.050	0.004	0.050	0.017	0.027	0.22
1200	0.05	0.038	0.038	0.016	0.062	0.13	0.050	0.004	0.050	0.017	0.021	0.18
1250	0.05	0.028	0.028	0.003	0.057	0.13	0.050	0.002	0.050	0.017	0.018	0.17
1300	0.05	0.028	0.028	0.005	0.051	0.12	0.050	0.002	0.050	0.017	0.016	0.17
1350	0.06	0.024	0.024	0.004	0.044	0.13	0.050	0.001	0.050	0.017	0.014	0.17
1400	0.06	0.023	0.023	0.002	0.045	0.15	0.050	-0.002	0.050	0.017	0.014	0.19
1450	0.05	0.021	0.021	0.004	0.028	0.18	0.050	0.000	0.050	0.017	0.015	0.20
1500	0.04	0.022	0.022	0.004	0.019	0.20	0.050	0.001	0.050	0.017	0.014	0.22
1550	0.05	0.031	0.031	0.004	0.049	0.37	0.050	0.157	0.050	0.017	-0.095	0.42
1600	0.11	0.065	0.065	0.015	0.061	0.57	0.050	-0.155	0.050	0.017	-0.135	0.63

4 Data Analysis of the comparison

The data analysis described in this section will lead to values and uncertainty of the unilateral degree of equivalence (DoE) for the participant laboratories. The DoE is the difference between the participating laboratory results and the key comparison reference value (KCRV) from the CCPR K2.a key comparison [1]. The data analysis to obtain the DoE follows Appendix A of the Guidelines for RMO PR Key Comparisons CCPR-G6 [2]. For this comparison the situation as described in section A.2.3 of the guideline is applicable: there are two link laboratories, with the pilot laboratory being one of the link laboratories.

4.1 Temperature correction to the transfer detector responsivities

The first analysis step is to calculate the responsivity at 23 °C (S_{ij}^{23}) from the participant data via:

$$S_{ij}^{23} = S_{ij} - c_R \times \left(R_{ij} - R^{23}\right), \tag{8}$$

where c_R is the sensitivity coefficient of the responsivity for temperature, as reported in Section 3.3. S_{ij} and R_{ij} are the responsivity and resistance of participant i, detector j, respectively. The uncertainty u_{C_R} associated to the sensitivity coefficient is based on the standard deviation of these measurements. The uncertainty resulting from the temperature correction is given by:

$$u_{\mathrm{temp}}\left(S_{ij}\right) = u_{C_R} \times \left(R_{ij} - R^{23}\right), \tag{9}$$

where $R^{23} = 109.18\ \Omega$, as calculated from Equation (1). The uncertainty on the resistance measurement has not been reported by the participant laboratories and is considered negligible.

4.2 Uniformity and beam size

The following beam sizes have been reported by the participating laboratories:

Table 7. Overview of the detectors as measured by the participants

Laboratory	Beam shape and size
VSL	4 mm, circular
CMI	4 mm, circular
GUM	2 mm, square
JV	2 mm, square
NPL	4 mm, circular
SP	4 mm, circular
UME	4 mm, circular

For laboratories having a beam size and shape that is different from the default parameters (see section 4.3.6 in the Technical protocol), an additional uncertainty contribution $u_{\mathrm{i,unif}}^2\left(S_{ij}\right)$ to the transfer uncertainty has been determined based on the actual beam parameters and the uniformity of the detector responsivity (see section 3.5). This is only the case for GUM and JV. For random variation of the detector homogeneity the uncertainty for 2x2 mm^2 square

beam size is estimated to be about 1.8× the uncertainty for the 4 mm diameter round beam (Table 4). The factor 1.8 is equal to the square root of the ratio of the area of the round and square beam, respectively. Probably this is an over-estimate, since the responsivity dominantly shows a linear slope as a function of spatial position (see Figure 6). To first order the responsivity then is independent from the spot size, when the spot is aligned to the center of the detector.

The combined uncertainty consists of the uncertainty reported by the participant and contributions resulting from temperature correction and homogeneity:

$$u_c^2(S_{ij}^{23}) = u^2(S_{ij}) + u_{\mathrm{temp}}^2(S_{ij}) + u_{\mathrm{unif}}^2(S_{ij}). \tag{10}$$

4.3 Analysis method

Starting with the responsivity data at 23 °C (see Section 4.1), the data analysis consists of the following steps:

1. Calculate the relative difference Δ_{ij} for each lab i and each photodiode j compared to the VSL measurement:

$$\Delta_{ij} = \frac{S_{ij}^{23}}{S_{ij}^{23,\mathrm{VSL}}} - 1. \tag{11}$$

Here the VSL responsivity is calculated from the pre- and post-measurement of detector j:

$$S_{ij}^{23,\mathrm{VSL}} = \frac{1}{2}\left[S_{ij}^{23,\mathrm{VSL}}(\mathrm{pre}) + S_{ij}^{23,\mathrm{VSL}}(\mathrm{post})\right]. \tag{12}$$

2. Determine the mean relative difference between VSL and lab *i* averaged over the 3 detectors: $\overline{\Delta}_i$. Since all detectors are of the same type here simply the arithmetic mean over the three detectors is taken for all participant:

$$\overline{\Delta}_i = \frac{1}{3}\sum_{j=1}^{3} \Delta_{ij.} \tag{13}$$

3. Determine the unilateral DoE for laboratory

The unilateral DoE for the participant *i, calculated through the pilot* is:

$$D_{i(p)} = D_p + \overline{\Delta}_i, \tag{14}$$

where D_{p} is the unilateral DoE for the pilot-linking laboratory as calculated during the CC Key comparison.

The unilateral DoE for laboratory *i*, *calculated through the pilot and the link* laboratory is given by

$$D_{i(l)} = D_l + \overline{\delta}_l + \overline{\Delta}_i, \tag{15}$$

where $\mathrm{D_l}$ is the unilateral DoE for the link laboratory as calculated during the CC Key comparison for the link l.

Here we introduced the quantity $\bar{\delta}_l$, which is based on the responsivity measurements of the three detectors measured by the link laboratory and the pilot. Here a *weighted average* is applied to determine $\bar{\delta}_l$ from the responsivity measurements of the three detectors. From the relative data it appeared that 2 out of 3 detectors measured by the linking laboratory (NPL) showed significant drift, i.e. showing differences between pre- and post-measurement comparable to the combined standard uncertainty of NPL and VSL (see results in Section 5). This detector drift was most notable for the detectors involved in the NPL- VSL comparison (DGT6 and DGT8) and significant because of the relatively small measurement uncertainty of NPL. Since NPL is the linking laboratory, it was considered appropriate to apply a weighting to these detectors before calculating the DoE for all participants via the linking laboratory.

Weighting of the transfer detectors as measured by link laboratory

To determine the weighted average, we follow the same approach as the CCPR K2.a comparison piloted by NIST [1]. Here the weighting is based on the total transfer uncertainty, which includes a contribution based on detector drift. The uncertainty associated to the stability of the transfer detectors is based on the difference between pre and post measurements, assuming a rectangular distribution:

$$u_{\mathrm{stab}}\left(S_{lj}^{23,\mathrm{VSL}}\right) = \frac{1}{2\sqrt{3}} \times \frac{\left|S_{lj}^{23,\mathrm{VSL}}(\mathrm{pre}) - S_{lj}^{23,\mathrm{VSL}}(\mathrm{post})\right|}{S_{lj}^{23,\mathrm{VSL}}}. \tag{16}$$

Here l, refers to the link lab, and j is the detector label (1-3).

The transfer uncertainty is based on the drift of the detector in combination with other transfer uncertainty components. The total transfer uncertainty is:

$$u_{\mathrm{t}}^2\left(\delta_{lj}\right) = u_{\mathrm{r}}^2\left(S_{lj}\right) + u_{\mathrm{r}}^2\left(S_{pj}\right) + u_{\mathrm{stab}}^2\left(S_{lj}^{\mathrm{VSL}}\right) + \left(u_{\mathrm{c},lj}^{\mathrm{T}}\right)^2. \tag{17}$$

Here $u_{\mathrm{r}}^2\left(S_{lj}\right)$ and $u_{\mathrm{r}}^2\left(S_{pj}\right)$ are the standard deviations of the mean of the measurements for each detector *j* for pilot and link laboratory, respectively. $u_{\mathrm{c},lj}^{\mathrm{T}}$ contains the combined additional uncertainty contributions due to bandwidth and wavelength uncertainty of the pilot and link (Table 6) and a contribution for the temperature sensitivity of the detectors:

$$\left(u_{\mathrm{c},lj}^{\mathrm{T}}\right)^2 = \left(u_{\mathrm{w},pj}^{\mathrm{T}}\right)^2 + \left(u_{\mathrm{w},lj}^{\mathrm{T}}\right)^2 + \left(u_{\mathrm{bp},pj}^{\mathrm{T}}\right)^2 + \left(u_{\mathrm{bp},lj}^{\mathrm{T}}\right)^2 + \left(u_{\mathrm{t},lp,j}^{\mathrm{T}}\right)^2, \tag{18}$$

where:

$$u_{\mathrm{t},lp,j}^{\mathrm{T}} = u_{C_R} \times \mathrm{MAX}\left|R_{pj} - R_{lj}\right|. \tag{19}$$

Here R_{lj} and R_{pj} are the reported resistances of the temperature sensor of detector *j* for link and pilot laboratory, respectively. For simplicity, and since reported temperatures at one laboratory are very close, the maximum difference between reported pilot and link resistance is taken over the 3 detectors involved. A transfer uncertainty contribution due to different spot size is not included, since the pilot and link laboratory nominally operate at the same spot geometry.

The weighted mean of the difference between link laboratory and pilot is calculated from:

$$\bar{\delta}_l = \sum_{j=1}^{3} w_{lj} \cdot \delta_{lj}, \tag{20}$$

where:

$$w_{lj} = \frac{u_{\mathrm{t}}^{-2}(\delta_{lj})}{\sum_{j=1}^{3} u_{\mathrm{t}}^{-2}\ (\delta_{lj})} \tag{21}$$

and:

$$\delta_{lj} = \frac{S_{lj}^{23,\mathrm{VSL}}}{S_{lj}^{23}} - 1. \tag{22}$$

Note the difference between Eq.(22) and Eq.(11).

Based on the weighted value $\bar{\delta}_l$, the DoE of the participant via the link laboratory $\mathrm{D_{i(}}_{l)}$ is calculated using Eq. (15).

The uncertainties involved in the weighting of the three detectors and the resulting weighting factors are summarized in the table below.

Table 8. Uncertainty contributions due to wavelength and bandpass effects for pilot and link and random effects of the pilot for DGT6,7,8.

λ/nm	$u_{\mathrm{w},pj}^{\mathrm{T}}$ /%	$u_{\mathrm{w},lj}^{\mathrm{T}}$ /%	$u_{\mathrm{bp},pj}^{\mathrm{T}}$ /%	$u_{\mathrm{bp},lj}^{\mathrm{T}}$ /%	$u_{\mathrm{r},pj}$ /%
900	0.058	0.015	0.004	0.000	0.133
950	0.050	0.013	0.001	0.000	0.115
1000	0.043	0.012	-0.002	0.000	0.099
1050	0.036	0.011	0.000	0.000	0.091
1100	0.032	0.010	0.000	0.000	0.087
1150	0.027	0.008	0.004	0.000	0.085
1200	0.021	0.007	0.004	0.000	0.081
1250	0.018	0.007	0.002	0.000	0.076
1300	0.016	0.006	0.002	0.000	0.078
1350	0.014	0.006	0.001	0.000	0.081
1400	0.014	0.005	-0.002	0.000	0.081
1450	0.015	0.012	0.000	0.000	0.071
1500	0.014	0.018	0.001	0.000	0.068
1550	-0.095	0.025	0.157	0.000	0.089
1600	-0.135	0.031	-0.155	0.000	0.139

Table 9. Uncertainty contributions due to detector stability, temperature and random effects at the link laboratory for DGT6, DGT7 and DGT8.

λ /nm	$u_{\mathrm{stab}}(S^{\mathrm{VSL}}_{l,DGT6})$ /%	$u^{\mathrm{T}}_{\mathrm{t},lp,DGT6}$ /%	$u_{\mathrm{r}}(S_{l,DGT6})$ /%	$u_{\mathrm{stab}}(S^{\mathrm{VSL}}_{l,DGT7})$ /%	$u^{\mathrm{T}}_{\mathrm{t},lp,DGT7}$ /%	$u_{\mathrm{r}}(S_{l,DGT7})$ /%	$u_{\mathrm{stab}}(S^{\mathrm{VSL}}_{l,DGT8})$ /%	$u^{\mathrm{T}}_{\mathrm{t},lp,DGT8}$ /%	$u_{\mathrm{r}}(S_{l,DGT8})$ /%
900	0.38	0.24	0.037	0.15	0.27	0.05	0.36	0.25	0.04
950	0.35	0.23	0.117	0.11	0.26	0.12	0.33	0.24	0.12
1000	0.33	0.20	0.088	0.08	0.22	0.13	0.30	0.21	0.08
1050	0.30	0.19	0.080	0.04	0.20	0.08	0.28	0.19	0.08
1100	0.28	0.18	0.062	0.02	0.18	0.08	0.25	0.17	0.05
1150	0.25	0.16	0.056	0.00	0.17	0.06	0.22	0.16	0.06
1200	0.26	0.15	0.051	0.04	0.15	0.05	0.22	0.15	0.04
1250	0.27	0.14	0.051	0.07	0.14	0.05	0.23	0.13	0.05
1300	0.25	0.12	0.045	0.09	0.12	0.05	0.22	0.12	0.05
1350	0.24	0.11	0.054	0.10	0.11	0.05	0.20	0.10	0.06
1400	0.22	0.11	0.066	0.10	0.11	0.06	0.18	0.11	0.05
1450	0.20	0.07	0.078	0.11	0.07	0.08	0.17	0.07	0.06
1500	0.19	0.05	0.066	0.11	0.05	0.07	0.16	0.05	0.08
1550	0.16	0.12	0.067	0.13	0.12	0.12	0.13	0.12	0.14
1600	0.10	0.16	0.077	0.15	0.15	0.08	0.03	0.15	0.08

The resulting total uncertainties and weighting factors of VSL and NPL for the calculation of the DoE are shown in the table below.

Table 10. Total transfer uncertainty and weighting factors for DGT6, DGT7 and DGT8.

λ/nm	$u_t(\delta_{l,DGT6})$/%	$u_t(\delta_{l,DGT7})$/%	$u_t(\delta_{l,DGT8})$/%	$w_{l,DGT6}$	$w_{l,DGT7}$	$w_{l,DGT8}$
900	0.47	0.35	0.46	0.26	0.48	0.27
950	0.46	0.33	0.44	0.25	0.48	0.27
1000	0.41	0.29	0.39	0.24	0.49	0.27
1050	0.38	0.24	0.36	0.22	0.54	0.24
1100	0.35	0.22	0.32	0.21	0.53	0.25
1150	0.32	0.20	0.29	0.21	0.54	0.25
1200	0.31	0.19	0.28	0.20	0.56	0.24
1250	0.32	0.18	0.29	0.19	0.58	0.23
1300	0.29	0.18	0.26	0.20	0.55	0.25
1350	0.28	0.17	0.24	0.20	0.53	0.27
1400	0.27	0.18	0.23	0.22	0.49	0.29
1450	0.24	0.16	0.21	0.23	0.48	0.30
1500	0.22	0.16	0.20	0.24	0.46	0.29
1550	0.30	0.29	0.30	0.34	0.34	0.32
1600	0.32	0.34	0.30	0.33	0.30	0.37

As a result, DGT7 shows stronger weighting for wavelengths up to 1500 nm compared to the other 2 detectors, since detector drift is significantly smaller, as can be concluded from Table 9.

Degree of Equivalence of the participating laboratories

The degree of equivalence for the participating laboratory *i* is calculated via:

$$\mathrm{D_i} = \mathrm{W_p D_{i(p)}} + \mathrm{W}_l \mathrm{D_{i(}}_l\mathrm{)} \qquad \mathrm{W_P} + \mathrm{W_l} = 1. \tag{23}$$

The weighing factors for pilot and link laboratory $\mathrm{W_p}$ and $\mathrm{W_l}$ are determined from the following equations:

$$\mathrm{W_p} = \frac{\bar{W}}{\bar{\sigma}_\mathrm{p}^2 - \mathrm{u}_{\mathrm{p,r,RMO}}^2 - \mathrm{s}_{\mathrm{RMO}}^2}, \qquad \mathrm{W}_l = \frac{\bar{\mathrm{W}}}{\bar{\sigma}_\mathrm{l}^2 + \mathrm{u}_{\mathrm{p,r,RMO}}^2}, \tag{24}$$

where:

$$\bar{\mathrm{W}} = \frac{\left(\bar{\sigma}_\mathrm{l}^2 + \mathrm{u}_{\mathrm{p,r,RMO}}^2\right)\left(\bar{\sigma}_\mathrm{p}^2 - \mathrm{u}_{\mathrm{p,r,RMO}}^2 - \mathrm{s}_{\mathrm{RMO}}^2\right)}{\bar{\sigma}_\mathrm{p}^2 + \bar{\sigma}_\mathrm{l}^2 - \mathrm{s}_{\mathrm{RMO}}^2}, \tag{25}$$

$$\bar{\sigma}_\mathrm{p}^2 = \mathrm{s}_{\mathrm{KC}}^2 + \mathrm{s}_{\mathrm{RMO}}^2 + \mathrm{u}_{\mathrm{p,st}}^2 + \mathrm{u}_{\mathrm{p,r,KC}}^2 + \mathrm{u}_{\mathrm{p,r,RMO,}}^2$$

$$\bar{\sigma}_l^2 = \mathrm{s}_{\mathrm{KC}}^2 + \mathrm{s}_{\mathrm{RMO}}^2 + \mathrm{u}_{l,\mathrm{st}}^2 + \mathrm{u}_{l,\mathrm{r,KC}}^2 + \mathrm{u}_{l,\mathrm{r,RMO}}^2.$$

Note the asymmetry in Eq.(24), which results from the fact that the pilot provides a direct link, while the other link laboratory serves as a link through the pilot.

The standard uncertainty on the DoE for participant *i* is calculated from:

$$\mathrm{u}^2(\mathrm{D_i}) = \mathrm{u}_{i,\mathrm{c}}^2 + \left(\mathrm{W_p}^2 - 2\mathrm{W_p}\mathrm{w_p} + \mathrm{W_l}^2 - 2\mathrm{W_l}\mathrm{w_l}\right)\mathrm{s}_{\mathrm{KC}}^2 + u^2(\mathrm{x_{ref}}) + \mathrm{W_p}^2\left(\mathrm{u}_{\mathrm{p,st}}^2 + \mathrm{u}_{\mathrm{p,r,KC}}^2 + \mathrm{u}_{\mathrm{p,r,RMO}}^2\right) + \mathrm{W_l}^2\left(\mathrm{u}_{l,\mathrm{st}}^2 + \mathrm{u}_{l,\mathrm{r,KC}}^2 + \mathrm{u}_{l,\mathrm{r,RMO}}^2\right) + \left(\mathrm{W_l}^2 + 1\right)\mathrm{s}_{\mathrm{RMO}}^2 + 2\mathrm{W_l}\,\mathrm{u}_{\mathrm{p,r,RMO}}^2. \quad (26)$$

Here the combined uncertainty $\mathrm{u}_{\mathrm{i,c}}^2$ is the arithmetic mean for participant i of $u_{\mathrm{c}}^2\left(S_{ij}^{23}\right)$, as defined in Eq.(10)

The variables in the equations above are summarized in the table below.

Table 11. Overview of variables used for the determination of DoE and its associated uncertainty, also showing the origin of the data.

Quantity	Description	Source of data
$\mathrm{D_i}$	Unilateral DoE for the laboratory i	Calculated from other quantities
D_p	Unilateral DoE for the link laboratory as calculated during the CC Key comparison for the pilot p	CC KC report
$\mathrm{D_l}$	Unilateral DoE for the link laboratory as calculated during the CC Key comparison for the link l	CC KC report
$S_{lj}^{23,\mathrm{VSL}}$	Responsivity of detector j as measured by pilot (VSL) related to link laboratory	VSL responsivity data as measured for this comparison
S_{lj}^{23}	Responsivity of detector j measured by link laboratory (NPL)	NPL responsivity data measured for this comparison
$\mathrm{D_{i(p)}}$	The unilateral DoE for laboratory *i*, *calculated via the pilot*	Calculated from other quantities
$D_{i(l)}$	The unilateral DoE for laboratory *i*, *calculated through the pilot and the link*	Calculated from other quantities
W_p	Weighting for pilot laboratory	Calculated from other quantities
W_l	Weighting for link laboratory	Calculated from other quantities
s_{KC}	Transfer uncertainty of the CC KC: The additional term s as added during a Mandel-Paule approach that has been used to obtain consistency of the CC KC results	From CC KC report if applicable. This may also be an uncertainty due to artifact instability calculated from known effects. The transfer uncertainty is not defined in the CC comparison. Assume $s_{\mathrm{KC}} = 0$.
s_{RMO}	Standard transfer uncertainty of the RMO comparison. This may be based on known effects (e.g. artifact instability), or from the similar term in the CC KC	RMO KC or CC KC report. Not available from CC KC report, there is no specific indication for artifact instability that needs to be taken into account. Consider $s_{\mathrm{RMO}} = 0$.
$u_{p,\mathrm{st}}$	Standard uncertainty associated with reproducibility of pilot laboratory scale	This value is based on the uncertainty associated to drift/aging of the reference detector of VSL (GT3) and the uncertainty associated to the cryogenic radiometer.
$u_{p,\mathrm{r,KC}}$	Standard uncertainty associated with uncorrelated (random) effects at the pilot laboratory in the CC KC	CC KC report, table 7.8 Take the average of $u_{\mathrm{r}}\left(\bar{s}_{i,x}\right)$ for $\mathrm{x} = 1,2,3$.
$u_{p,\mathrm{r,RMO}}$	Standard uncertainty associated with uncorrelated (random) effects at the pilot laboratory in the RMO KC	Uncorrelated uncertainty contributions from VSL for this KC.
$u_{l,\mathrm{st}}$	Standard uncertainty associated with reproducibility of linking laboratory scale	Stability of scale from NPL technical report.
$u_{l,\mathrm{r,KC}}$	Standard uncertainty associated with uncorrelated (random) effects at the link laboratory in the CC KC	CC KC report, table 7.9 Take the average of $u_{\mathrm{r}}\left(\bar{s}_{i,x}\right)$ for $\mathrm{x} = 1,2,3$.

$u_{l,\mathrm{r,RMO}}$	Standard uncertainty associated with uncorrelated (random) effects at the link laboratory in the RMO KC	Uncorrelated uncertainty contributions from NPL technical report for this KC.
u_i	Uncertainty on the responsivity of the participant to be linked	Uncertainty as reported by participant *i* in this KC
$u_{\mathrm{temp}}(S_{ij})$	Temperature contribution to transfer uncertainty	This KC, based on uncertainty on temperature sensitivity and reported temperature (in Ω by the participant, averaged over 3 detectors.
$\mathrm{u_{unif}}(S_{ij})$	Uncertainty due to detector uniformity (for labs with different spot size)	This KC, based on detector uniformity and reported spot size and shape.
$\mathrm{u_c}(S_{ij})$	Combined uncertainty of the 3 variables above for participant i	Calculated from other quantities
$\mathrm{u_{i,c}}$	Arithmetic mean of the combined uncertainty over the 3 detectors	Calculated from other quantities
$\mathrm{w_p}$	Weight of pilot lab in the calculation of KCRV	CC KC report, table 7.19
$\mathrm{w_l}$	Weight of link lab in the calculation of KCRV	CC KC report, table 7.19
$\mathrm{u(x_{ref})}$	Standard uncertainty associated with KCRV	CC KC report, table 7.21

In the table below an overview of the input parameters that are used to determine the weighting for the DoE is shown and the resulting weighting factors. Here $s_{\mathrm{KC}} = s_{\mathrm{RMO}} = 0$.

Table 12. Overview of variables used for the determination of DoE and its associated uncertainty.

Wavelength /nm	$\mathrm{u_{p,st}}$ /%	$\mathrm{u_{p,r,KC}}$ /%	$\mathrm{u_{p,r,RMO}}$ /%	$\mathrm{u_{l,st}}$ /%	$\mathrm{u_{l,r,KC}}$ /%	$\mathrm{u_{l,r,RMO}}$ /%	W_p	W_l
900	0.02	0.04	0.13	0.01	0.05	0.04	0.92	0.08
950	0.01	0.03	0.12	0.01	0.05	0.12	0.97	0.03
1000	0.04	0.06	0.10	0.01	0.03	0.10	0.79	0.21
1050	0.07	0.05	0.09	0.01	0.03	0.08	0.69	0.31
1100	0.13	0.04	0.09	0.01	0.03	0.06	0.41	0.59
1150	0.13	0.04	0.09	0.01	0.03	0.06	0.39	0.61
1200	0.07	0.02	0.08	0.01	0.03	0.05	0.65	0.35
1250	0.07	0.03	0.08	0.01	0.02	0.05	0.62	0.38
1300	0.05	0.02	0.08	0.01	0.02	0.05	0.76	0.24
1350	0.06	0.01	0.08	0.01	0.03	0.06	0.72	0.28
1400	0.11	0.02	0.08	0.01	0.03	0.06	0.49	0.51
1450	0.14	0.02	0.07	0.01	0.01	0.07	0.35	0.65
1500	0.17	0.01	0.07	0.01	0.01	0.07	0.24	0.76
1550	0.17	0.02	0.09	0.01	0.01	0.11	0.41	0.59
1600	0.26	0.05	0.14	0.01	0.03	0.08	0.28	0.72

It is noted that for some wavelengths (particularly 900 nm to 1000 nm) the weighting of the pilot laboratory is much larger than the link laboratory. The origin of this and the impact is further discussed in Section 6.

In the table below other input parameters from the CC key comparison that are needed to calculate the DoE for the participants and their associated uncertainty are shown.

Table 13. Other input parameters from the CC key comparison used to calculate the DoE for the participants and their associated uncertainty.

λ /nm	D_p /%	$\mathrm{D_l}$ /%	$\mathrm{w_p}$	$\mathrm{w_l}$	$\mathrm{u(x_{ref})}$ /%
900	0.66	0.37	0.02	0.15	0.09
950	0.16	0.47	0.04	0.15	0.08
1000	0.50	0.13	0.03	0.16	0.07
1050	0.30	0.14	0.04	0.16	0.07
1100	0.26	0.22	0.05	0.16	0.06
1150	0.18	0.17	0.07	0.16	0.06
1200	0.14	0.31	0.08	0.15	0.06
1250	0.21	0.24	0.09	0.17	0.05
1300	0.21	0.22	0.10	0.17	0.05
1350	0.10	0.31	0.10	0.16	0.05
1400	0.20	0.15	0.11	0.16	0.06
1450	0.25	0.25	0.12	0.12	0.06
1500	0.27	0.25	0.11	0.15	0.06
1550	0.34	0.25	0.04	0.16	0.07
1600	0.40	0.20	0.02	0.16	0.07

5 Results from participating laboratories

In this section the responsivity values and their corresponding uncertainty for the detectors are reported for all participants. The tables presented below show the responsivity and calculated responsivity at 23 °C and the uncertainty components resulting from the temperature correction and the nonuniformity of the detector (for laboratories with different beam shape). The combined uncertainty as calculated from Eq.(10) is also included. The responsivity as measured by the pilot and the uncertainty of the pilot are reported for each detector.

The DoE as calculated from Eq.(26) and its associated uncertainty are shown for each participating laboratory both in a table and as a graph. Since this is an RMO comparison only for the non-link laboratories the DoE has been determined.

The technical reports of every participating laboratory are enclosed as annexes at the end of this report. The technical reports contain information on the measurement method and setup, traceability and the uncertainty associated to the responsivity calibration.

5.1 NPL (United Kingdom) – link laboratory

Table 14. Results of NPL, DGT6

NPL_DGT6

λ /nm	S_{ij} /(A/W)	$u(S_{ij})$ /%	S_{ij}^{23} /(A/W)	$u_{temp}(S_{ij})$ /%	$u_{unif}(S_{ij})$ /%	$u_c(S_{ij})$ /%	$S_{ij}^{23,VSL}$ /(A/W)	$u(S_{ij}^{23,VSL})$ /%
900	0.4517	0.08	0.4536	0.16	0.00	0.18	0.4602	0.24
950	0.5073	0.23	0.5088	0.13	0.00	0.26	0.5153	0.21
1000	0.5571	0.22	0.5585	0.11	0.00	0.25	0.5640	0.19
1050	0.5983	0.20	0.5996	0.10	0.00	0.22	0.6059	0.19
1100	0.6361	0.19	0.6372	0.10	0.00	0.21	0.6426	0.21
1150	0.6725	0.19	0.6734	0.09	0.00	0.21	0.6788	0.20
1200	0.7087	0.19	0.7095	0.08	0.00	0.21	0.7143	0.18
1250	0.7428	0.19	0.7435	0.08	0.00	0.20	0.7484	0.15
1300	0.7774	0.19	0.7780	0.07	0.00	0.20	0.7823	0.15
1350	0.8100	0.19	0.8105	0.06	0.00	0.20	0.8148	0.15
1400	0.8390	0.19	0.8393	0.06	0.00	0.20	0.8440	0.17
1450	0.8674	0.19	0.8675	0.04	0.00	0.19	0.8716	0.19
1500	0.8935	0.19	0.8934	0.03	0.00	0.19	0.8963	0.21
1550	0.8988	0.20	0.9007	0.07	0.00	0.21	0.9068	0.37
1600	0.6421	0.21	0.6545	0.09	0.00	0.23	0.6679	0.60

Table 15. Results of NPL DGT7

NPL_DGT7

λ /nm	S_{ij} /(A/W)	$u(S_{ij})$ /%	S_{ij}^{23} /(A/W)	$u_{temp}(S_{ij})$ /%	$u_{unif}(S_{ij})$ /%	$u_c(S_{ij})$ /%	$S_{ij}^{23,VSL}$ /(A/W)	$u(S_{ij}^{23,VSL})$ /%
900	0.3972	0.08	0.3992	0.19	0.00	0.21	0.4036	0.24
950	0.4585	0.25	0.4600	0.14	0.00	0.29	0.4653	0.21
1000	0.5173	0.24	0.5187	0.12	0.00	0.27	0.5234	0.19
1050	0.5686	0.22	0.5699	0.11	0.00	0.25	0.5758	0.19
1100	0.6158	0.21	0.6169	0.10	0.00	0.23	0.6225	0.21
1150	0.6610	0.21	0.6619	0.09	0.00	0.23	0.6678	0.20
1200	0.7049	0.21	0.7057	0.08	0.00	0.23	0.7116	0.17
1250	0.7455	0.21	0.7462	0.08	0.00	0.22	0.7526	0.15
1300	0.7862	0.21	0.7868	0.07	0.00	0.22	0.7928	0.15
1350	0.8240	0.21	0.8245	0.06	0.00	0.22	0.8311	0.15
1400	0.8565	0.21	0.8568	0.06	0.00	0.22	0.8641	0.17
1450	0.8907	0.21	0.8908	0.04	0.00	0.21	0.8978	0.19
1500	0.9202	0.21	0.9201	0.03	0.00	0.21	0.9267	0.21
1550	0.9353	0.24	0.9372	0.07	0.00	0.25	0.9460	0.37
1600	0.6872	0.23	0.6998	0.08	0.00	0.24	0.7170	0.61

Table 16. Results of NPL, DGT 8

NPL_DGT8

λ /nm	S_{ij} /(A/W)	$u(S_{ij})$ /%	S_{ij}^{23} /(A/W)	$u_{temp}(S_{ij})$ /%	$u_{unif}(S_{ij})$ /%	$u_c(S_{ij})$ /%	$S_{ij}^{23,VSL}$ /(A/W)	$u(S_{ij}^{23,VSL})$ /%
900	0.4293	0.08	0.4313	0.18	0.00	0.19	0.4366	0.24
950	0.4918	0.22	0.4933	0.13	0.00	0.26	0.4986	0.20
1000	0.5518	0.20	0.5532	0.11	0.00	0.23	0.5576	0.18
1050	0.6047	0.18	0.6060	0.10	0.00	0.21	0.6116	0.18
1100	0.6515	0.17	0.6526	0.10	0.00	0.20	0.6583	0.20
1150	0.6946	0.18	0.6955	0.09	0.00	0.20	0.7006	0.20
1200	0.7331	0.17	0.7339	0.08	0.00	0.19	0.7389	0.17
1250	0.7685	0.17	0.7692	0.07	0.00	0.19	0.7744	0.15
1300	0.8041	0.17	0.8047	0.07	0.00	0.18	0.8097	0.15
1350	0.8397	0.17	0.8402	0.06	0.00	0.18	0.8446	0.15
1400	0.8713	0.17	0.8716	0.06	0.00	0.18	0.8763	0.17
1450	0.9055	0.18	0.9056	0.04	0.00	0.18	0.9106	0.19
1500	0.9371	0.18	0.9370	0.03	0.00	0.18	0.9405	0.21
1550	0.9506	0.20	0.9525	0.06	0.00	0.21	0.9588	0.37
1600	0.6850	0.19	0.6976	0.08	0.00	0.21	0.7123	0.62

As discussed above DGT6 and DGT8 showed a large drift, as appeared from the results of pre- and post-measurements of these detectors by the pilot laboratory. However, the average between pre- and post-measurements of all detectors are relatively close. This also appears from the graph below, showing δ_{lj} for the three detectors and the weighted average value $\overline{\delta}_l$. The wavelength dependence of the difference shows a shape that is similar to that of Figure 4, showing the temperature dependence of the responsivity. A potential explanation of the difference might be the occurrence of temperature gradients between the sensitive area of the photodiode and the Pt100 sensor either during the measurements, or during the determination of the temperature sensitivity coefficient. In view of time not all DGTx detectors have been characterized individually for temperature dependence, but as can be seen from Figure 4, there is a spread on the measured coefficients. This has been taken into account as a measurement uncertainty. Compared to other laboratories NPL has a relatively large temperature difference from the nominal value (0.8 Ω) and is therefore the results are more sensitive to the temperature sensitivity coefficient compared to other labs.

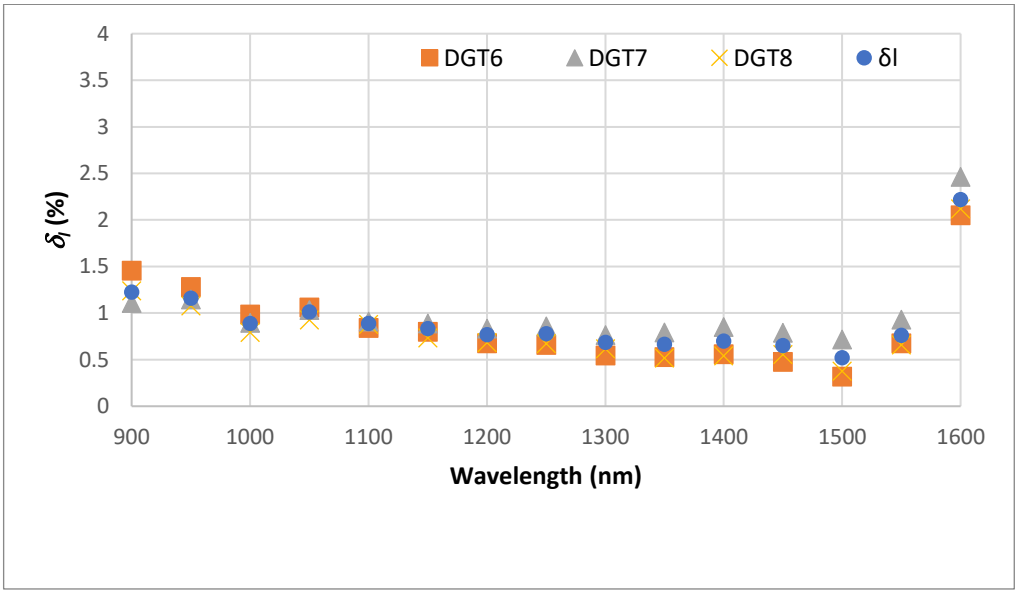

Figure 8. Relative difference between link and pilot for the individual detectors and the weighted average as defined in Eq.(22) and Eq.(20), respectively.

5.2 CMI (Czech Republic)

Table 17. Results of CMI, DGT1

CMI_DGT1

λ /nm	S_{ij} /(A/W)	$u(S_{ij})$ /%	S_{ij}^{23} /(A/W)	$u_{temp}(S_{ij})$ /%	$u_{unif}(S_{ij})$ /%	$u_e(S_{ij})$ /%	$S_{ij}^{23,VSL}$ /(A/W)	$u(S_{ij}^{23,VSL})$ /%
900	0.4438	0.51	0.4442	0.04	0.00	0.51	0.4479	0.24
950	0.4972	0.49	0.4976	0.04	0.00	0.49	0.4994	0.21
1000	0.5450	0.23	0.5454	0.03	0.00	0.23	0.5471	0.19
1050	0.5891	0.23	0.5895	0.03	0.00	0.23	0.5905	0.19
1100	0.6256	0.23	0.6259	0.03	0.00	0.23	0.6280	0.20
1150	0.6612	0.23	0.6615	0.03	0.00	0.23	0.6627	0.20
1200	0.6924	0.23	0.6926	0.02	0.00	0.23	0.6944	0.16
1250	0.7225	0.23	0.7227	0.02	0.00	0.23	0.7240	0.15
1300	0.7539	0.23	0.7541	0.02	0.00	0.23	0.7548	0.15
1350	0.7867	0.23	0.7868	0.02	0.00	0.23	0.7868	0.15
1400	0.8189	0.23	0.8190	0.02	0.00	0.23	0.8185	0.17
1450	0.8527	0.23	0.8527	0.01	0.00	0.23	0.8521	0.19
1500	0.8853	0.23	0.8853	0.01	0.00	0.23	0.8834	0.21
1550	0.9066	0.23	0.9072	0.02	0.00	0.23	0.9079	0.37
1600	0.6789	0.30	0.6824	0.02	0.00	0.30	0.6948	0.60

Table 18. Results of CMI, DGT3

CMI_DGT3

λ /nm	S_{ij} /(A/W)	$u(S_{ij})$ /%	S_{ij}^{23} /(A/W)	$u_{temp}(S_{ij})$ /%	$u_{unif}(S_{ij})$ /%	$u_e(S_{ij})$ /%	$S_{ij}^{23,VSL}$ /(A/W)	$u(S_{ij}^{23,VSL})$ /%
900	0.4209	0.51	0.4213	0.04	0.00	0.51	0.4262	0.24
950	0.4787	0.49	0.4791	0.04	0.00	0.49	0.4820	0.21
1000	0.5318	0.23	0.5322	0.03	0.00	0.23	0.5351	0.19
1050	0.5821	0.23	0.5825	0.03	0.00	0.23	0.5844	0.19
1100	0.6242	0.23	0.6245	0.03	0.00	0.23	0.6275	0.20
1150	0.6649	0.23	0.6652	0.03	0.00	0.23	0.6668	0.20
1200	0.6996	0.23	0.6998	0.02	0.00	0.23	0.7021	0.16
1250	0.7320	0.23	0.7322	0.02	0.00	0.23	0.7339	0.15
1300	0.7650	0.23	0.7652	0.02	0.00	0.23	0.7662	0.15
1350	0.7990	0.23	0.7991	0.02	0.00	0.23	0.7994	0.15
1400	0.8307	0.23	0.8308	0.02	0.00	0.23	0.8305	0.17
1450	0.8666	0.23	0.8666	0.01	0.00	0.23	0.8660	0.19
1500	0.9007	0.23	0.9007	0.01	0.00	0.23	0.8985	0.21
1550	0.9235	0.23	0.9241	0.02	0.00	0.23	0.9243	0.37
1600	0.6860	0.30	0.6897	0.02	0.00	0.30	0.7014	0.60

Table 19. Results of CMI, DGT12

CMI_DGT12

λ /nm	S_{ij} /(A/W)	$u(S_{ij})$ /%	S_{ij}^{23} /(A/W)	$u_{temp}(S_{ij})$ /%	$u_{unif}(S_{ij})$ /%	$u_e(S_{ij})$ /%	$S_{ij}^{23,VSL}$ /(A/W)	$u(S_{ij}^{23,VSL})$ /%
900	0.4218	0.51	0.4221	0.03	0.00	0.51	0.4280	0.24
950	0.4813	0.49	0.4816	0.03	0.00	0.49	0.4855	0.20
1000	0.5334	0.23	0.5337	0.03	0.00	0.23	0.5376	0.19
1050	0.5802	0.23	0.5805	0.02	0.00	0.23	0.5836	0.18
1100	0.6200	0.23	0.6202	0.02	0.00	0.23	0.6245	0.20
1150	0.6616	0.23	0.6618	0.02	0.00	0.23	0.6650	0.20
1200	0.7006	0.23	0.7008	0.02	0.00	0.23	0.7046	0.16
1250	0.7383	0.23	0.7385	0.02	0.00	0.23	0.7417	0.15
1300	0.7757	0.23	0.7758	0.02	0.00	0.23	0.7785	0.14
1350	0.8115	0.23	0.8116	0.01	0.00	0.23	0.8135	0.15
1400	0.8419	0.23	0.8420	0.01	0.00	0.23	0.8437	0.17
1450	0.8734	0.23	0.8734	0.01	0.00	0.23	0.8749	0.19
1500	0.9009	0.23	0.9009	0.01	0.00	0.23	0.9012	0.21
1550	0.9178	0.23	0.9182	0.02	0.00	0.23	0.9208	0.37
1600	0.6916	0.30	0.6944	0.02	0.00	0.30	0.7078	0.59

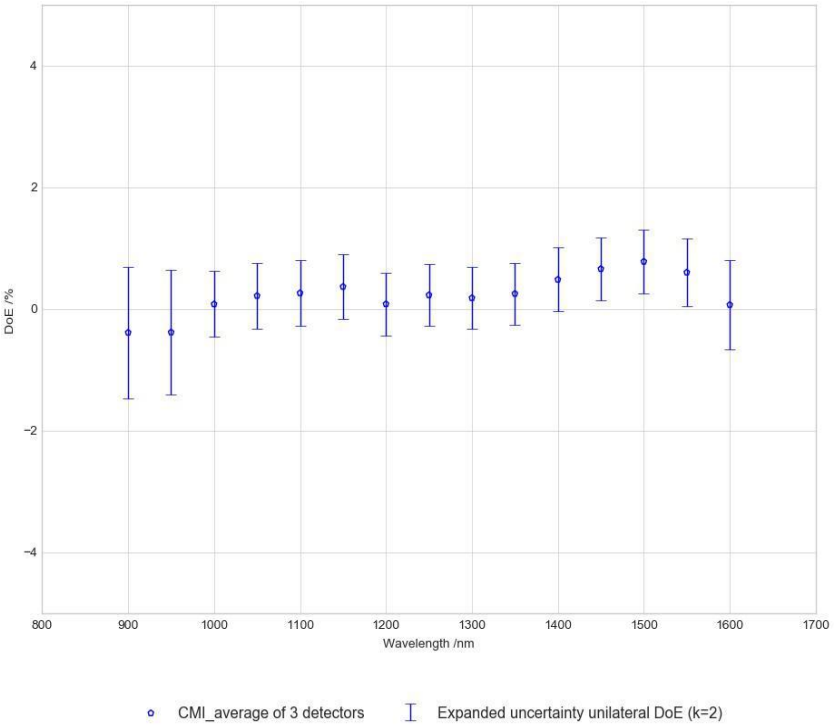

Figure 9. DoE of CMI

5.3 GUM (Poland)

Table 20. Results of GUM, DGT1

GUM_DGT1

λ /nm	S_{ij} /(A/W)	$u(S_{ij})$ /%	S_{ij}^{23} /(A/W)	$u_{temp}(S_{ij})$ /%	$u_{unif}(S_{ij})$ /%	$u_c(S_{ij})$ /%	$S_{ij}^{23,VSL}$ /(A/W)	$u(S_{ij}^{23,VSL})$ /%
900	0.4369	0.46	0.4366	0.02	0.17	0.49	0.4498	0.24
950	0.4993	0.38	0.4992	0.01	0.13	0.40	0.5010	0.21
1000	0.5483	0.26	0.5481	0.02	0.11	0.28	0.5492	0.19
1050	0.5911	0.39	0.5910	0.01	0.10	0.40	0.5924	0.19
1100	0.6297	0.29	0.6296	0.01	0.09	0.31	0.6299	0.20
1150	0.6653	0.32	0.6652	0.01	0.09	0.33	0.6644	0.20
1200	0.6965	0.34	0.6965	0.01	0.09	0.35	0.6964	0.17
1250	0.7270	0.32	0.7269	0.01	0.09	0.33	0.7260	0.16
1300	0.7579	0.32	0.7578	0.01	0.09	0.33	0.7568	0.15
1350	0.7901	0.29	0.7901	0.01	0.10	0.31	0.7884	0.15
1400	0.8228	0.29	0.8228	0.00	0.10	0.31	0.8203	0.17
1450	0.8577	0.31	0.8577	0.00	0.08	0.32	0.8539	0.19
1500	0.8906	0.31	0.8906	0.00	0.07	0.32	0.8851	0.21
1550	0.9138	0.36	0.9135	0.01	0.12	0.38	0.9100	0.38
1600	0.6976	0.50	0.6965	0.01	0.20	0.54	0.6970	0.60

Table 21. Results of GUM, DGT3

GUM_DGT3

λ /nm	S_{ij} /(A/W)	$u(S_{ij})$ /%	S_{ij}^{23} /(A/W)	$u_{temp}(S_{ij})$ /%	$u_{unif}(S_{ij})$ /%	$u_c(S_{ij})$ /%	$S_{ij}^{23,VSL}$ /(A/W)	$u(S_{ij}^{23,VSL})$ /%
900	0.4196	0.50	0.4194	0.02	0.17	0.53	0.4297	0.24
950	0.4851	0.49	0.4848	0.02	0.13	0.51	0.4858	0.22
1000	0.5391	0.32	0.5390	0.01	0.11	0.34	0.5388	0.19
1050	0.5882	0.34	0.5881	0.01	0.10	0.35	0.5872	0.18
1100	0.6321	0.35	0.6320	0.01	0.09	0.36	0.6296	0.21
1150	0.6729	0.40	0.6728	0.01	0.09	0.41	0.6686	0.20
1200	0.7082	0.44	0.7081	0.01	0.09	0.45	0.7052	0.17
1250	0.7404	0.39	0.7403	0.01	0.09	0.40	0.7383	0.16
1300	0.7731	0.40	0.7730	0.01	0.09	0.41	0.7718	0.15
1350	0.8068	0.40	0.8068	0.00	0.10	0.41	0.8052	0.16
1400	0.8394	0.43	0.8394	0.01	0.10	0.44	0.8360	0.18
1450	0.8751	0.39	0.8751	0.00	0.08	0.40	0.8703	0.19
1500	0.9089	0.39	0.9089	0.00	0.07	0.40	0.9012	0.21
1550	0.9307	0.38	0.9305	0.01	0.12	0.40	0.9254	0.38
1600	0.7003	0.56	0.6992	0.01	0.20	0.59	0.7032	0.61

Table 22. Results of GUM, DGT12

GUM_DGT12

λ /nm	S_{ij} /(A/W)	$u(S_{ij})$ /%	S_{ij}^{23} /(A/W)	$u_{temp}(S_{ij})$ /%	$u_{unif}(S_{ij})$ /%	$u_e(S_{ij})$ /%	$S_{ij}^{23,VSL}$ /(A/W)	$u(S_{ij}^{23,VSL})$ /%
900	0.4139	0.41	0.4135	0.04	0.17	0.44	0.4294	0.24
950	0.4844	0.40	0.4840	0.04	0.13	0.42	0.4869	0.21
1000	0.5379	0.23	0.5376	0.03	0.11	0.26	0.5387	0.19
1050	0.5834	0.33	0.5831	0.02	0.10	0.35	0.5846	0.19
1100	0.6256	0.28	0.6254	0.02	0.09	0.30	0.6252	0.21
1150	0.6666	0.32	0.6664	0.02	0.09	0.33	0.6654	0.20
1200	0.7059	0.32	0.7057	0.02	0.09	0.33	0.7049	0.18
1250	0.7434	0.30	0.7433	0.01	0.09	0.31	0.7422	0.16
1300	0.7803	0.31	0.7802	0.01	0.09	0.32	0.7786	0.15
1350	0.8160	0.28	0.8159	0.01	0.10	0.30	0.8134	0.15
1400	0.8469	0.30	0.8469	0.01	0.10	0.32	0.8431	0.17
1450	0.8780	0.31	0.8780	0.01	0.08	0.32	0.8743	0.19
1500	0.9056	0.33	0.9056	0.00	0.07	0.34	0.9007	0.22
1550	0.9231	0.39	0.9228	0.01	0.12	0.41	0.9202	0.38
1600	0.7083	0.54	0.7066	0.01	0.20	0.58	0.7064	0.61

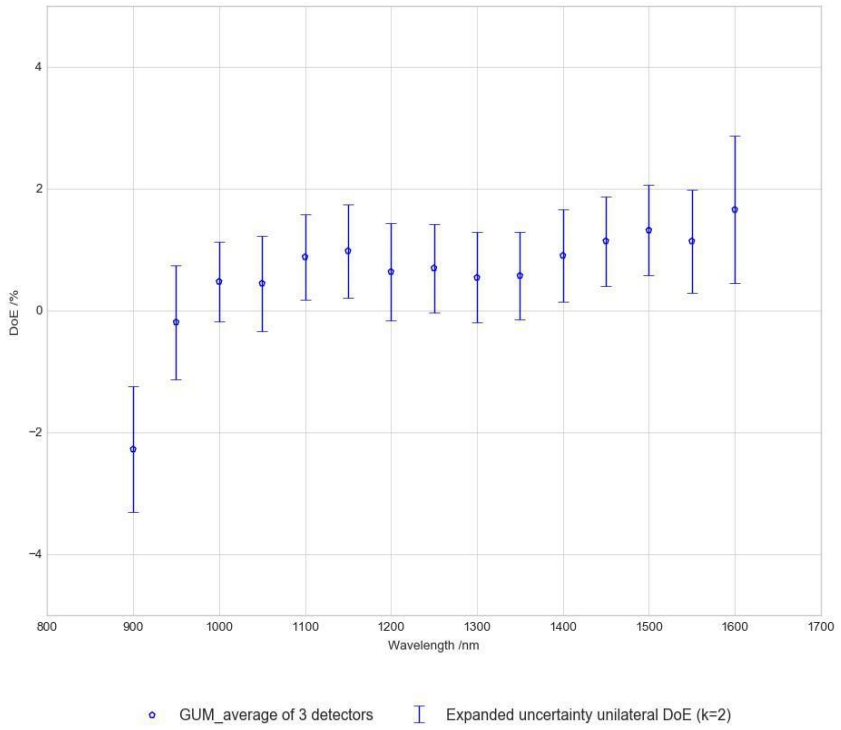

Figure 10. DoE of GUM

5.4 JV (Norway)

Table 23. Results of JV, DGT9

JV_DGT9

λ /nm	S_{ij} /(A/W)	$u(S_{ij})$ /%	S_{ij}^{23} /(A/W)	$u_{temp}(S_{ij})$ /%	$u_{unif}(S_{ij})$ /%	$u_e(S_{ij})$ /%	$S_{ij}^{23,VSL}$ /(A/W)	$u(S_{ij}^{23,VSL})$ /%
900	0.4309	0.46	0.4313	0.04	0.17	0.49	0.4362	0.24
950	0.4883	0.26	0.4887	0.04	0.13	0.30	0.4922	0.21
1000	0.5381	0.34	0.5385	0.03	0.11	0.36	0.5427	0.19
1050	0.5829	0.30	0.5832	0.03	0.10	0.32	0.5868	0.19
1100	0.6212	0.31	0.6215	0.03	0.09	0.33	0.6257	0.21
1150	0.6606	0.28	0.6608	0.02	0.09	0.30	0.6641	0.20
1200	0.6986	0.29	0.6988	0.02	0.09	0.30	0.7014	0.16
1250	0.7339	0.28	0.7341	0.02	0.09	0.29	0.7366	0.15
1300	0.7701	0.28	0.7703	0.02	0.09	0.30	0.7719	0.15
1350	0.8039	0.29	0.8040	0.02	0.10	0.31	0.8055	0.15
1400	0.8331	0.28	0.8332	0.02	0.10	0.30	0.8346	0.17
1450	0.8634	0.28	0.8634	0.01	0.08	0.29	0.8649	0.19
1500	0.8899	0.29	0.8899	0.01	0.07	0.30	0.8902	0.21
1550	0.9049	0.30	0.9054	0.02	0.12	0.32	0.9073	0.37
1600	0.6658	0.42	0.6691	0.02	0.20	0.47	0.6832	0.60

Table 24. Results of JV, DGT10

JV_DGT10

λ /nm	S_{ij} /(A/W)	$u(S_{ij})$ /%	S_{ij}^{23} /(A/W)	$u_{temp}(S_{ij})$ /%	$u_{unif}(S_{ij})$ /%	$u_e(S_{ij})$ /%	$S_{ij}^{23,VSL}$ /(A/W)	$u(S_{ij}^{23,VSL})$ /%
900	0.3839	0.59	0.3843	0.04	0.17	0.61	0.3880	0.25
950	0.4441	0.36	0.4445	0.04	0.13	0.39	0.4479	0.21
1000	0.5001	0.43	0.5005	0.03	0.11	0.45	0.5042	0.19
1050	0.5524	0.42	0.5527	0.03	0.10	0.43	0.5552	0.19
1100	0.5974	0.42	0.5977	0.03	0.09	0.43	0.6016	0.20
1150	0.6455	0.42	0.6457	0.02	0.09	0.43	0.6477	0.20
1200	0.6894	0.43	0.6896	0.02	0.09	0.44	0.6919	0.16
1250	0.7303	0.42	0.7305	0.02	0.09	0.43	0.7329	0.15
1300	0.7715	0.42	0.7717	0.02	0.09	0.43	0.7730	0.15
1350	0.8098	0.42	0.8099	0.01	0.10	0.43	0.8108	0.15
1400	0.8410	0.44	0.8411	0.01	0.10	0.45	0.8436	0.17
1450	0.8745	0.43	0.8745	0.01	0.08	0.44	0.8768	0.19
1500	0.9058	0.43	0.9058	0.01	0.07	0.44	0.9063	0.21
1550	0.9231	0.46	0.9235	0.02	0.12	0.47	0.9251	0.37
1600	0.6792	0.47	0.6821	0.02	0.20	0.51	0.6946	0.60

Table 25. Results of JV, DGT11

JV_DGT11

λ /nm	S_{ij} /(A/W)	$u(S_{ij})$ /%	S_{ij}^{23} /(A/W)	$u_{temp}(S_{ij})$ /%	$u_{unif}(S_{ij})$ /%	$u_e(S_{ij})$ /%	$S_{ij}^{23,VSL}$ /(A/W)	$u(S_{ij}^{23,VSL})$ /%
900	0.3955	0.63	0.3957	0.02	0.17	0.65	0.3979	0.25
950	0.4505	0.50	0.4507	0.02	0.13	0.52	0.4520	0.21
1000	0.5004	0.50	0.5006	0.02	0.11	0.51	0.5021	0.19
1050	0.5463	0.46	0.5465	0.01	0.10	0.47	0.5469	0.19
1100	0.5848	0.54	0.5849	0.01	0.09	0.55	0.5870	0.21
1150	0.6263	0.45	0.6264	0.01	0.09	0.46	0.6268	0.20
1200	0.6646	0.47	0.6647	0.01	0.09	0.48	0.6651	0.16
1250	0.7000	0.45	0.7001	0.01	0.09	0.46	0.7008	0.15
1300	0.7375	0.44	0.7376	0.01	0.09	0.45	0.7371	0.15
1350	0.7740	0.44	0.7741	0.01	0.10	0.45	0.7732	0.15
1400	0.8064	0.46	0.8064	0.01	0.10	0.47	0.8075	0.17
1450	0.8413	0.46	0.8413	0.00	0.08	0.47	0.8423	0.19
1500	0.8738	0.43	0.8738	0.00	0.07	0.44	0.8733	0.21
1550	0.8976	0.45	0.8978	0.01	0.12	0.47	0.8983	0.37
1600	0.6717	0.48	0.6731	0.01	0.20	0.52	0.6831	0.60

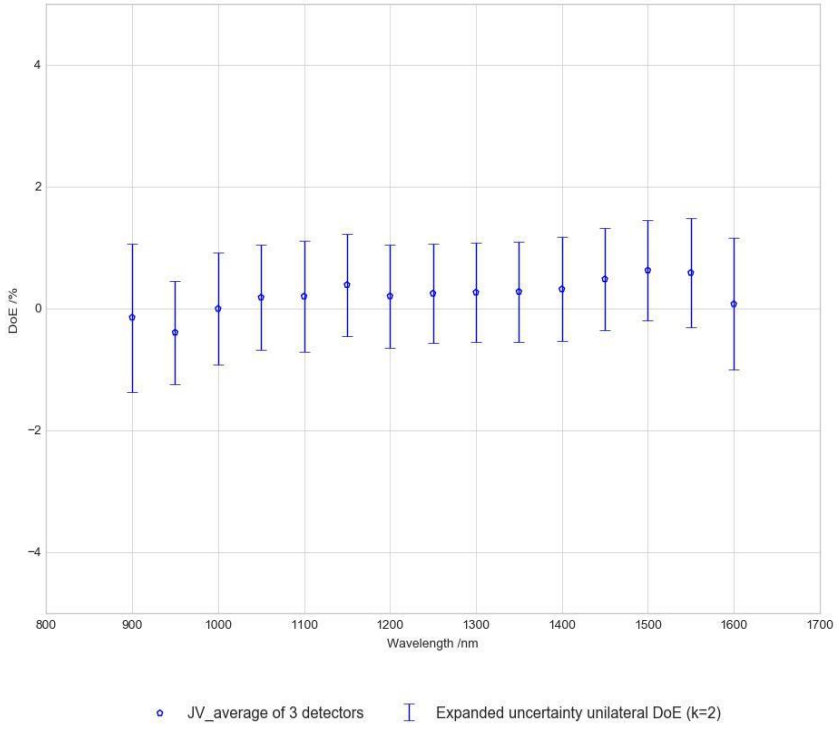

Figure 11. DoE of JV

5.5 SP (Sweden)

Table 26. Results of SP, DGT6

SP_DGT6

λ /nm	S_{ij} /(A/W)	$u(S_{ij})$ /%	S_{ij}^{23} /(A/W)	$u_{temp}(S_{ij})$ /%	$u_{unif}(S_{ij})$ /%	$u_e(S_{ij})$ /%	$S_{ij}^{23,VSL}$ /(A/W)	$u(S_{ij}^{23,VSL})$ /%
900	0.4510	0.86	0.4491	0.17	0.00	0.88	0.4531	0.23
950	0.5050	0.82	0.5031	0.17	0.00	0.84	0.5083	0.20
1000	0.5560	0.82	0.5542	0.14	0.00	0.84	0.5573	0.18
1050	0.6010	0.83	0.5994	0.13	0.00	0.84	0.5997	0.18
1100	0.6410	0.82	0.6396	0.12	0.00	0.83	0.6369	0.20
1150	0.6760	0.82	0.6749	0.11	0.00	0.83	0.6737	0.20
1200	0.7100	0.82	0.7090	0.11	0.00	0.83	0.7093	0.16
1250	0.7420	0.82	0.7411	0.10	0.00	0.83	0.7434	0.15
1300	0.7770	0.82	0.7762	0.09	0.00	0.83	0.7777	0.15
1350	0.8090	0.83	0.8084	0.07	0.00	0.83	0.8104	0.15
1400	0.8420	0.84	0.8416	0.08	0.00	0.84	0.8400	0.17
1450	0.8720	0.84	0.8719	0.05	0.00	0.84	0.8680	0.19
1500	0.8990	1.03	0.8991	0.03	0.00	1.03	0.8931	0.21
1550	0.8860	1.12	0.8836	0.09	0.00	1.12	0.9045	0.37
1600	0.6660	1.82	0.6502	0.11	0.00	1.83	0.6677	0.60

Table 27. Results of SP, DGT7

SP_DGT7

λ /nm	S_{ij} /(A/W)	$u(S_{ij})$ /%	S_{ij}^{23} /(A/W)	$u_{temp}(S_{ij})$ /%	$u_{unif}(S_{ij})$ /%	$u_e(S_{ij})$ /%	$S_{ij}^{23,VSL}$ /(A/W)	$u(S_{ij}^{23,VSL})$ /%
900	0.4030	0.82	0.4010	0.19	0.00	0.85	0.4046	0.24
950	0.4640	0.81	0.4621	0.19	0.00	0.83	0.4662	0.21
1000	0.5230	0.82	0.5212	0.16	0.00	0.83	0.5242	0.19
1050	0.5780	0.82	0.5763	0.14	0.00	0.84	0.5764	0.18
1100	0.6270	0.82	0.6256	0.13	0.00	0.83	0.6230	0.20
1150	0.6700	0.82	0.6688	0.12	0.00	0.83	0.6681	0.20
1200	0.7130	0.82	0.7120	0.11	0.00	0.83	0.7114	0.16
1250	0.7520	0.82	0.7510	0.10	0.00	0.83	0.7520	0.15
1300	0.7930	0.83	0.7922	0.09	0.00	0.83	0.7920	0.14
1350	0.8310	0.84	0.8303	0.07	0.00	0.85	0.8300	0.15
1400	0.8670	0.86	0.8666	0.08	0.00	0.86	0.8630	0.17
1450	0.9030	0.86	0.9029	0.05	0.00	0.86	0.8964	0.19
1500	0.9340	1.05	0.9341	0.03	0.00	1.05	0.9251	0.21
1550	0.9250	1.12	0.9225	0.09	0.00	1.13	0.9439	0.37
1600	0.7180	1.82	0.7018	0.11	0.00	1.82	0.7164	0.59

Table 28. Results of SP, DGT8

SP_DGT8

λ /nm	S_{ij} /(A/W)	$u(S_{ij})$ /%	S_{ij}^{23} /(A/W)	$u_{temp}(S_{ij})$ /%	$u_{unif}(S_{ij})$ /%	$u_e(S_{ij})$ /%	$S_{ij}^{23,VSL}$ /(A/W)	$u(S_{ij}^{23,VSL})$ /%
900	0.4300	0.85	0.4280	0.18	0.00	0.87	0.4311	0.24
950	0.4910	0.83	0.4891	0.17	0.00	0.85	0.4931	0.20
1000	0.5510	0.83	0.5492	0.15	0.00	0.85	0.5521	0.18
1050	0.6080	0.85	0.6064	0.13	0.00	0.86	0.6063	0.18
1100	0.6580	0.85	0.6566	0.12	0.00	0.86	0.6533	0.20
1150	0.6990	0.86	0.6979	0.11	0.00	0.87	0.6961	0.20
1200	0.7360	0.85	0.7350	0.10	0.00	0.86	0.7345	0.16
1250	0.7700	0.85	0.7691	0.10	0.00	0.86	0.7698	0.15
1300	0.8060	0.84	0.8052	0.09	0.00	0.85	0.8054	0.14
1350	0.8410	0.86	0.8404	0.07	0.00	0.86	0.8406	0.15
1400	0.8760	0.87	0.8756	0.07	0.00	0.87	0.8726	0.17
1450	0.9120	0.86	0.9119	0.05	0.00	0.87	0.9072	0.19
1500	0.9450	1.06	0.9451	0.03	0.00	1.06	0.9375	0.21
1550	0.9380	1.14	0.9355	0.08	0.00	1.15	0.9564	0.37
1600	0.7150	1.84	0.6989	0.11	0.00	1.84	0.7127	0.60

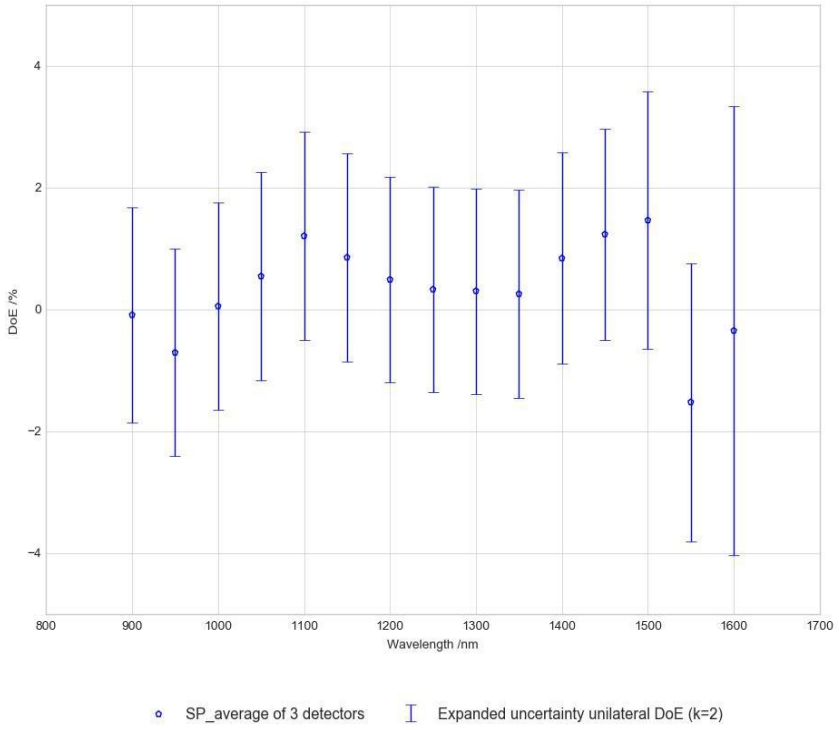

Figure 12. DoE SP

5.6 UME (Turkey)

Table 29. Results of UME, DGT9

UME_DGT9

λ /nm	R_i /(A/W)	$u(R_i)/\%$	$R_0/(A/W)$	$u(R_0)/\%$
900	0.4349	0.92	0.4387	0.24
950	0.4931	0.92	0.4947	0.21
1000	0.5488	0.92	0.5452	0.19
1050	0.5925	0.92	0.5893	0.19
1100	0.6322	0.92	0.6279	0.21
1150	0.6750	0.91	0.6661	0.21
1200	0.7163	0.91	0.7038	0.18
1250	0.7550	0.91	0.7392	0.16
1300	0.7921	0.91	0.7743	0.15
1350	0.8273	0.91	0.8077	0.16
1400	0.8529	0.91	0.8368	0.19
1450	0.8860	0.91	0.8670	0.19
1500	0.9066	0.91	0.8921	0.21
1550	0.9092	0.97	0.9100	0.38
1600	0.6612	0.97	0.6872	0.61

Table 30. Results of UME, DGT10

UME_DGT10

λ /nm	S_{ij} /(A/W)	$u(S_{ij})$ /%	S_{ij}^{23} /(A/W)	$u_{temp}(S_{ij})$ /%	$u_{unif}(S_{ij})$ /%	$u_c(S_{ij})$ /%	$S_{ij}^{23,VSL}$ /(A/W)	$u(S_{ij}^{23,VSL})$ /%
900	0.3956	0.92	0.3947	0.09	0.00	0.92	0.3933	0.24
950	0.4580	0.92	0.4571	0.08	0.00	0.92	0.4533	0.21
1000	0.5186	0.92	0.5178	0.07	0.00	0.92	0.5095	0.19
1050	0.5692	0.92	0.5684	0.06	0.00	0.92	0.5607	0.19
1100	0.6153	0.92	0.6147	0.06	0.00	0.92	0.6067	0.21
1150	0.6648	0.91	0.6643	0.05	0.00	0.91	0.6523	0.20
1200	0.7121	0.91	0.7116	0.05	0.00	0.91	0.6964	0.17
1250	0.7553	0.91	0.7549	0.04	0.00	0.91	0.7374	0.16
1300	0.7961	0.91	0.7958	0.04	0.00	0.91	0.7773	0.15
1350	0.8346	0.92	0.8343	0.03	0.00	0.92	0.8147	0.15
1400	0.8634	0.92	0.8632	0.03	0.00	0.92	0.8473	0.18
1450	0.9000	0.92	0.8999	0.02	0.00	0.92	0.8805	0.20
1500	0.9239	0.92	0.9240	0.01	0.00	0.92	0.9091	0.22
1550	0.9274	1.01	0.9264	0.04	0.00	1.01	0.9281	0.38
1600	0.6771	1.05	0.6702	0.05	0.00	1.05	0.6965	0.60

Table 31. Results of UME, DGT11

UME_DGT11

λ /nm	S_{ij} /(A/W)	$u(S_{ij})$ /%	S_{ij}^{23} /(A/W)	$u_{temp}(S_{ij})$ /%	$u_{unif}(S_{ij})$ /%	$u_c(S_{ij})$ /%	$S_{ij}^{23,VSL}$ /(A/W)	$u(S_{ij}^{23,VSL})$ /%
900	0.3979	0.94	0.3968	0.11	0.00	0.95	0.4014	0.26
950	0.4549	0.93	0.4539	0.10	0.00	0.94	0.4555	0.21
1000	0.5099	0.92	0.5089	0.09	0.00	0.92	0.5058	0.20
1050	0.5550	0.92	0.5541	0.08	0.00	0.92	0.5504	0.20
1100	0.5957	0.92	0.5949	0.08	0.00	0.92	0.5901	0.21
1150	0.6405	0.92	0.6399	0.07	0.00	0.92	0.6299	0.21
1200	0.6829	0.92	0.6823	0.06	0.00	0.92	0.6684	0.18
1250	0.7221	0.92	0.7215	0.06	0.00	0.92	0.7038	0.16
1300	0.7608	0.92	0.7603	0.05	0.00	0.92	0.7401	0.16
1350	0.7997	0.92	0.7993	0.04	0.00	0.92	0.7760	0.15
1400	0.8327	0.92	0.8325	0.05	0.00	0.92	0.8101	0.18
1450	0.8714	0.92	0.8713	0.03	0.00	0.92	0.8446	0.19
1500	0.9001	0.92	0.9002	0.02	0.00	0.92	0.8760	0.21
1550	0.9123	1.00	0.9108	0.05	0.00	1.00	0.9008	0.38
1600	0.6751	1.04	0.6657	0.07	0.00	1.04	0.6836	0.62

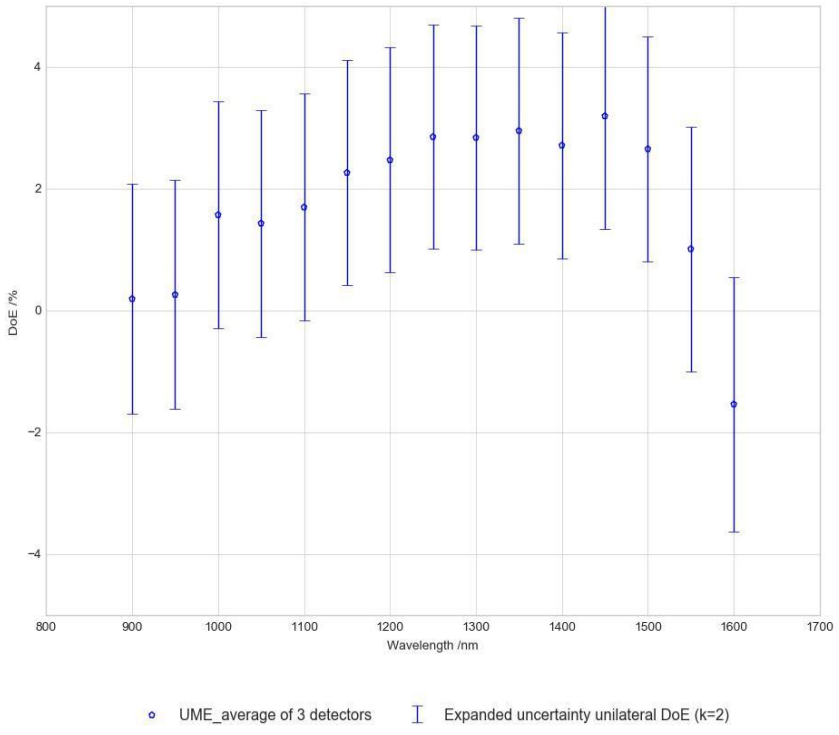

Figure 13. DoE of UME

6 Discussion and conclusion

To summarize the results, the unilateral Degree of Equivalence (DoE) and its uncertainty are shown in Table 32 below for each participant. The results are also plotted in Figure 14.

Table 32. Unilateral DoE and its associated expanded uncertainty for all participants.

λ /nm	D_{CMI}/%	$U(D_{\mathrm{CMI}})$/%	D_{GUM}/%	$U(D_{\mathrm{GUM}})$/%	D_{JV}/%	$U(D_{\mathrm{JV}})$/%	D_{SP}/%	$U(D_{\mathrm{SP}})$/%	D_{UME}/%	$U(D_{\mathrm{UME}})$/%
900	-0.38	1.08	-2.27	1.03	-0.14	1.22	-0.08	1.76	0.20	1.89
950	-0.38	1.02	-0.19	0.94	-0.39	0.85	-0.70	1.70	0.27	1.88
1000	0.09	0.54	0.48	0.65	0.00	0.92	0.06	1.70	1.58	1.87
1050	0.22	0.54	0.45	0.78	0.19	0.86	0.55	1.71	1.44	1.86
1100	0.27	0.54	0.89	0.70	0.21	0.91	1.21	1.71	1.70	1.86
1150	0.37	0.53	0.98	0.77	0.40	0.83	0.86	1.70	2.27	1.85
1200	0.09	0.52	0.64	0.79	0.21	0.85	0.50	1.69	2.48	1.84
1250	0.24	0.51	0.70	0.73	0.25	0.82	0.34	1.69	2.86	1.84
1300	0.19	0.51	0.55	0.74	0.27	0.81	0.31	1.69	2.84	1.84
1350	0.26	0.51	0.58	0.72	0.28	0.83	0.26	1.71	2.96	1.85
1400	0.49	0.53	0.91	0.76	0.33	0.85	0.85	1.74	2.72	1.85
1450	0.67	0.52	1.15	0.74	0.49	0.84	1.24	1.73	3.20	1.85
1500	0.79	0.52	1.32	0.74	0.63	0.82	1.47	2.11	2.66	1.85
1550	0.61	0.56	1.15	0.85	0.59	0.90	-1.51	2.28	1.02	2.01
1600	0.08	0.73	1.66	1.21	0.08	1.08	-0.34	3.68	-1.53	2.09

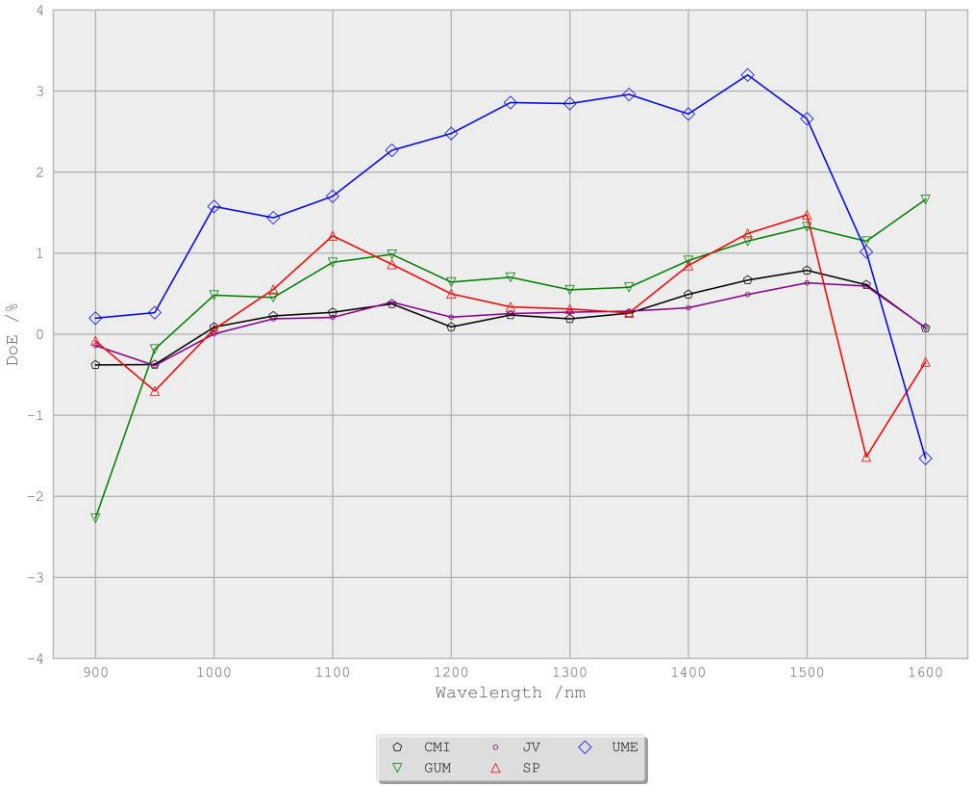

Figure 14. Summary of DoE of participating laboratories with the CCPR KCRV. Uncertainties have been omitted for clarity.

Discussion on weighting

As shown in Table 12, the weighting of the pilot laboratory for the wavelength range 900 nm – 1000 nm is dominant, so the DoE of participants with the CCPR KCRV is almost fully based on the link via the pilot laboratory. The reason for the strong weighting is the relatively large contribution of random effects ($u_{p,r,RMO}$) in Eq.(21) for these wavelengths. To estimate the impact of the weighting on the DoE, we have calculated the DoE for the case that the weighting of the link laboratory is artificially set to be at least 0.25. This (rather arbitrary) threshold only impacts the wavelengths 900 nm, 950 nm and 1000 nm. The maximum change in DoE we observe, is about 0.3% at 950 nm (smaller at the other wavelengths), which is far within the uncertainty of the participants at this wavelength. The impact on the E_n value is small (there is no lab for which the E_n value changes from below 1 to above 1 or vice versa when applying the minimum weight of 0.25 for the link laboratory).

Although the impact of the weighting on the calculated DoE is thus limited in this case, it is recommended to be aware of the impact of relatively large random effects on the weighting of pilot and link laboratory and take this into account e.g. when selecting comparison artefacts.

Conclusion

Seven laboratories, including pilot and link laboratory, participated in a EURAMET comparison of spectral responsivity measurements for the near-infrared spectral range (900 nm – 1600 nm). This key comparison links the EURAMET participants to the CCPR-K2.a-2003 comparison. Most laboratories show a DoE within 1 % from the CCPR KCRV for almost the full wavelength range (with some slightly larger differences mostly above 1450 nm). One laboratory (UME) shows larger deviations, up to 3%. Within the uncertainty on the DoE, SP and JV fully agree with the KCRV that was established with the CCPR-k2.a-2003 comparison, while CMI almost fully agrees, except a small deviation around 1500 nm. GUM has some deviations slightly larger than the uncertainty on the DoE for a few wavelengths, while UME shows larger deviations outside the uncertainty on the DoE for the central part of the wavelength range.

References

[1] Steven W Brown, Thomas C Larason and Yoshi Ohno (2010). Final report on the key comparison CCPR-K2.a-2003: Spectral responsivity in the range of 900 nm to 1600 nm, Metrologia, **47-**02002, doi: 10.1088/0026-1394/47/1A/02002

[2] Guidance documents: CCPR-G2 and CCPR-G6: https://www.bipm.org/en/committees/cc/ccpr/publications-cc.html#gd

[3] K D Stock, R Heine and H Hofer, 'Spectral characterization of Ge trap detectors and photodiodes used as transfer standards', Metrologia 40 (1) (2003)

A Appendix – Technical reports of participating laboratories

The Technical Reports of the participants are included in the sections below.

During the Pre-Draft-A Process 3: Review of Relative Data the following corrections to data were made.

- the spectral responsivity of DGT3 by GUM at 1550 nm was updated due to a typo in the submitted data file: change 0.8307 to 0.9307.
- A typo in the NPL uncertainty budget on detector bandwidth was corrected.
- Typo in CMI Technical report corrected (wording ‘’enhanced uncertainty” replaced by “expanded uncertainty”).

The following corrections have been made to the Technical Reports of the participants as a response to the Draft A1 version of the EURAMET.PR-K2.a report. These changes have been included in Draft A2.

- CMI provided an update of the description of their measurement facility and included explanatory text to the breakdown of their measurement uncertainty.
- A typo was corrected in the date of the CMI measurement results for DGT12 and DGT3 and the Technical Report (4 JAN 2011 was replaced by 4 JAN 2012).
- JV provided an updated version of their report with improved typographic readability of the equations.

A.1 CMI (Czech Republic)

Technical (Measurement) report

Description of the measurement facility and method (Including measurement facility schematic):

Type of primary standard:

CMI primary standard is an absolute cryogenic radiometer, mechanically cooled, laser based. Kr-Ion laser is used as an optical radiation source, delivering set of eight UV, Visible and NIR lines. The system includes an external power stabilizer (for performance parameters see uncertainty budget attached).

Laboratory transfer standards used: Set of or hemispherical pyro electric detectors with golden black covered LiNb crystal are used as a reference standard for relative spectral responsivity in the spectral range from 900 nm to 1670 nm. (For performance parameters see uncertainty budget attached).

Set of three silicon trap detector CMI 1, CMI 2, CMI 3, consisting three 10 mm x 10 mm Hamamatsu S1337 photodiodes arranged in a light trapping configuration, electrically connected in parallel, and terminated by a standard BNC connector acts as an absolute transfer standard. While providing the periodical re-calibration of transfer standard Si-Trap detectors on CMI absolute cryogenic radiometer, usually in the period of 2 years. Typical degradation drift of our Si-Traps between two calibrations is 0,04% . For three stated laser lines the shift appears to be at approximately same level.

Monochromator used:

McPHERSON 2035D double grating monochromator, subtractive setup. Detailed description and schematic diagram of the measuring facility see below.

Laboratory primary reference detector used

Temperature stabilised single-element InGaAs detector CMI-SRNIR-03 consisting in GPD Optoelectronics GAP 5000 window less photodiode chip with an active area of diameter 5 mm mounted in the front of a cylindrical housing.

Laboratory primary reference InGaAs detector CMI-SRNIR-03 is calibrated for its relative spectral responsivity with hemispherical pyro electric detectors with golden black covered crystal, the absolute calibration is provided with the set of three silicon trap detectors CMI 1, CMI 2, CMI 3.

Detailed description and schematic diagram of the measuring facility

The measurements were performed using the CMI reference monochromator based facility developed in CMI (see fig.1)

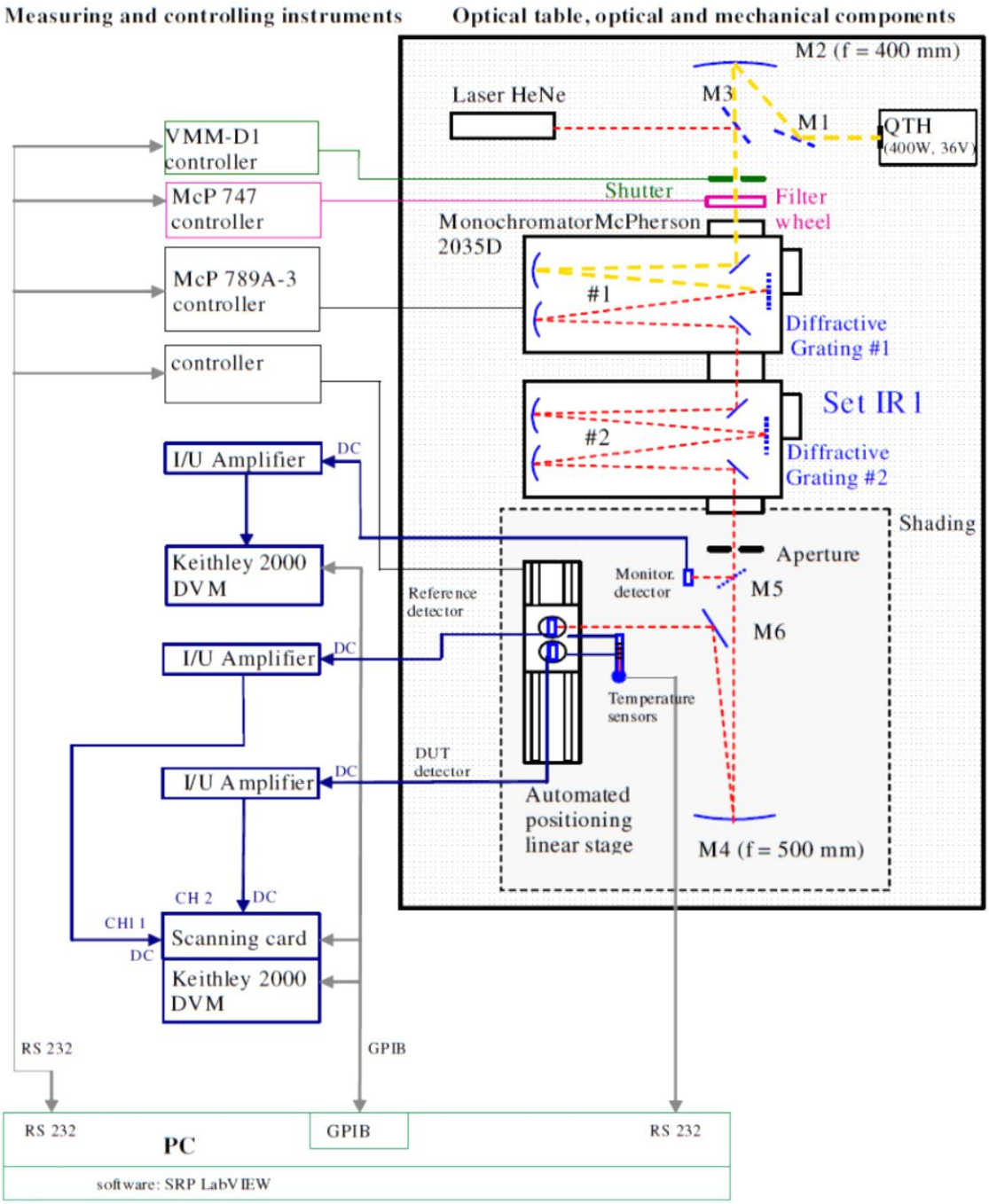

fig.1: Schematic drawing of the CMI reference monochromator based facility. M2, M4 – concave spherical mirrors; M1, M3, M5, M6 – moveable plane mirrors; Filter wheel – order sorting filters; *HeNe laser used for aligning optical system.*

CMI monochromator based reference facility for spectral responsivity measurement in spectral region 900 nm to 1670 nm uses double grating monochromator McPHERSON 2035D with subtractive dispersion, focal length 350 mm. One couple of ruled gratings 600 G/mm blazed at 1280 nm is used for dispersing the beam in this spectral range.

The Quartz Tungsten Halogen (QTH) lamp 400 W is used for illuminating the entrance slit.

The filter-wheel with a set of order sorting filters is used for suppressing higher diffraction orders at the entrance slit of the monochromator. The optical shutter is applied at the entrance slit side of the monochromator facility.

The motorized linear stage is used for both reference and DUT detectors positioning. All measurement is fully automated.

Parameters used at the CMI laboratory

The spectral bandwidth of 5 nm FWHM was used throughout this comparison.

The reflective optics of f/# at about f/8 was used after the double monochromator's exit slit.

A 4 mm diameter circular spot was imaged into the geometrical centre of input aperture of the calibrated Ge detectors. The reference plane was set at the 6 mm Ge aperture front plane normal to the beam axis.

The Monitor detector was used to compensate for time fluctuations of radiant flux of measuring quasi-monochromatic beam.

Breakdown of uncertainty:

Measurement repeatability evaluation in this CMI uncertainty breakdown represents the values of measurements involving the realignment of whole calibration system including removing and re-adjusting the detectors. It is evaluated for each step of standard detectors realisation.

The 'Pyro stability' uncertainty contribution below in the spreadsheet represents an estimation of the drift of the PYRO (+its electronic) response in a short-term period between its two independent absolute calibrations.

The internal stray-light of our double monochromator system was measured by the 'NPL cut-off filter method' and reached the value approximately 5E-5 relatively. Then the uncertainty evaluates the modelled difference between the right value measured theoretically with completely pure beam and modelled result raising from including spectrally uniform stray-light of the measured level.

The CMI InGaAs drift value was evaluated with respect to the time period of roughly one month from the last CMI INGaAs3 detector calibration. For simplicity the 'worst case envelop value' was chosen for the whole spectral range.

Primary reference Laser based CR							
Source of uncertainty	**Spectral range [nm]**	**Type**	**Value [%]**	**Distribution**	**Divider (coefficient)**	**Ci**	**Ui [%]**
Window transmittance	λ = 799.3 λ = 647.1 λ = 568.1	A	0.005	standard	1	1	0.0050
Scattered and diffracted light		B	10	standard	2	0.0001	0.0005
Cavity absorptance		B	0.001	rectangular	1.732	1	0.0006
Electrical power measurements		B	0.002	standard	2	1	0.0010
Radiometer sensitivity		B	0.001	rectangular	1.732	1	0.0006
Changes in scatter and thermal radiation		B	0.001	rectangular	1.732	1	0.0006
Measurement repeatability		A	0.001509	standard	1	1	0.0015
uncertainty							**0.0054**

Transfer standards (Si-Traps)							
Source of uncertainty	**Spectral range [nm]**	**Type**	**Value [%]**	**Distribution**	**Divider (coefficient)**	**Ci**	**Ui [%]**
Optical power measurement (Primary reference Laser based CR)		B	0.0054	standard	1	1	0.0054
Calibration of DVM for detectors	λ = 799.3 λ = 647.1 λ = 568.1	B	0.0005	rectangular	1.732	1	0.0003
drift DVM for detectors		B	0.0005	rectangular	1.732	1	0.0003
I/U transducer calibration		B	0.01	rectangular	1.732	1	0.0058
Drift of I/U transducer		B	0.001	rectangular	1.732	1	0.0006
Spot diameter influence		B	0.005	rectangular	1.732	1	0.0029
Laser stability		B	0.005	rectangular	1.732	1	0.0029
Alignment repeatability		B	0.005	standard	2	1	0.0025
Transfer standards temporal stab.		B	0.04	rectangular	1.732	1	0.0231
Measurement repeatability		A	0.000566	standard	1	1	0.0006
Combined standard uncertainty k = 1							**0.0249**

Relative calibration of CMI reference detector InGaAs3 at monochromator based facility (Standard =Spectrally flat detector PYRO)							
Source of uncertainty	**Spectral range [nm]**	**Type**	**Value [%]**	**Distribution**	**Divider (coefficient)**	**Ci**	**Ui [%]**
PYRO residual wavelength dependence	$900 \le \lambda \le 1650$	B	0.1	rectangular	1.732	1	0.06
PYRO uniformity	$900 \le \lambda \le 1650$	B	0.02	rectangular	1.732	1	0.01
PYRO stability	$900 \le \lambda \le 1650$	B	0.02	rectangular	1.732	1	0.01
Measurement repeatability (Standard deviation of the mean STDEM of PYRO signal)	$900 \le \lambda < 960$	A	0.14	standard	1	1	0.14
	$960 \le \lambda \le 1630$		0.07				0.07
			[nm]			[%.nm^{-1}]	[%]
Wavelength calibration	**$\lambda = 1307.5$**	B	0.05	rectangular	1.732	0.17	0.005
	$\lambda = 900$		0.30			0.76	0.13
	$\lambda = 950$		0.30			0.41	0.07
	$960 \le \lambda \le 1630$		0.30			0.30	0.05
			[°C]			[%.°C^{-1}]	[%]
Teperature dependence of InGaAs	$\lambda = 900$		0.2	rectangular	1.732	0.13	0.02
	$\lambda = 950$		0.2			0.11	0.01
	$960 \le \lambda \le 1630$		0.2			0.1	0.01
Bandwidth effects	$900 \le \lambda < 960$		0.6		1.732	1	0.35
	$960 \le \lambda \le 1630$		0.1				0.06
			positioning [mm]			[%.mm^{-1}]	[%]
Uniformity of InGaAs	$900 \le \lambda < 960$	B	0.25	rectangular	1.732	0.70	0.10
	$960 \le \lambda \le 1630$		0.25			0.42	0.06
Lock in amplifier linearity	$900 \le \lambda \le 1650$	B	0.17	rectangular	1.732	1	0.10
Voltmeter linearity	$900 \le \lambda \le 1650$	B	0.01	rectangular	1.732	1	0.01
Amplifier linearity	$900 \le \lambda \le 1650$	B	0.02	rectangular	1.732	1	0.01
Combined standard uncertainty k = 1	**$\lambda = 1307.5$**			**standard**			**0.16**
	$\lambda = 900$						**0.43**
	$\lambda = 950$						**0.41**
	$960 \le \lambda \le 1630$						**0.17**

Absolute Calibration of CMI reference detector InGaAs3 at monochromator based facility							
Source of uncertainty	**Spectral range [nm]**	**Type**	**Value [%]**	**Distribution**	**Divider (coefficient)**	**Ci**	**Ui [%]**
Relative calibration of CMI reference detector with PYRO	**λ = 1307.5** λ = 900 λ = 950 960 ≤ λ ≤ 1630	B	0.16 0.43 0.41 0.17	standard	1	1	0.16 0.43 0.41 0.17
Transfer standards (Si-detector)	λ = 653.75	B	0.10	standard	2	1	0.050
Transfer Si standards Drift	λ = 653.75	B	0.05	rectangular	1.732	1	0.029
Uniformity Si	λ = 653.75	B	0.1	rectangular	1.732	1	0.058
Linearity Si	λ = 653.75	B	0.01	rectangular	1.732	1	0.006
Polarization dependence Si	λ = 653.75	B	0.0001	rectangular	1.732	1	0.0001
Temperature dependence of Si	λ = 653.75	B	0.0005	rectangular	1.732	1	0.0003
PYRO residual wavelength dependence	900 ≤ λ ≤ 1650	B	0.1	rectangular	1.732	1	0.058
Bandwidth effects	λ = 653.75, λ = 1307.5	B	0.05	rectangular	1.732	1	0.029
Voltmeter linearity	900 ≤ λ ≤ 1650	B	0.005	rectangular	1.732	1	0.003
I/U transducer dut detector	900 ≤ λ ≤ 1650	B	0.01	standard	2	1	0.005
I/U transducer standard detector	900 ≤ λ ≤ 1650	B	0.01	standard	2	1	0.005
Stray light	900 ≤ λ ≤ 1650	B	0.026	rectangular	1.732	1	0.015
Measurement repeatability	λ = 653.75, λ = 1307.5	A	0.037	standard	1	1	0.037
Combined standard uncertainty k = 1	λ = 900 λ = 950 960 ≤ λ ≤ 1630			standard			0.44 0.43 0.20
Expanded uncertainty k = 2	λ = 900 λ = 950 960 ≤ λ ≤ 1630			**standard**			**0.88** **0.85** **0.40**

Calibration of EURAMET KC K2.a comparison transfer Ge detectors							
Source of uncertainty	**Spectral range [nm]**	**Type**	**Value**	**Distribution**	**Divider (coefficient)**	**Ci**	**Ui [%]**
CMI Reference detector	λ = 900 λ = 950 960 ≤ λ ≤ 1630	B	0.44 0.43 0.20	standard	1	1	0.44 0.43 0.20
			[°C]			[%.°C^{-1}]	[%]
Temperature dependence of Ge *)	900 ≤ λ ≤ 1550 λ = 1600	B	0.2 0.2	rectangular	1.732	0.15 0.95	0.02 0.11
Bandwidth effects	900 ≤ λ < 960 960 ≤ λ < 1550 1550 ≤ λ < 1630		0.4 0.1 0.1	rectangular	1.732	1	0.23 0.06 0.06
CMI InGaAs drift	900 ≤ λ ≤ 1650	B	0.05	rectangular	1.732	1	0.029
Voltmeter linearity	900 ≤ λ ≤ 1650	B	0.005	rectangular	1.732	1	0.003
I/U transducer dut detector	900 ≤ λ ≤ 1650	B	0.01	standard	2	1	0.005
I/U transducer standard detector	900 ≤ λ ≤ 1650	B	0.01	standard	2	1	0.005
Stray light	900 ≤ λ ≤ 1650	B	0.002	rectangular	1.732	1	0.001
			positioning [mm]			[%.mm^{-1}]	[%]
Uniformity of Ge *)	900 ≤ λ < 1000 1000 ≤ λ < 1550 1550 ≤ λ ≤ 1650	B	0.25 0.25 0.25	rectangular	1.732	0.5 0.5 0.5	0.07 0.07 0.07
Measurement repeatability	900 ≤ λ ≤ 1550 λ = 1600	A	0.03 0.03	standard	1	1	0.03 0.03
			[nm]			[%.nm-1]	[%]
Wavelength calibration	900 ≤ λ ≤ 1550 λ = 1600	B	0.30 0.30	rectangular	1.732	0.30 0.95	0.05 0.16
Combined standard uncertainty k = 1	λ = 900 λ = 950 960 ≤ λ ≤ 1550 λ = 1600			standard			0.51 0.49 0.23 0.30
Expanded uncertainty k = 2	λ = 900 λ = 950 960 ≤ λ ≤ 1550 λ = 1600			**standard**			**1.01** **0.99** **0.47** **0.60**

*Data extimated according CMI Ge working standard detector

Description of calibration laboratory conditions: e.g. temperature, humidity etc

All measurements were made in air conditioned dust free laboratory. The room temperature was maintained at (22,9 ± 0,5) °C during the calibration, relative humidity air (40 ± 10)%. The reference detector was temperature stabilised to keep its temperature within 22,9 °C ± 0,2 °C. The real temperature of detectors was monitored.

Measurement results:

Type of Standard Ge **Reference number** DGT1

Wavelength / **nm**	Spectral Responsivity **A/W**	STD **A/W**	Num of measurements /**n**	Temperature /**Ohm**	Combined standard uncertainty (k=1) /%
900	0.4438	0.00022	10	108.960	0.51
950	0.4972	0.00023	10	108.959	0.49
1000	0.5450	0.00005	10	108.953	0.23
1050	0.5891	0.00005	10	108.956	0.23
1100	0.6256	0.00014	10	108.955	0.23
1150	0.6612	0.00003	10	108.953	0.23
1200	0.6924	0.00003	10	108.951	0.23
1250	0.7225	0.00004	10	108.949	0.23
1300	0.7539	0.00005	10	108.954	0.23
1350	0.7867	0.00011	10	108.952	0.23
1400	0.8189	0.00007	10	108.955	0.23
1450	0.8527	0.00008	10	108.954	0.23
1500	0.8853	0.00012	10	108.957	0.23
1550	0.9066	0.00007	10	108.954	0.23
1600	0.6789	0.00011	10	108.961	0.30

Laboratory: Czech metrology institute

Date: **4 JAN 2012** **Signature**

Marek Smid
Head of Radiometry and Photometry department

Measurement results:

Type of Standard Ge **Reference number** DGT12

Wavelength **/ nm**	Spectral Responsivity **A/W**	STD **A/W**	Num of measurements **/n**	Temperature **/Ohm**	Combined standard uncertainty (k=1) **/%**
900	0.4218	0.00043	10	109.009	0.51
950	0.4813	0.00026	10	109.013	0.49
1000	0.5334	0.00011	10	109.009	0.23
1050	0.5802	0.00009	10	109.011	0.23
1100	0.6200	0.00004	10	109.006	0.23
1150	0.6616	0.00006	10	109.005	0.23
1200	0.7006	0.00005	10	109.006	0.23
1250	0.7383	0.00004	10	109.007	0.23
1300	0.7757	0.00002	10	109.007	0.23
1350	0.8115	0.00011	10	109.005	0.23
1400	0.8419	0.00013	10	109.007	0.23
1450	0.8734	0.00005	10	109.006	0.23
1500	0.9009	0.00010	10	109.006	0.23
1550	0.9178	0.00007	10	109.004	0.23
1600	0.6916	0.00015	10	109.009	0.30

Laboratory: Czech metrology institute

Date: 4 JAN 2012 **Signature**

Marek Smid
Head of Radiometry and Photometry department

Type of Standard Ge **Reference number** DGT3

Wavelength **/ nm**	Spectral Responsivity **A/W**	STD **A/W**	Num of measurements **/n**	Temperature **/Ohm**	Combined standard uncertainty (k=1) **/%**
900	0.4209	0.00015	10	108.951	0.51
950	0.4787	0.00007	10	108.955	0.49
1000	0.5318	0.00008	10	108.949	0.23
1050	0.5821	0.00008	10	108.952	0.23
1100	0.6242	0.00007	10	108.952	0.23
1150	0.6649	0.00005	10	108.949	0.23
1200	0.6996	0.00005	10	108.949	0.23
1250	0.7320	0.00008	10	108.947	0.23
1300	0.7650	0.00008	10	108.951	0.23
1350	0.7990	0.00007	10	108.950	0.23
1400	0.8307	0.00009	10	108.948	0.23
1450	0.8666	0.00017	10	108.946	0.23
1500	0.9007	0.00009	10	108.950	0.23
1550	0.9235	0.00011	10	108.948	0.23
1600	0.6860	0.00018	10	108.951	0.30

Laboratory: Czech metrology institute

Date: 4 JAN 2012 **Signature**

Marek Smid
Head of Radiometry and Photometry department

Laboratory: CMI Prague, CZ

Date: 4 January 2012 Signature:

Marek Smid

Head of Radiometry and Photometry department

End of protocol

A.2 GUM (Poland)

Technical (Measurement) report

Description of the measurement facility and method (Including measurement facility schematic):

The direct comparative method is used, in which monochrome radiation with the wavelength λ is directed first to the reference receiver and then to the receiver being tested. This method is in accordance with CIE 202: 2011 Spectral responsiveness measurement of detectors, radiometers and photometers.

The measuring stand for calibration of spectral sensitivity standards in the spectral range (900 - 1600 nm) includes: monochromator with Spectra Pro-500 Czerny-Turner holographic grid manufactured by Acton Research Corporation with ARC Spectra Drive; Mirror illumination with 600W quartz-halogen lamp, 120V; Tronic Elektronic DC power supply; LMT photocurrent meter; reference receiver - germanium photodiodes.

Type of primary standard:

Photodiode germanium UDT type 260.

Laboratory transfer standards used if any:

-

Monochromator used:

Monochromator Spectra Pro-500 Czerny-Turner Acton Research Corporation, serial number 500147S with a holographic grid, serial number 12-120-H

Primary reference or traceability route of primary reference and breakdown of uncertainty:

Photodiode was calibrated in PTB in December 2010.

Description of calibration laboratory conditions: e.g. temperature, humidity etc

Ambient temperature (23 ± 1)° C.

Measurement results (the same as form 8.1 of the protocol):

Wavelength [nm]	Uncertainty of reference standard [%]	Repeatability [%]	Wavelength calibration [%]	Short term instability of source [%]	Stray light [%]	Bandwidth effects [%]	Standard deviation of series [%]	Combined standard uncertainty (relative) [%]
900	0,3407	0,2779	0,0286	0,01	0,01	0,02	0,1275	0,46
950	0,3173	0,1782	0,0020	0,01	0,01	0,02	0,0932	0,38
1000	0,1459	0,1468	0,0156	0,01	0,01	0,02	0,1478	0,26
1050	0,1597	0,2739	0,0131	0,01	0,01	0,02	0,2300	0,39
1100	0,1545	0,1353	0,0113	0,01	0,01	0,02	0,2033	0,29
1150	0,1578	0,1490	0,0094	0,01	0,01	0,02	0,2317	0,32
1200	0,1694	0,1736	0,0088	0,01	0,01	0,02	0,2392	0,34
1250	0,1534	0,1297	0,0085	0,01	0,01	0,02	0,2498	0,32
1300	0,1927	0,1537	0,0085	0,01	0,01	0,02	0,2079	0,32
1350	0,1527	0,1404	0,0083	0,01	0,01	0,02	0,2035	0,29
1400	0,1539	0,1183	0,0085	0,01	0,01	0,02	0,2159	0,29
1450	0,1527	0,1497	0,0077	0,01	0,01	0,02	0,2248	0,31
1500	0,1516	0,1351	0,0052	0,01	0,01	0,02	0,2312	0,31
1550	0,2942	0,1276	0,0473	0,01	0,01	0,02	0,1607	0,36
1600	0,4628	0,1554	0,0473	0,01	0,01	0,02	0,1002	0,50

Where:

Uncertainty of reference standard: Uncertainty in the certificate reference calibration photodiode divided by 2. The thus obtained value was then referenced to the sensitivity of the photodiode for a given wavelength and multiplied by 100%.

Repeatability: Calculation of the standard deviation (For 12 or 13 measurement of spectral sensitivity for a given wavelength) relative to the spectral sensitivity obtained for the reference photodiode, multiplied by 100%.

Wavelength calibration: Example: With the selected wavelength of 900 nm and 950 nm was measured spectral sensitivity. Reproducibility reading wavelength, measured in the calibration certificate monochromator, ± better than ± 0.1 nm.

Short term instability of source: On the basis of the lamp manufacturer, and its experience in using this type of light source estimated the effect of the source of instability at 0.01%.

Stray light: Based on knowledge of the characteristics of the monochromator estimated share of stray light at 0.01%.

Bandwidth effects: The effect of bandwidth on was estimated 0,02 %.

Measurement results

Type of Standard Ge detector **Reference Number DGT 1**

Wavelength nm	Spectral Responsivity A / W	Relative Std Dev. A/W	Num of measurements	Temperature /·10^3 Ohm	Uncertainty / %
900	0,4369	0,001214	12	109,34	0,46
950	0,4993	0,000890	12	109,26	0,38
1000	0,5483	0,000805	12	109,30	0,26
1050	0,5911	0,001619	12	109,28	0,39
1100	0,6297	0,000852	12	109,27	0,29
1150	0,6653	0,000991	12	109,27	0,32
1200	0,6965	0,001209	12	109,24	0,34
1250	0,7270	0,000943	12	109,26	0,32
1300	0,7579	0,001165	12	109,26	0,32
1350	0,7901	0,001109	12	109,26	0,29
1400	0,8228	0,000973	12	109,23	0,29
1450	0,8577	0,001284	12	109,23	0,31
1500	0,8906	0,001203	12	109,26	0,31
1550	0,9138	0,001166	12	109,30	0,36
1600	0,6976	0,001084	12	109,26	0,50

Laboratory: Photometry and Radiometry Laboratory, Central Office of Measures.....

Date: 28-07-2014..... Signature: .....

Measurement results

Type of Standard Ge detector **Reference Number DGT 3**

Wavelength nm	Spectral Responsivity A / W	Relative Std Dev. A/W	Num of measurements	Temperature /·10^3 Ohm	Uncertainty / %
900	0,4196	0,001636	13	109,30	0,50
950	0,4851	0,001969	13	109,33	0,49
1000	0,5391	0,001150	13	109,27	0,32
1050	0,5882	0,001101	13	109,26	0,34
1100	0,6321	0,001444	13	109,25	0,35
1150	0,6729	0,001943	13	109,30	0,40
1200	0,7082	0,002089	13	109,28	0,44
1250	0,7404	0,002018	13	109,26	0,39
1300	0,7731	0,002309	13	109,30	0,40
1350	0,8068	0,002513	13	109,23	0,40
1400	0,8394	0,002757	13	109,26	0,43
1450	0,8751	0,002545	13	109,26	0,39
1500	0,9089	0,002431	13	109,26	0,39
1550	0,9307	0,001481	13	109,27	0,38
1600	0,7003	0,001776	13	109,26	0,56

Laboratory: Photometry and Radiometry Laboratory, Central Office of Measures

Date: 28-07-2014..... Signature: Szojna

Measurement results

Type of Standard Ge detector **Reference Number DGT 12**

Wavelength nm	Spectral Responsivity A / W	Relative Std Dev. A/W	Num of measurements	Temperature /·10³ Ohm	Uncertainty / %
900	0,4139	0,001058	12	109,40	0,41
950	0,4844	0,000918	12	109,40	0,40
1000	0,5379	0,000454	12	109,38	0,23
1050	0,5834	0,000960	12	109,37	0,33
1100	0,6256	0,000624	12	109,35	0,28
1150	0,6666	0,001060	12	109,37	0,32
1200	0,7059	0,000979	12	109,36	0,32
1250	0,7434	0,000838	12	109,32	0,30
1300	0,7803	0,001061	12	109,34	0,31
1350	0,8160	0,001047	12	109,35	0,28
1400	0,8469	0,001093	12	109,33	0,30
1450	0,8780	0,001464	12	109,32	0,31
1500	0,9056	0,001748	12	109,32	0,33
1550	0,9231	0,001772	12	109,31	0,39
1600	0,7083	0,001784	12	109,30	0,54

Laboratory: Photometry and Radiometry Laboratory, Central Office of Measures...

Date: 28-07-2014..... Signature: Szejma.....

A.3 JV (Norway)

Description of the measurement facility and method

The Germanium detectors were calibrated against JVs transfer standards in the spectral response setup. This setup consists of a tungsten lamp, a double-grating monochromator, shutter and order-sorting filters, imaging optics, a detector translation stage and readout electronics. The output optics and detector stage is enclosed in a light tight box. The monochromator output slit used in the measurements was 1 mm, giving a spectral width of 3 nm FWHM. The signals from the two detectors were amplified and read by a digital voltmeter. The whole system is computer controlled and fully automated.

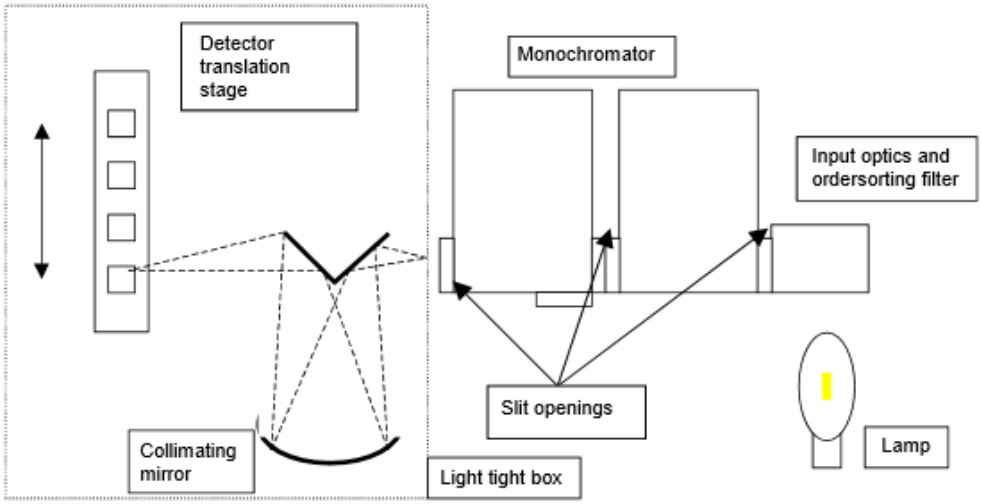

Figure 1. Spectral response set-up.

Square spot of 2 mm imaged on single Germanium detectors.
F/#: f/6

Type of primary standard:

Si trap detector (RA-SPR-37)

Laboratory transfer standards used if any:

InGaAs detectors (RA-SPR-32, RA-SPR-33)

Monochromator used:

McPherson Inc 2035, 0.35 Meter Scanning Monochromator

Primary reference or traceability route of primary reference and breakdown of uncertainty:

Primary standard:
At Justervesenet an independent spectral response scale is realised with the hybrid self-calibration method (Gran, 2005) [1]. The method is based on a physical model of silicon photodiodes. Parameters in the model of the silicon trap detector are estimated to find the responsivity of the detector over the spectral range from 400 – 1100 nm. The uncertainty in the responsivity values are shown in Fig. 2. We call the responsivity values and their associated uncertainty

$$R(Trap) \pm u_{Trap} \quad (1)$$

Transfer standard:
The transfer standards used in the measurements was two of our InGaAs detectors. They were calibrated relative against our spectrally invariant cavity pyroelectric detector (CPD) over the spectral range from 800 – 1700 nm with 25 nm spacing. This detector has an active element with a platinum black coating inside an aluminium reflective hemisphere. The CPD needs a preamplifier, a chopper and a lock-in amplifier to give a dc-equivalent signal. The relative InGaAs response is calculated as

$$V_{rel}(IG) = \frac{V(IG)}{V(pyro)}, \tag{2}$$

with an associated uncertainty given as the standard deviation in the relative measurement as

$$u_{rel}(IG) = \sigma(V_{rel}(IG)). \tag{3}$$

The absolute calibration of the InGaAs detectors was against a silicon trap detector in the spectrally overlapping range from 800 to 1100 nm.

$$R(IG) = \frac{V(IG)}{V(Trap)} \cdot R(Trap) \tag{4}$$

with the uncertainty from 800 to 1100 nm calculated as

$$u_R(IG) = \frac{V(IG)}{V(Trap)} \cdot u_{Trap} + R(Trap) \cdot \sigma\left(\frac{V(IG)}{V(Trap)}\right) \tag{5}$$

In order to make the relative measurement in (2) absolute, a scaling constant is multiplied to the relative measurement as

$$R(IG)_i = V_{rel}(IG)_i \cdot K, \tag{6}$$

with uncertainty calculated as

$$u_R(IG) = \frac{\partial R}{\partial V_{rel}} \cdot u_{rel}(IG) + \frac{\partial R}{\partial K} \cdot u_K = K \cdot u_{rel}(IG) + V_{rel} \cdot u_K \tag{7}$$

The scaling constant K is calculated from the spectral range from 800 to 1100 nm where we have absolute responsivity values of the InGaAs from its calibration to the trap detector in (4) as

$$K = \frac{1}{n}\sum_i K_i = \frac{1}{5}\sum_{i=900}^{1000} \frac{R(IG)_i}{V_{rel}(IG)_i}, \tag{8}$$

with the observed standard deviation of K_i values as the uncertainty in the scaling constant. Because eq (3) is large at wavelengths below 900 nm and (5) is large for wavelengths above 1000 nm we only used values between 900 and 1000 nm in the estimation of K and its uncertainty. The responsivity values by direct calibration to a trap detector (4) were used up to 975 nm and the responsivity calculation by (6) was used from 1000 nm because these calculations gave the lowest uncertainty in the responsivity values.

Germanium detectors:
Eq. (7) is our type A uncertainty in the estimation of the InGaAs transfer standard uncertainty. Then Type B components were added afterwards. The total uncertainty was used in the estimation of the Ge detectors uncertainty. The values are calculated as

$$R(Ge) = \frac{V_{Ge}}{V_{IG}} \cdot R(IG), \tag{9}$$

with the Type A uncertainty calculated as

$$u_R(Ge) = \frac{V_{Ge}}{V_{IG}} \cdot u_R(IG)_{total} + R(IG) \cdot \sigma\left(\frac{V_{Ge}}{V_{IG}}\right). \tag{10}$$

The Germanium detectors were calibrated against the InGaAs transfer standard detectors in two independent series. The first series is measured with 8 repetitions at each wavelength, and the second series with 4 repetitions at each wavelength. All measurements were used in the estimation of the Ge detector's responsivity.

Uncertainty budget:

The primary standard combined relative uncertainty is shown in figure 2.

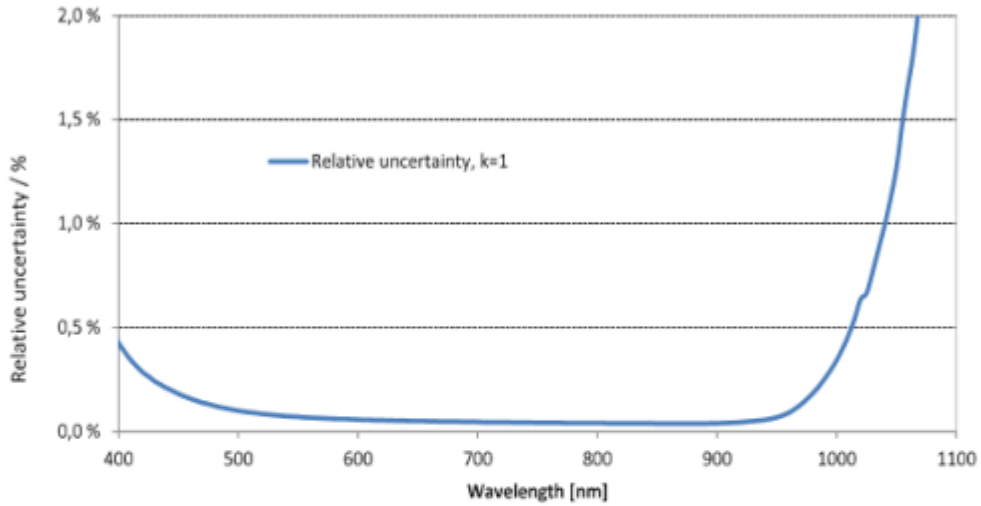

Figure 2. Trap 22 (RA-SPR-37) *relative uncertainty as a function of wavelength.*

InGaAs transfer standard:

The spectrally dependent InGaAs transfer standard uncertainty is shown in Table 1a for InGaAs 12 (RA-SPR-32) and 1b for InGaAs 13 (RA-SPR-33). In addition to the Type A uncertainty calculation given in eqs. (2) - (8), the following components were used:

Pyroelectric detector, non-black	0.06%
Straylight	0.03%
InGaAs nonuniformity	0.1%
Electrical calibration	0.02%
Bandwidth	neglectable

Table 1a. InGaAs 12 uncertainty budget

Wavelength	Response	Uncertainty component [%]				Total uncertainty
[nm]	[A/W]	Type A	Temperature	Wavlength	Total Type B	[%]
900	0,3626	0,22	0,10	0,30	0,33	0,39
950	0,6496	0,24	0,10	0,09	0,17	0,29
1000	0,7700	0,38	0,05	0,02	0,13	0,40
1050	0,7977	0,37	0,05	0,03	0,13	0,39
1100	0,8642	0,35	0,05	0,03	0,14	0,38
1150	0,9165	0,37	0,05	0,01	0,13	0,39
1200	0,9477	0,37	0,05	0,02	0,13	0,39
1250	0,9959	0,36	0,05	0,02	0,13	0,38
1300	1,0305	0,36	0,05	0,01	0,13	0,38
1350	1,0486	0,36	0,05	0,01	0,13	0,38
1400	1,0782	0,37	0,05	0,02	0,13	0,39
1450	1,1209	0,37	0,05	0,01	0,13	0,39
1500	1,1520	0,37	0,05	0,00	0,13	0,39
1550	1,1533	0,38	0,05	0,00	0,13	0,40
1600	1,1338	0,37	0,05	-0,02	0,13	0,39

Table 1b. InGaAs 13 uncertainty budget

Wavelength	Response	Uncertainty component [%]				Total uncertainty
[nm]	[A/W]	Type A	Temperature	Wavlength	Total Type B	[%]
900	0,3520	0,07	0,10	0,35	0,38	0,38
950	0,6556	0,11	0,10	0,05	0,16	0,19
1000	0,7589	0,22	0,05	0,04	0,14	0,26
1050	0,8032	0,19	0,05	0,01	0,13	0,24
1100	0,8516	0,19	0,05	0,04	0,14	0,24
1150	0,9172	0,18	0,05	0,01	0,13	0,22
1200	0,9470	0,18	0,05	0,02	0,13	0,23
1250	0,9900	0,19	0,05	0,02	0,13	0,23
1300	1,0327	0,18	0,05	0,01	0,13	0,22
1350	1,0513	0,19	0,05	0,01	0,13	0,23
1400	1,0728	0,19	0,05	0,01	0,13	0,23
1450	1,1118	0,19	0,05	0,02	0,13	0,23
1500	1,1526	0,20	0,05	0,01	0,13	0,24
1550	1,1684	0,19	0,05	-0,01	0,13	0,23
1600	1,1429	0,19	0,05	-0,01	0,13	0,23

The uncertainties in the estimate of the responsivity of Germanium detectors are derived from Table 1a and 1b. Ge 9 is calibrated against InGaAs 13 and Ge 10 and Ge 11 are calibrated against InGaAs 12. Each of the Germanium detectors was calibrated twice against the same InGaAs detector after realignment of the detectors. The difference in responsivity between the two series was included as an uncertainty component for the reproducibility. Otherwise, the same components as for our transfer standards were used except for a stray-light component of 0.05%. The numerical values of the wavelength components are different due to the difference in spectral shape, but the same 0.2 nm uncertainty in the wavelength is used.

Description of calibration laboratory conditions: e.g. temperature, humidity etc

The laboratory has climate controlled temperature and humidity.
Temperature in laboratory: 22.2 °C ± 0.2 °C
Humidity: 44 % ± 3.0 % RH

References:

[1] Gran, J.: "Accurate and independent spectral response scale based on silicon trap detectors and spectrally invariant detectors", Oslo (2005), ISSN 1501-7710 No. 434.

Measurement results:

Type of Standard: Germanium detector

Reference Number: DGT9

Wavelength	Spectral Responsivity	STD	Num of measurements	Temperature	Combined standard uncertainty (k=1)
/ nm	A / W	A / W	/n	/ Ohm	/ %
900	0,4309	0,00102	2	108,972	0,46
950	0,4883	0,00017	2	108,971	0,26
1000	0,5381	0,00124	2	108,971	0,34
1050	0,5829	0,00066	2	108,970	0,30
1100	0,6212	0,00114	2	108,970	0,31
1150	0,6606	0,00074	2	108,970	0,28
1200	0,6986	0,00069	2	108,970	0,29
1250	0,7339	0,00079	2	108,970	0,28
1300	0,7701	0,00051	2	108,970	0,28
1350	0,8039	0,00066	2	108,970	0,29
1400	0,8331	0,00045	2	108,971	0,28
1450	0,8634	0,00078	2	108,971	0,28
1500	0,8899	0,00042	2	108,972	0,29
1550	0,9049	0,00050	2	108,972	0,30
1600	0,6658	0,00251	2	108,973	0,42

Laboratory: Justervesenet (JV)

Date: 17.02.12

Type of Standard: Germanium detector

Reference Number: DGT10

Wavelength	Spectral Responsivity	STD	Num of measurements	Temperature	Combined standard uncertainty (k=1)
/ nm	A / W	A / W	/n	/ Ohm	/ %
900	0,3839	0,00210	2	108,980	0,59
950	0,4441	0,00062	2	108,982	0,36
1000	0,5001	0,00024	2	108,984	0,43
1050	0,5524	0,00002	2	108,986	0,42
1100	0,5974	0,00107	2	108,988	0,42
1150	0,6455	0,00033	2	108,989	0,42
1200	0,6894	0,00003	2	108,991	0,43
1250	0,7303	0,00054	2	108,992	0,42
1300	0,7715	0,00006	2	108,993	0,42
1350	0,8098	0,00013	2	108,995	0,42
1400	0,8410	0,00101	2	108,996	0,44
1450	0,8745	0,00083	2	108,998	0,43
1500	0,9058	0,00030	2	108,999	0,43
1550	0,9231	0,00130	2	109,000	0,46
1600	0,6792	0,00062	2	109,001	0,47

Laboratory: Justervesenet (JV)

Date: 17.02.12

Type of Standard: Germanium detector

Reference Number: DGT11

Wavelength	Spectral Responsivity	STD	Num of measurements	Temperature	Combined standard uncertainty (k=1)
/ nm	A / W	A / W	/n	/ Ohm	/ %
900	0,3955	0,00245	2	109,087	0,63
950	0,4505	0,00242	2	109,088	0,50
1000	0,5004	0,00175	2	109,089	0,50
1050	0,5463	0,00141	2	109,090	0,46
1100	0,5848	0,00293	2	109,091	0,54
1150	0,6263	0,00138	2	109,092	0,45
1200	0,6646	0,00182	2	109,092	0,47
1250	0,7000	0,00185	2	109,093	0,45
1300	0,7375	0,00128	2	109,094	0,44
1350	0,7740	0,00150	2	109,094	0,44
1400	0,8064	0,00202	2	109,095	0,46
1450	0,8413	0,00206	2	109,095	0,46
1500	0,8738	0,00042	2	109,096	0,43
1550	0,8976	0,00038	2	109,096	0,45
1600	0,6717	0,00011	2	109,097	0,48

Laboratory: Justervesenet (JV)

Date: 17.02.12

A.4 NPL (United Kingdom)

1. DESCRIPTION OF THE MEASUREMENT FACILITY AND METHOD

1.1 MEASUREMENT FACILITY

The measurement facility used to measure the spectral responsivity of the EURAMET.PR-K2.a detectors is shown in Figure 1 below.

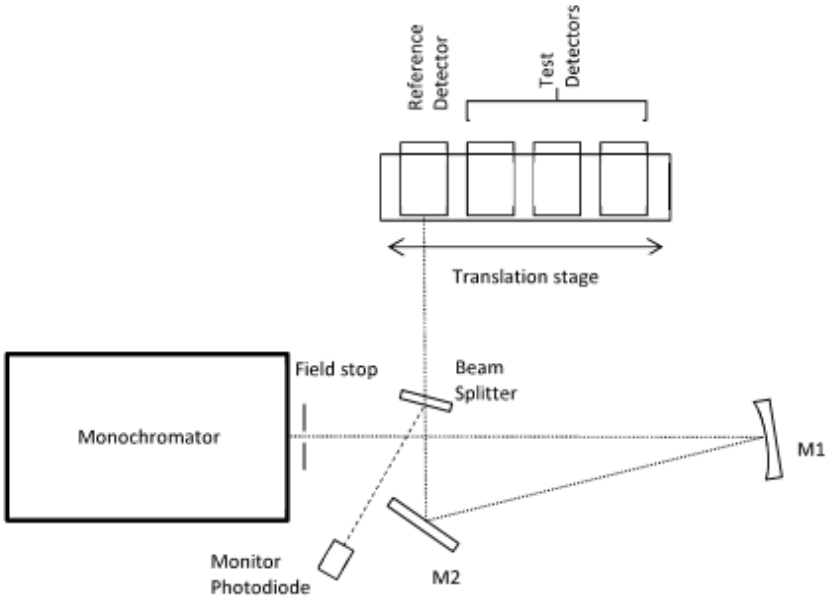

Figure 1: NPL Spectral Responsivity Facility. M1 is a spherical mirror. M2 is a plane mirror. Not shown: source and optics located before the monochromator (source, mirrors, shutter and chopper), the monitor screen, the detector enclosure, and the electrical system.

A quartz tungsten halogen source was imaged into the monochromator using mirrors. A shutter and a chopper (used for relative measurements against the pyroelectric reference detector) were positioned before the entrance port of the monochromator. The chopping frequency was 71 Hz.

A McPherson model 2035 double subtractive Czerny-Turner monochromator was used, which had an f/number of f/4.8. The entrance and exit slits of each half of the monochromator were variable in both width and height. The width was set to 1.25 mm to give a bandwidth of 5 nm (triangular), and the height was set to 2 mm. Built-in order sorting filters were located immediately before the entrance slit. The gratings installed in the monochromator for these measurements were blazed at 1.25 µm, and had a groove density of 600 g/mm.

A variable aperture, placed after the monochromator, was used as a field stop. It was used to control the f/number of the beam. A spherical mirror (M1) was used to form a one-to-one image of the exit port of the monochromator and a turning mirror (M2) was used to steer the image to the reference and test detectors. A beam splitter was used to reflect a small percentage of the power in the beam to a monitor detector, which was used to monitor any change in power of the beam during the measurements. The monitor detector was screened from the other detectors as much as possible.
The detectors were mounted on a computer-controlled translation stage in order to ensure reproducible positioning of each detector with respect to the beam. Alignment aids were used to align

the detectors normal to, and centred about, the optical axis in each of the respective measurement positions on this translation stage. The distance between the detector surface and mirror M2 was adjusted according to the size of irradiated area required i.e.:

- The reference trap detectors were positioned such that they were underfilled, and so that an image of the exit port of the monochromator was formed on the last (third) detector.
- The pyroelectric detector was positioned such that the beam passed through the port of the hemisphere (fixed to the front of the detector) without clipping.
- The comparison detectors were positioned such that the beam falling on the detector surface was approximately circular, and approximately 4 mm in diameter.

The detector side of the system (i.e. from the monochromator exit port onwards) was enclosed within a light tight enclosure.

Each detector was connected to a transimpedance amplifier. The output from the amplifier was then measured by a voltmeter (directly for d.c. measurements and via a lock-in amplifier for a.c. measurements).

The temperature within the enclosure was monitored using a platinum resistance thermometer (PRT).

1.2 MEASUREMENT METHODOLOGY

To achieve the best possible measurement uncertainty for the measurement of the comparison detectors, absolute measurements were made directly against reference silicon trap detectors at wavelengths from 900 nm to 920 nm and these were combined with relative measurements against a reference cavity pyroelectric detector from 900 nm to 1600 nm. The overlap points, defined as the wavelengths at which both absolute and relative measurements were made, were used to determine a normalisation constant. The normalisation constant was applied to all of the relative data points to calculate the absolute spectral responsivity at these wavelengths. This allowed the absolute spectral responsivity of the comparison detectors to be determined at each wavelength required for the comparison (see Section 1.5 for more details.)

Measurements were automated using the control program. The sequence for each measurement scan was as follows:

1. Set the monochromator to the first (lowest) wavelength required.
2. Record the light and dark readings (made with the shutter open and closed respectively) from the reference detector.
3. Repeat step 2 for each individual test detector in turn.
4. Set the monochromator to the next wavelength required.
5. Repeat steps 2 and 3.
6. Repeat steps 4 and 5 until all required wavelengths have been measured.

The monitor detector was measured simultaneously and was used to correct for any change in the output of the source during the course of the measurements.

Up to eight repeated scans were carried out, depending on the signal-to-noise, to form one 'independent measurement'. The mean and standard deviation of the scans forming each independent measurement were calculated. A number of independent measurements were carried out (four in the case of the absolute measurements and three in the case of the relative measurements) and these were averaged to obtain the final measurement result. All the detectors (reference and test) were realigned between each independent measurement.

1.3 ABSOLUTE MEASUREMENTS

Absolute measurements were made by reference to NPL's three-element reference silicon trap detectors. The spectral responsivity of the trap detectors had been calibrated against the NPL Primary Standard Cryogenic Radiometer at several Krypton ion lines in the UV, visible and NIR. The responsivity of the trap detectors at wavelengths longer than 799.3 nm was extrapolated from the responsivity at 799.3 nm by assuming constant quantum efficiency.

Absolute measurements of the EURAMET DGTx detectors were made against the trap detectors at 900 nm, 910 nm and 920 nm. Collectively these were known as the 'overlap points'. The 900 nm measurement is reported as part of the intercomparison. The other wavelengths were only used to determine a normalisation constant (see Section 1.5) and are not reported as part of this comparison.

Measurement parameters:

Modulation frequency	d.c.
f/number	At least f/21

1.4 RELATIVE MEASUREMENTS

Relative measurements of the EURAMET DGTx detectors were made by reference to the NPL reference cavity pyroelectric detector, which incorporates a gold hemisphere [1]. Measurements were made at all wavelengths required by the comparison (including 900 nm) and at the additional overlap points of 910 nm and 920 nm. The absolute and relative overlap points were then used to determine a normalisation constant, as described in Section 1.5.

Measurement parameters:

Modulation frequency	a.c.
f/number	Approximately f/9

1.5 NORMALISATION CONSTANT

As described in Section 1.2, the absolute responsivity values were obtained by applying a normalisation constant, $C_{\mathrm{norm,avg}}$, to the relative spectral responsivity values determined from the measurements against the pyroelectric reference detector. In other words, the absolute responsivity $R(\lambda_i)$ at wavelength λ_i was calculated from the corresponding relative spectral responsivity value, $R_{\mathrm{rel}}(\lambda_i)$, using:

$$R(\lambda_i) = C_{\mathrm{norm,avg}} * R_{\mathrm{rel}}(\lambda_i). \qquad \text{Equation 1}$$

The normalisation constant at each overlap point λ_j (i.e. 900 nm, 910 nm and 920 nm, where measurements were made against the traps and the pyroelectric detector) was calculated as the ratio of absolute response at that wavelength, $R_{\mathrm{abs}}(\lambda_j)$ (obtained from the measurements against the trap detectors) to the relative response at that wavelength, $R_{\mathrm{rel}}(\lambda_j)$ (obtained from measurements against the pyroelectric detector):

$$C_{\mathrm{norm}}(\lambda_j) = \frac{R_{\mathrm{abs}}(\lambda_j)}{R_{\mathrm{rel}}(\lambda_j)} \qquad \text{Equation 2}$$

The average normalisation constant $C_{\mathrm{norm,avg}}$ was then calculated using the weighted mean of the results from these 3 overlap wavelengths using:

$$C_{\text{norm,avg}} = \sum_1^3 C_{\text{norm}}(\lambda_j)\omega(\lambda_j) \qquad \text{Equation 3}$$

where the weights $\omega(\lambda_j)$ are given by:

$$\omega(\lambda_j) = \frac{1/u^2_{\text{abs,c}}(\lambda_j)}{\sum_1^3(1/u^2_{\text{abs,c}}(\lambda_j))} \qquad \text{Equation 4}$$

Here $u_{\text{abs,c}}(\lambda_j)$ is the combined standard uncertainty associated with the absolute responsivity at each of the overlap wavelengths λ_j (see Section 5.2.2).

The reproducibility of the 3 individual normalisation constants used to calculate the mean (each corresponding to a different 'overlap' wavelength) was allowed for as an additional component in the uncertainty budget (see Table 3). The mean of the uncertainties of the absolute responsivities at the normalisation wavelengths was also included.

2. TYPE OF PRIMARY STANDARD

The primary standard was the NPL Primary Standard Cryogenic Radiometer. The dissemination route is shown in section 5.

3. LABORATORY TRANSFER STANDARDS USED

NPL-designed three-element silicon trap detectors were used as the reference transfer standard to provide measurements of the absolute spectral response and a cavity pyroelectric detector was used to provide the relative spectral responsivity of the comparison detectors at all wavelengths specified in the EURAMET-K2.a Technical Protocol. Further details are given in Sections 1.3 and 1.4 above.

4. MONOCHROMATOR USED

This is described in section 1.1.

5. PRIMARY REFERENCE OR TRACEABILITY ROUTE OF PRIMARY REFERENCE AND BREAKDOWN OF UNCERTAINTY

5.1 TRACEABILITY ROUTE

The measurements made by NPL in this comparison are traceable to the NPL Primary Standard Cryogenic Radiometer. The traceability route is shown in Figure 2.

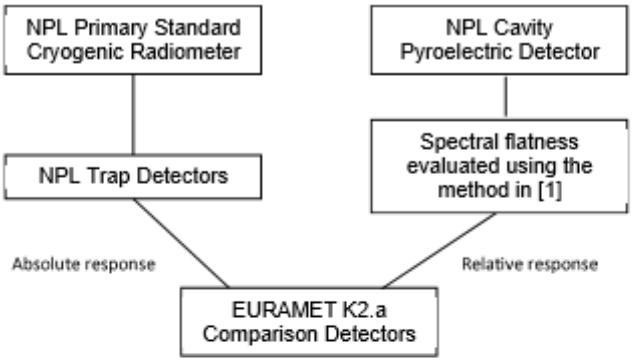

Figure 2: Traceability chain for the NPL measurements for the EURAMET K2.a comparison

5.2 UNCERTAINTIES ASSOCIATED WITH THE CALIBRATION OF THE COMPARISON DETECTORS

5.2.1 Uncertainty in the calibration of the trap detectors against the cryogenic radiometer

The expanded uncertainty associated with the calibration of the trap detectors was taken to be 0.02 % at all wavelengths used in this comparison (i.e. 900 nm, 910 nm and 920 nm). Table 1 shows the breakdown of uncertainties for calibration of a trap detector against the NPL cryogenic radiometer [2]. It should be noted that the NPL spectral responsivity scale at wavelengths above 799.3 nm (the highest wavelength at which a direct measurement of the trap detectors against the NPL cryogenic radiometer was carried out) is based on an assumption that the quantum efficiency of the traps does not change over the wavelength range 800 nm to 920 nm. This assumption defines the NPL spectral responsivity scale over this wavelength range; therefore no additional uncertainty is included for extrapolation effects in the uncertainty budget shown in Table 1.

Table 1: Uncertainty budget for calibration of the trap detectors against the NPL cryogenic radiometer.

Source of Uncertainty	Type	Value ±%	Prob. Dist.	Divisor	C_i	U_i ±%
cavity absorptance	B	0.001	rectangular	1.732	1	0.0006
window transmittance	A	0.005	normal	1	1	0.005
window scatter	B	10	normal	2	1/10000	0.0005
sensitivity of radiometer	B	0.001	rectangular	1.732	1	0.0006
electrical power measurement	B	0.002	normal	2	1	0.0010
changes in scattered & thermal radiation	B	0.001	rectangular	1.732	1	0.0006
measurement repeatability (cryogenic radiometer)	A	0.0014	normal	1	1	0.0014
optical power measurement	B	0.0108	normal	2	1	0.0054
detector dvm calibration	B	0.0005	rectangular	1.732	1	0.0003
detector dvm drift	B	0.0005	rectangular	1.732	1	0.0003
amplifier calibration	B	0.01	rectangular	1.732	1	0.0058
amplifier drift	B	0.001	rectangular	1.732	1	0.0006
beam size	B	0.005	rectangular	1.732	1	0.0029
laser stability	B	0.005	rectangular	1.732	1	0.0029

positional reproducibility	B	0.005	normal	2	1	0.0025
measurement repeatability (trap)	A	0.0015	normal	1	1	0.0015
combined standard uncertainty			**normal**			**0.0094**
expanded uncertainty			**normal**			**0.02**

5.2.2 Uncertainty in the calibration of the comparison detectors against the trap detectors

The comparison detectors were calibrated in terms of their absolute spectral responsivity against the NPL reference trap detectors at 900 nm, 910 nm and 920 nm. The results at 900 nm are reported in Tables 4 to 6. These results were combined with those obtained by measurements at 910 nm and 920 nm against the pyroelectric reference detector to determine a normalisation constant for each comparison detector, which was used to transform the relative measurements (from calibration against the pyroelectric detector) to absolute values, as described in Section 1.5. The uncertainty budget for this calibration is given in Table 2; details of the uncertainty contributions are given in Sections 5.2.2.1 to 5.2.2.10.

5.2.2.1 Uncertainty due to trap detector calibration

This was taken from Table 1.

5.2.2.2 Uncertainty due to ageing of the traps

No correction was made for potential ageing of the trap detectors since the time of last calibration, but an allowance for this effect was included in the uncertainty budget, based on historical data obtained over a number of years.

5.2.2.3 Uncertainty due to wavelength

The standard uncertainty associated with the measured spectral responsivity of the comparison detectors due to uncertainty in the wavelength scale of the monochromator was estimated to be [3]:

$$\frac{S_R(\lambda)}{S_T(\lambda)}\frac{\partial}{\partial\lambda}\left\{\frac{S_T(\lambda)}{S_R(\lambda)}\right\}\frac{u(\lambda)}{\sqrt{3}} \qquad \text{Equation 5}$$

where $S_T(\lambda)$ and $S_R(\lambda)$ are the signals from the reference and test detector respectively, and $u(\lambda)$ is the semi-range for the wavelength scale uncertainty, estimated to be 0.1 nm. The differential term was estimated by:

$$\frac{\phi(\lambda_{i+1})-\phi(\lambda_i)}{\lambda_{i+1}-\lambda_i}+\frac{\phi(\lambda_{i-1})-\phi(\lambda_i)}{\lambda_{i-1}-\lambda_i} \qquad \text{Equation 6}$$

where $\phi(\lambda)=S_T(\lambda)/S_R(\lambda)$.

Table 2 Uncertainty budget for calibration of comparison detectors against NPL reference trap detectors.

Source of uncertainty	Type	Value +-%			Prob. Dist.	Div.	C_i	U_i +- %		
		900 nm	910 nm	920 nm				900 nm	910 nm	920 nm
trap detector calibration	B	0.02	0.02	0.02	normal	2	1	0.01	0.01	0.01
ageing since calibration	B	0.03	0.03	0.03	rectangular	1.732	1	0.0175	0.0175	0.0175
monochromator wavelength*	B	0.016	0.014	0.014	rectangular	1.732	1	0.009	0.008	0.008
monochromator bandwidth*	B	0	0	0	rectangular	1.732	1	0	0	0
temperature	B	0	0	0	rectangular	1.732	1	0	0	0
non-uniformity	B	0.02	0.02	0.02	rectangular	1.732	1	0.0116	0.0116	0.0116
stray light	B	0	0	0	rectangular	1.732	1	0	0	0
electronics	B	0.024	0.024	0.024	rectangular	1.732	1	0.014	0.014	0.014
scan repeatability#	A	0.02	0.01	0.02	normal	1	1	0.02	0.01	0.02
independent meas. repeatability#	A	0.03	0.01	0.03	normal	1	1	0.03	0.01	0.03
polarisation	B	0	0	0	rectangular	1.732	1	0	0	0
beam divergence	B	0.05	0.05	0.05	rectangular	1.732	1	0.0289	0.0289	0.0289
vignetting	B	0	0	0	rectangular	1.732	1	0	0	0
combined standard uncertainty#					**normal**			**0.0772**	**0.0605**	**0.0638**
expanded uncertainty*					**normal**			**0.16**	**0.12**	**0.13**

* Uncertainty expressed in terms of responsivity – see Sections 5.2.2.3 and 5.2.2.4 for details

Typical value; actual value calculated individually for each set of results

5.2.2.4 Uncertainty due to bandwidth

Measurements were made using a bandwidth of 5 nm, in accordance with the protocol, and therefore it was not necessary to apply any bandwidth correction to the results. Nevertheless, the difference between the spectral responsivity profiles of the reference and comparison detectors meant that the influence of bandwidth on the results had to be considered in the evaluation of the measurement uncertainty. The uncertainty due to bandwidth was estimated by calculating the size of the bandwidth correction (the correction to be applied to obtain the 'true' value for infinitely narrow bandwidth), using a 3-point correction method and assuming a triangular bandpass function [3] i.e. using:

$$C_0 = \left[-\frac{\Delta^2}{12\delta^2}\right] M_{-1} + \left[1 + \frac{\Delta^2}{6\delta^2}\right] M_0 + \left[-\frac{\Delta^2}{12\delta^2}\right] M_{+1} \qquad \text{Equation 7}$$

where C_0 is the corrected value for the wavelength being considered, Δ is the bandwidth, δ is the measurement step interval and M_0, M_{-1} and M_{+1} are, respectively, the measured values at the wavelength being considered, the wavelength point one below this and the wavelength point one above this. The difference between C_0 and M_0 was found to be very small in all cases, meaning that even if the uncertainty due to bandwidth was taken as being equal to the size of the resultant bandwidth correction (a gross over-estimate of the likely uncertainty), it had negligible impact on the final measurement uncertainty.

5.2.2.5 Uncertainty due to temperature

The temperature coefficient of response of trap detectors was determined in the CCPR-K2.b comparison and was taken to be representative of the NPL three element reference trap detectors as these are made from the same type of diodes (i.e. Hamamatsu S1337) [5]. The temperature of the trap detectors was highly stable during the course of the measurements and therefore this temperature coefficient was estimated to have a negligible impact on the measurement uncertainty.

The temperature of the comparison detectors was measured and is reported as part of the results (in the form of the measured resistance of the associated PRT). The variations in the temperature of the comparison detectors during measurement were small and therefore the associated uncertainty was assumed to be negligible.

5.2.2.6 Uncertainty due to detector non-uniformity

The uncertainty due to non-uniformity of the reference trap detectors was based on previous research [2]. The test detectors were realigned several times during the course of the measurements, with the orientation being changed as part of each realignment. As a result, the uncertainties due to due to non-uniformities in the test detectors and/or beam were included as part of the 'independent measurement repeatability' component of the uncertainty budget.

5.2.2.7 Uncertainty due to stray light

The stray light performance of the monochromator has been estimated in the past using combinations of filters. As expected for a well-designed double monochromator, the stray light performance was found to be good, and to have negligible impact on the measurement uncertainty.

5.2.2.8 Uncertainty due to electronics

The uncertainty associated with the electronics (lock-in, chopper and dvm, including linearity and frequency stability effects) was estimated based on the associated electrical calibration uncertainties, historical data relating to drift in the calibration values over time, and manufacturer's data. The range of signal levels used during the measurements was small, meaning that uncertainties due to linearity in particular were also small.

Table 3 Uncertainty budget for calibration of comparison detectors against NPL reference pyroelectric detector (note uncertainties vary slowly with wavelength – results at 200 nm intervals only are quoted).

Source of uncertainty	Type	Value ±%				Prob. Dist.	Div.	c_i	u_i ± %			
		1000 nm	1200 nm	1400 nm	1600 nm				1000 nm	1200 nm	1400 nm	1600 nm
pyroelectric spectral flatness	B	0.1	0.1	0.1	0.1	rectangular	1.732	1	0.058	0.058	0.058	0.058
monochromator wavelength*	B	0.012	0.007	0.004	0.031	rectangular	1.732	1	0.012	0.007	0.005	0.031
monochromator bandwidth*	B	0	0	0	0	rectangular	1.732	1	0	0	0	0
temperature	B	0.15	0.15	0.15	0.15	rectangular	1.732	1	0.087	0.087	0.087	0.087
non-uniformity	B	0.08	0.08	0.08	0.08	rectangular	1.732	1	0.046	0.046	0.046	0.046
stray light	B	0	0	0	0	rectangular	1.732	1	0	0	0	0
electronics	B	0.025	0.025	0.025	0.025	rectangular	1.732	1	0.014	0.014	0.014	0.014
non-linearity	B	0.1	0.1	0.1	0.1	rectangular	1.732	1	0.058	0.058	0.058	0.058
scan repeatability#	A	0.07	0.05	0.07	0.08	normal	1	1	0.07	0.05	0.07	0.08
independent meas. repeatability#	A	0.09	0.03	0.04	0.07	normal	1	1	0.09	0.03	0.04	0.07
polarisation/beam geometry	B	0	0	0	0	rectangular	1.732	1	0	0	0	0
normalisation#	A	0.093	0.093	0.093	0.093	normal	1	1	0.093	0.093	0.093	0.093
absolute responsivity from traps#	B	0.135	0.135	0.135	0.135	normal	2	1	0.067	0.067	0.067	0.067
combined standard uncertainty#						**normal**			**0.217**	**0.187**	**0.187**	**0.206**
expanded uncertainty#						**normal**			**0.45**	**0.39**	**0.39**	**0.43**

* Uncertainty expressed in terms of responsivity – see Sections 5.2.2.3 and 5.2.2.4 for details
# Typical value; actual value calculated individually for each set of results

5.2.2.9 Uncertainties due to random effects ('scan repeatability' and 'independent measurement repeatability')

The standard uncertainties due to random effects for an individual determination of detector responsivity was estimated as the standard error associated with the mean (SEOM) for a series of spectral scans, given by:

$$\sigma_{\text{scan}}=\sigma/\sqrt{N} \qquad \text{Equation 8}$$

where N is the number of spectral scans (usually 8) and σ is the standard deviation of these scans. By its nature, the random error varied for each independent determination of detector responsivity. However, it was observed that for a given detector at a given wavelength, the SEOM was similar for each determination, and it was therefore reasonable to take the average value of SEOM from the 3 or 4 independent measurements for the uncertainty budget. This is included in the uncertainty budget under the heading 'scan repeatability'.

The detectors were realigned for each independent measurement, as described in Section 1.2, and this would be expected to result in some additional random variation in the results, beyond that determined from the SEOM of the repeated scans. This additional uncertainty, $u_{\text{repro}}(\lambda)$, was calculated using:

$$\text{If } \sigma_{\text{repeat}}(\lambda) \le u^2_{\text{scan}}(\lambda) \text{ then } u_{\text{repro}}(\lambda) = 0,$$

$$\text{otherwise } u_{\text{repro}}(\lambda) = \sqrt{\sigma^2_{\text{repeat}}(\lambda) - u^2_{\text{scan}}(\lambda)} \qquad \text{Equation 9}$$

where $\sigma_{\text{repeat}}(\lambda)$ is the standard error associated with the mean (SEOM) for the series of independent measurements. This is included in the uncertainty budget under the heading 'independent measurement repeatability'. As indicated in 5.2.2.6, this also included the uncertainty due to detector non-uniformity since the detector was realigned (and re-orientated) for each independent measurement.

5.2.2.10 Uncertainties due to polarisation and beam geometry

The uncertainties associated with polarisation and beam geometry (vignetting of the trap and beam divergence effects) were all considered to be negligible, based on the results of previous investigations.

5.2.3 Uncertainty in the measurement of the comparison detectors against the cavity pyroelectric detector

As discussed previously, the comparison detectors were calibrated in terms of their relative spectral responsivity against the NPL reference cavity pyroelectric detector at 910 nm and 920 nm as well as at all the defined comparison wavelengths. The results at 900 nm, 910 nm and 920 nm were combined with those from measurements against the reference trap detectors to determine a normalisation constant for each comparison detector, which was used to transform the relative measurements at 950 nm and above to absolute values, as described in Section 1.5.

The uncertainty budget for the absolute calibration at 950 nm and above is given in Table 3; details of the uncertainty contributions are given in Sections 5.2.3.1 to 5.2.3.9

5.2.3.1 Uncertainty due to spectral flatness of cavity pyroelectric detector

The spectral flatness of the cavity pyroelectric reference detector has been estimated by measuring the change in response of the pyroelectric detector with and without the cavity in place, following the method of Theocharous [1]; the associated uncertainty is included in the uncertainty budget. Since the pyroelectric detector was used only to determine the relative spectral responsivity, and not to assign absolute values, there was no need to include any additional uncertainty for its absolute calibration. Furthermore, there was no allowance made for ageing of the cavity pyroelectric reference detector, since measurements have shown this type of detector to be highly stable with time [1].

5.2.3.2 Uncertainty due to wavelength and bandwidth

These uncertainties were analysed as described in Sections 5.2.2.3 and 5.2.2.4 above. As in the case of the calibration of the comparison detectors against the trap detectors, the uncertainty due to bandwidth effects was found to be negligibly small for the calibration of the comparison detectors against the pyroelectric detector.

5.2.3.3 Uncertainty due to temperature

The temperature coefficient of response of the cavity pyroelectric reference detector was taken to be approximately 0.15 % $°C^{-1}$ based on previous measurements [1]. The temperature of the pyroelectric detector was controlled to well within ±1 °C during the course of the measurements and therefore the uncertainty due to temperature drifts for the pyroelectric was taken to be 0.15 % (rectangular).

The temperature of the comparison detectors was measured and is reported as part of the results (in the form of the measured resistance of the associated PRT). The variations in the temperature of the comparison detectors during measurement were small and therefore the associated uncertainty was assumed to be negligible.

5.2.3.4 Uncertainty due to detector uniformity

The uncertainty due to non-uniformity of the cavity pyroelectric reference detector was based on previous research [1]. The test detectors were realigned between each independent measurement, with the orientation being changed as part of each realignment. As a result, the uncertainties due to due to non-uniformities in the test detectors and/or beam were included as part of the 'independent measurement repeatability' component of the uncertainty budget.

5.2.3.5 Uncertainty due to stray light

As described in 5.2.2.7, the expected stray light performance of the double monochromator used for these measurements was found to be good, and to have negligible impact on the measurement uncertainty.

5.2.3.6 Uncertainty due to electronics

The uncertainty associated with the electronics (dvm, preamplifier and chopper) was estimated based on the associated electrical calibration uncertainties, historical data relating to drift in the calibration values over time, and manufacturer's data.

5.2.3.7 Uncertainty due to lock-in non- linearity

The uncertainty associated with the non-linearity of the lock-in amplifier was estimated based on manufacturer's data.

5.2.3.8 Uncertainties due to random effects ('scan repeatability' and 'independent measurement repeatability')

The standard uncertainties due random effects were evaluated as described in Section 5.2.2.9.

5.2.3.9 Uncertainties due to polarisation and beam geometry effects

The uncertainties associated with polarisation and beam geometry were considered to be negligible, based on the results of previous investigations.

5.2.3.10 Uncertainty due to normalisation

The reproducibility of the 3 individual normalisation constants (each corresponding to a different 'overlap point') was allowed for as an additional component in the uncertainty budget.

5.2.3.11 Uncertainty due to absolute responsivity against traps

The mean of the combined standard uncertainties associated with the absolute responsivity at each of the overlap wavelengths, $u_{\mathrm{abs,c}}(\lambda_j)$, obtained from calibration against the trap detectors (see Section 5.2.2), was allowed for as an additional component in the uncertainty budget.

6. CALIBRATION LABORATORY ENVIRONMENTAL CONDITIONS

The temperature in the laboratory was maintained in the range 20.8 °C to 21.6 °C during the course of the measurements. Humidity was not monitored but was controlled within the range 30 % RH to 60 % RH.

7. REFERENCES

[1] Theocharous, E., *The establishment of the NPL Infrared relative spectral responsivity scale using cavity pyroelectric detectors.* Metrologia, 2006, **43**: S115-S119.

[2] Fox, N.P., *Trap Detectors and their Properties* Metrologia, 1991, **28**: 197-202.

[3] Woolliams, E.R., Baribeau, R., Bialek, A., and Cox, M. G., *Spectrometer bandwidth correction for generalized bandpass functions.* Metrologia, 2011, **48**: 164–172.

[4] Kostkowski, H., *Reliable Spectroradiometry*. La Plata, USA: Spectroradiometry Consulting. 1997.

[5] R. Goebel and M. Stock., *Report on the key comparison CCPR-K2.b of spectral responsivity measurements in the wavelength range 300 nm to 1000 nm. Metrologia,* 2004, **41**: 02004.

8. MEASUREMENT RESULTS

Type of Standard: Germanium detector, temperature stabilised
Reference number: DGT6

Wavelength / nm	Spectral Responsivity A / W	STD A / W	Number of measurements /n	Temperature / Ohm	Combined standard uncertainty (k=1) / %
900	0.4517	0.0003	4	108.16	0.08
950	0.5073	0.0007	3*	108.38	0.23
1000	0.5571	0.0009	3*	108.38	0.22
1050	0.5983	0.0007	3*	108.38	0.20
1100	0.6361	0.0003	3*	108.38	0.19
1150	0.6725	0.0002	3*	108.38	0.19
1200	0.7087	0.0004	3*	108.38	0.19
1250	0.7428	0.0007	3*	108.38	0.19
1300	0.7774	0.0006	3*	108.38	0.19
1350	0.8100	0.0001	3*	108.38	0.19
1400	0.8390	0.0005	3*	108.38	0.19
1450	0.8674	0.0005	3*	108.38	0.19
1500	0.8935	0.0007	3*	108.38	0.19
1550	0.8988	0.0007	3*	108.38	0.20
1600	0.6421	0.0008	3*	108.38	0.21

*** 3 independent measurements were made on a relative basis only against the NPL cavity pyroelectric detectors; these were scaled using results from 4 independent sets of absolute measurements against the NPL trap detectors carried out in the range 900 nm - 920 nm.**

Laboratory: NPL
Date: 22 January 2015
Signature: Teresa Goodman

Type of Standard: Germanium detector, temperature stabilised
Reference number: DGT7

Wavelength / nm	Spectral Responsivity A / W	STD A / W	Number of measurements /n	Temperature / Ohm	Combined standard uncertainty (k=1) / %
900	0.3972	0.0004	4	108.14	0.08
950	0.4585	0.0002	3*	108.37	0.25
1000	0.5173	0.0004	3*	108.37	0.24
1050	0.5686	0.0005	3*	108.37	0.22
1100	0.6158	0.0007	3*	108.37	0.21
1150	0.6610	0.0002	3*	108.37	0.21
1200	0.7049	0.0001	3*	108.37	0.21
1250	0.7455	0.0005	3*	108.37	0.21
1300	0.7862	0.0006	3*	108.37	0.21
1350	0.8240	0.0005	3*	108.37	0.21
1400	0.8565	0.0009	3*	108.37	0.21
1450	0.8907	0.0012	3*	108.37	0.21
1500	0.9202	0.0006	3*	108.37	0.21
1550	0.9353	0.0019	3*	108.37	0.24
1600	0.6872	0.0010	3*	108.37	0.23

*** 3 independent measurements were made on a relative basis only against the NPL cavity pyroelectric detectors; these were scaled using results from 4 independent sets of absolute measurements against the NPL trap detectors carried out in the range 900 nm - 920 nm.**

Laboratory: NPL
Date: 22 January 2015
Signature: Teresa Goodman

Type of Standard: Germanium detector, temperature stabilised
Reference number: DGT8

Wavelength / nm	Spectral Responsivity A / W	STD A / W	Number of measurements /n	Temperature / Ohm	Combined standard uncertainty (k=1) / %
900	0.4293	0.0004	4	108.14	0.08
950	0.4918	0.0010	3*	108.37	0.22
1000	0.5518	0.0004	3*	108.37	0.20
1050	0.6047	0.0002	3*	108.37	0.18
1100	0.6515	0.0005	3*	108.37	0.17
1150	0.6946	0.0002	3*	108.37	0.18
1200	0.7331	0.0005	3*	108.37	0.17
1250	0.7685	0.0002	3*	108.37	0.17
1300	0.8041	0.0004	3*	108.37	0.17
1350	0.8397	0.0000	3*	108.37	0.17
1400	0.8713	0.0008	3*	108.37	0.17
1450	0.9055	0.0006	3*	108.37	0.18
1500	0.9371	0.0012	3*	108.37	0.18
1550	0.9506	0.0022	3*	108.37	0.20
1600	0.6850	0.0005	3*	108.37	0.19

*** 3 independent measurements were made on a relative basis only against the NPL cavity pyroelectric detectors; these were scaled using results from 4 independent sets of absolute measurements against the NPL trap detectors carried out in the range 900 nm - 920 nm.**

Laboratory: NPL
Date: 22 January 2015
Signature: Teresa Goodman

A.5 SP (Sweden)

Measurement facility and method

Measurements where performed in monochromator Zeiss MM12, fitted with motors for automatic wavelength and bandwidth setting. Round spot of 4 mm diameter imaged on the Germanium detectors with f/#: around f/6. As working standard a UDT 261 Ge s/n G306 NPL (SP500021) germanium diode was used. Assuming the same temperature dependence for the three measured artefacts and SP working standard the overall results are given for 21±1 °C (the temperature our standard is calibrated at) This increases the uncertainty for temperature dependence. The monochromator can be equipped with different prisms and lamps. For this comparison glass prisms and a tungsten halogen lamp was used for wavelengths from 900 nm and up to 1600 nm. The monochromator's basic wavelength calibration is made using a deuterium lamp. Typically a bandwidth of 7 nm has been used, although larger at higher wavelengths. Room temperature: 26±1 (recorded). Detector temperature was recorded during measurements. Each detector was measured in 6 series. Temperature over one series changed typically like for measurement 4 in Table 1.

Table 1: Temperature recording before and after measurement for measurement 4.

	TempDGT6	TempDGT7	TempDGT8
	Ohm	Ohm	Ohm
before	110,38	110,40	110,41
after	110,56	110,48	110,49

Temperature, min and max, registered for measured detector over the 6 series can be studied in Table 2.

Table 2: Min and max recorded temperature for each detector.

	TempDGT6	TempDGT7	TempDGT8
	Ohm	Ohm	Ohm
min	110,06	110,03	110,09
max	110,56	110,48	110,49

Reported temperatures in the results are average temperature over six series.

Basic traceability chain

SP is traceable to NPL for spectral responsivity in this wavelength range.

Measurement uncertainty

We are starting with uncertainty of our calibrated detector with traceability from NPL given for Each 50 nm wavelength between 900 and 1600 nm. The uncertainties are expressed in percent (%). In the tables below the calculated uncertainties is given for 1300 nm, 1450 nm, 1500 nm, 1550 nm and 1600 nm. The uncertainty calculation for 1300 nm represents the estimated uncertainties for 900 nm – 1400 nm.

Temperature: The laboratory's temperature was 26 ±1 °C during the measurements. The UDT Germanium detector had been calibrated at NPL at 21±1 °C. The temperature dependence of Germanium in spectral responsivity is reported in literature to be fairly small up to 1450 nm but after that the temperature dependence on the responsivity increases to reach several % at 1600 nm. Assuming similar temperature dependence for the three measured germanium artefacts and SP working standard the overall results are given for 21±1 °C with an increased uncertainty for the temperature dependence. Depending on the wavelength temperature contributes a certain amount to the overall uncertainty (from ±0,30 % at 900 nm – 1400 nm, ± 0,60 % at 1450 nm, ± 0,65 % 1500 nm, ± 0,66 % at 1550 nm and ± 1,14 % 1600 nm. Other components like repeatability and wavelength and bandwidth effects also have an increased uncertainty for λ ≥ 1450 nm.

Repeatability: Typically the standard deviations are calculated as mean values from five repeated measurements. This component is ± 0,30 %.

Linearity: Light from monochromator has a power in the order of 5-10 microW. Linearity effects are neglected in the uncertainty calculations.

Electrical measurements: The voltmeters and amplifiers used are calibrated at NMI for electricity. Also, all measurements are comparative, which almost completely will eliminate the small residual error. This component is assumed to be negligible in comparison to other uncertainties.

Others: Estimates for vingetting effects, reflections, polarizations, stray light, bandwidth effects, and to some extent non-uniformity, are type B estimates which are based on experience regarding the detector types used and the measurement set-up.

Source of uncertainty	**Estimate 1300 nm**	**Standard uncertainty (k=1) %**	**Estimate 1450 nm**	**Standard uncertainty (k=1)**
Calibration of NMI (SP) reference detector	*0,61*	*0,55*	*0,72*	*0,55*
Drift/contamination etc. since last calibration	*± 0,005*	*0,48*	*±0,006*	*0,48*
Calibration of VSL transfer detectors		*0,32*	*0,88*	*0,46*
Temperature dependence	*± 0,004*	*0,30*	*± 0,006*	*0,60*
Repeatability	*± 0,003*	*0,22*	*± 0,003*	*0,25*
Wavelength, bandwidth	*± 0,003*	*0,22*	*± 0,004*	*0,30*
Non-uniformity (detector surface)	*±0,001*	*0,07*	*±0,001*	*0,07*
Others (spot size, polarization, etc.)	*±0,001*	*0,07*	*±0,001*	*0,07*
Combined standard uncertainty k=1	*± 0,006*	*0,82*	*± 0,008*	*0,89*
Combined standard uncertainty k=2	*± 0,013*	*1,64*	*± 0,016*	*1,78*

Source of uncertainty	Estimate 1500 nm	Standard uncert-ainty (k=1) %	Estimate 1550 nm	Standard uncert-ainty (k=1)	Estimate 1600 nm	Standard uncert-ainty (k=1)
Calibration of NMI reference detector SP	*0,77*	*0,55*	*0,79*	*0,55*	*0,595*	*1,10*
Drift/contamination etc. since last calibration	*± 0,0065*	*0,50*	*±0,0072*	*0,54*	*±0,006*	*0,59*
Calibration of VSL transfer detectors	*0,908*	*0,316*	*0,895*	*0,462*	*0,673*	*0,462*
Temperature dependence	*± 0,010*	*0,65*	*± 0,011*	*0,66*	*± 0,013*	*1,14*
Repeatability	*± 0,003*	*0,19*	*± 0,005*	*0,33*	*± 0,006*	*0,48*
Wavelength, bandwidth	*± 0,003*	*0,19*	*± 0,005*	*0,33*	*± 0,006*	*0,48*
Non-uniformity (detector surface)	*±0,0008*	*0,05*	*±0,0008*	*0,05*	*±0,0008*	*0,07*
Others (spot size, polarization, etc.)	*±0,001*	*0,06*	*±0,001*	*0,07*	*±0,001*	*0,09*
Combined standard uncertainty k=1	*± 0,009*	*1,03*	*± 0,010*	*1,12*	*± 0,012*	*1,83*
Combined standard uncertainty k=2	*± 0,019*	*2,06*	*± 0,020*	*2,24*	*± 0,025*	*3,65*

Results

Table 4: Germanium Detector Reference Number: DGT6

Wavelength	Spectral Responivity	Stddev	Number of measurements	Temperature	Combined uncertainty	Combined uncertainty
nm	A/W	A/W	no	ohm	k=1/%	k=2
900	0,451	0,0027	6	110,223	0,864	1,73
950	0,505	0,0015	6	110,223	0,819	1,64
1000	0,556	0,0018	6	110,223	0,823	1,65
1050	0,601	0,0022	6	110,223	0,827	1,65
1100	0,641	0,0021	6	110,223	0,823	1,65
1150	0,676	0,0023	6	110,223	0,823	1,65
1200	0,710	0,0023	6	110,223	0,822	1,64
1250	0,742	0,0026	6	110,223	0,824	1,65
1300	0,777	0,0025	6	110,223	0,821	1,64
1350	0,809	0,0029	6	110,223	0,826	1,65
1400	0,842	0,0036	6	110,223	0,836	1,67
1450	0,872	0,0040	6	110,223	0,841	1,68
1500	0,899	0,0041	6	110,223	1,032	2,06
1550	0,886	0,0040	6	110,223	1,117	2,23
1600	0,666	0,0053	6	110,223	1,824	3,65

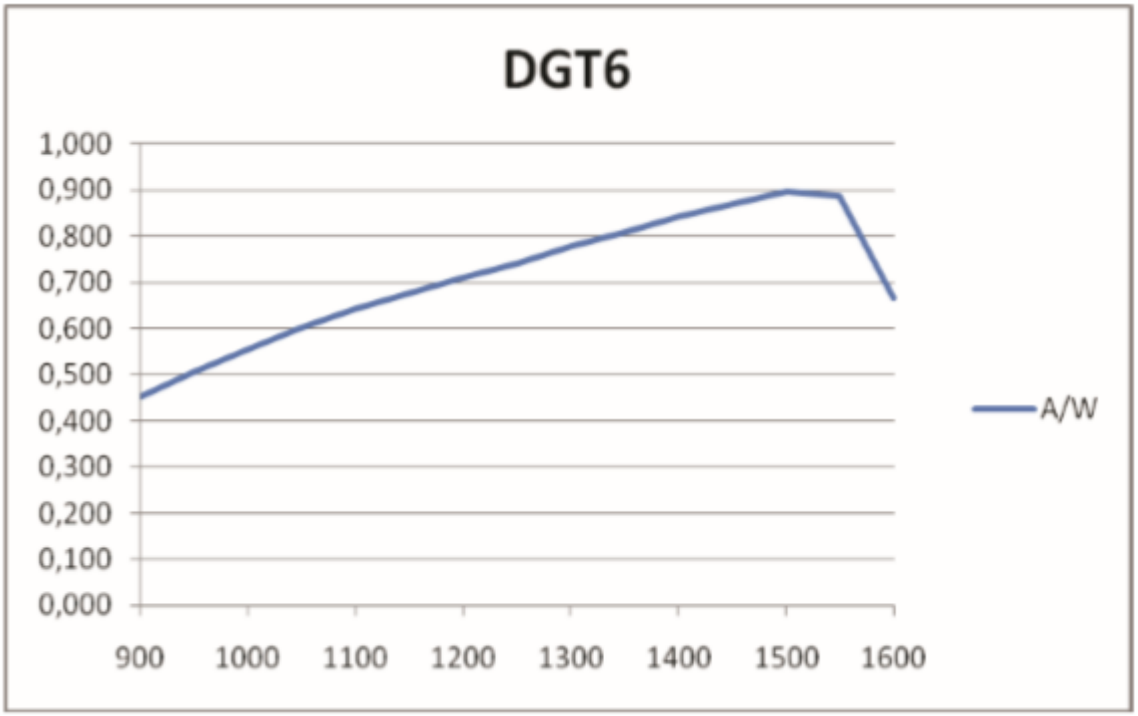

Table 5: Germanium Detector Reference Number: DGT7

Wavelength	Spectral Responivity	Stddev	Number of measurements	Temperature	Combined uncertainty	Combined uncertainty
nm	A/W	A/W	no	ohm	k=1/%	k=2
900	0,403	0,0014	6	110,251	0,823	1,65
950	0,464	0,0010	6	110,251	0,811	1,62
1000	0,523	0,0016	6	110,251	0,820	1,64
1050	0,578	0,0020	6	110,251	0,825	1,65
1100	0,627	0,0019	6	110,251	0,820	1,64
1150	0,670	0,0019	6	110,251	0,818	1,64
1200	0,713	0,0021	6	110,251	0,819	1,64
1250	0,752	0,0026	6	110,251	0,825	1,65
1300	0,793	0,0030	6	110,251	0,829	1,66
1350	0,831	0,0040	6	110,251	0,844	1,69
1400	0,867	0,0049	6	110,251	0,860	1,72
1450	0,903	0,0052	6	110,251	0,862	1,72
1500	0,934	0,0054	6	110,251	1,051	2,10
1550	0,925	0,0046	6	110,251	1,123	2,25
1600	0,718	0,0053	6	110,251	1,817	3,63

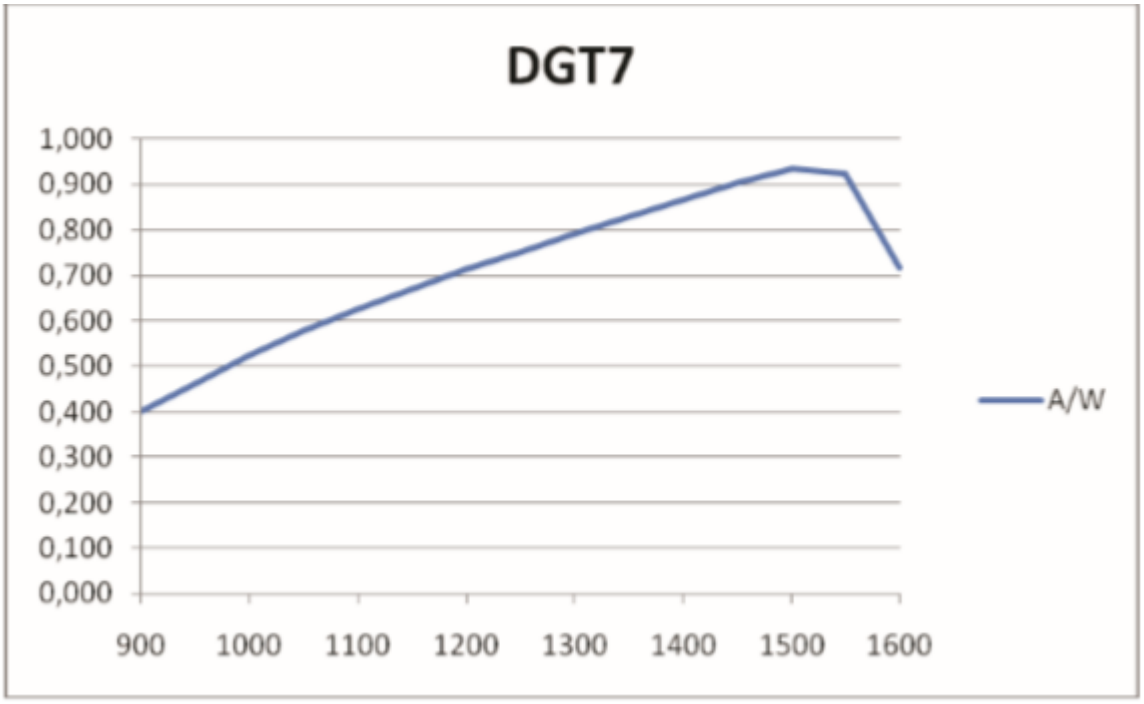

Table 6: Germanium Detector Detector Reference Number: DGT8

Wavelength	Spectral Responivity	Stddev	Number of measurements	Temperature	Combined uncertainty	Combined uncertainty
nm	A/W	A/W	no	ohm	k=1/%	k=2
900	0,430	0,00222	6	110,241	0,850	1,70
950	0,491	0,00179	6	110,241	0,827	1,65
1000	0,551	0,00227	6	110,241	0,833	1,67
1050	0,608	0,00306	6	110,241	0,848	1,70
1100	0,658	0,00352	6	110,241	0,853	1,71
1150	0,699	0,00396	6	110,241	0,859	1,72
1200	0,736	0,00396	6	110,241	0,854	1,71
1250	0,770	0,00401	6	110,241	0,851	1,70
1300	0,806	0,00394	6	110,241	0,845	1,69
1350	0,841	0,00465	6	110,241	0,857	1,71
1400	0,876	0,00537	6	110,241	0,869	1,74
1450	0,912	0,00539	6	110,241	0,864	1,73
1500	0,945	0,00588	6	110,241	1,058	2,12
1550	0,938	0,00591	6	110,241	1,142	2,28
1600	0,715	0,00649	6	110,241	1,840	3,68

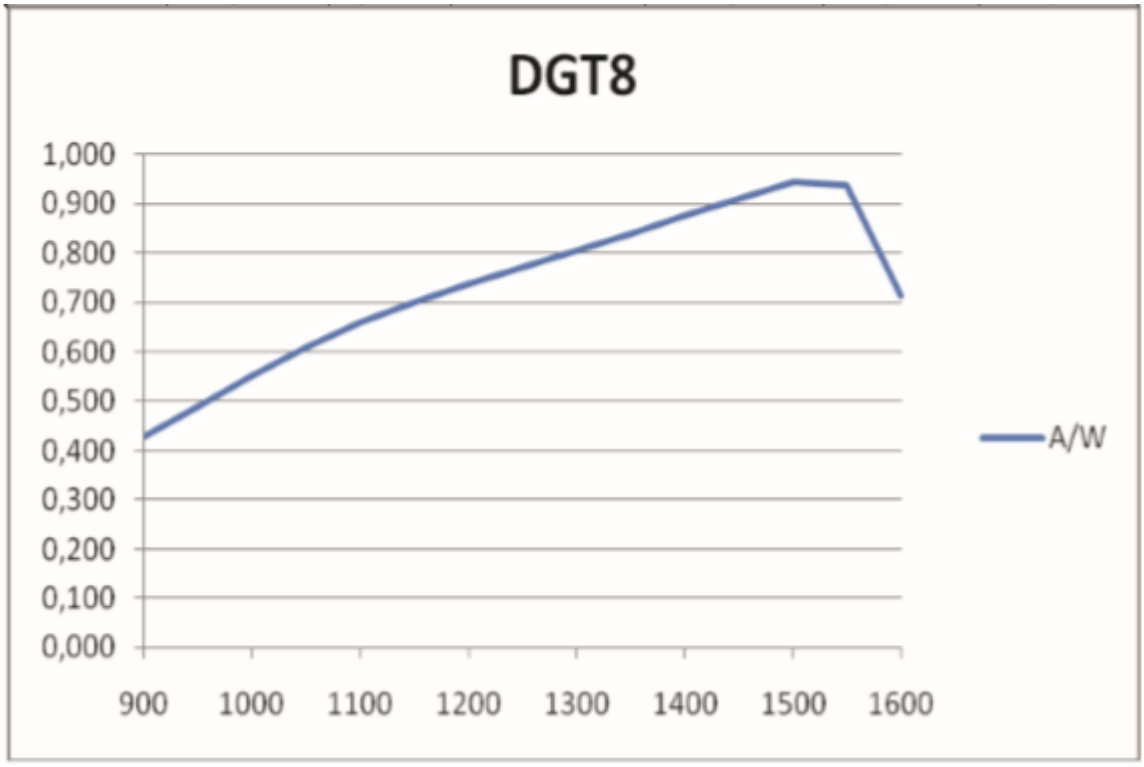

A.6 UME (Turkey)

1. Description of the measurement facility

The measurement system as shown in Figure 1 is consisting of a 400 Watt QTH lamp, a monochromator, output optics and detection system. The QTH lamp was operated at 395 Watt and used for the spectral range from 900 nm to 1600 nm. The monochromator (Type: DTM 300V Bentham Instruments Ltd, f = 300mm) is grating type with three diffraction gratings. The grating with 600 G/mm was used for these measurements. The band passes of monochromator were adjusted to about 8 nm. The off axis mirror was used to collimate the light beam, and variable apertures were used to adjust the beam diameter, minimize the background and stray light. The beam diameter for the measurements was adjusted to approximately 4 mm. The detectors were placed to the holders placed on translational stage and where they are separately connected to a transamplifier and a multimeter.

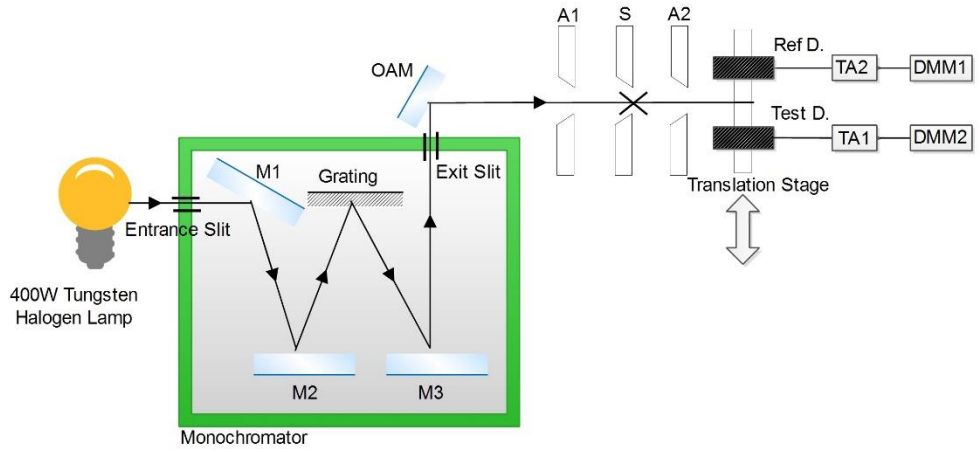

Figure1. The experimental setup for the spectral responsivity measurements. A1 and A2 are apertures; M1,M2 and M3 are mirrors; OAM: Off axis mirror; RefD, and Test D are reference and test detectors; TA: transimpedance amplifier; DMM: digital multimeter.

2. Description of the measuring technique

For the measurements, each time a reference detector and a test detector were put on the translational stage as shown in Figure1, where their optical alignments were done and sufficient time was allowed to let the detectors reach thermal equilibrium.

The reference and test detectors, via translation stage were moved against monochromatic beam at each wavelength from 900 nm to 1600 nm with 50 nm intervals and their current responses were recorded. By this way a set of six measurements were taken for each detector at different times. That is, the detectors were removed and realigned between each measurements. Moreover, for each measurement the internal PT-100 resistance of the

detectors was also measured. Responsivity values for the DUT were evaluated by multiplying the ratio of current response of DUT and reference with the reference detector responsivty.

3. Description of reference standard

Reference standard used in this comparison is GM10HS model germanium photodiode based detector. This detector is traceable to transfer standard named as Electrically Calibrated Pyroelectric Radiometer which is traceable to Electrical Substitution Cryogenic Radiometer.

4. Description of calibration laboratory conditions

The temperature and relative humidity of laboratory has been set to 23.0±0.5 °C and 45.0±5.0 %, respectively. During the whole measurement period average of recorded values of these two parameters were about 22.5 °C and 52.0 %.

5. Comments on detectors

Totally three detectors named as DGT09, DGT10 and DGT11 were measured. Before the measurements all the detectors were inspected for any damage and contamination. On all detectors no any fingerprints and dust particles were observed. No special cleaning process was applied especially during the measurements, apart from removing the dust particles from the surface of detectors with dry air.

6. Measurement results

The measurement results for the responsivity values of detectors are given in Table1, Table2 and Table3. Uncertainty components for spectral sesponsivity values of detectors are given in Table4, Table5 and Table6

Table1. Spectral Responsivity of DGT09 detector

Wavelength / nm	Spectral Responsivity A/W	STD A/W	Num of measurements /n	Temperature /Ohm	Combined relative standard uncertainty (k=1) /%
900	0,4358	4,7E-04	6	109,668	0,92
950	0,4940	2,7E-04	6	109,669	0,91
1000	0,5496	3,3E-04	6	109,670	0,92
1050	0,5933	3,0E-04	6	109,669	0,91
1100	0,6329	3,2E-04	6	109,671	0,91
1150	0,6756	2,6E-04	6	109,674	0,91
1200	0,7168	2,6E-04	6	109,676	0,91
1250	0,7554	2,5E-04	6	109,677	0,91
1300	0,7924	2,9E-04	6	109,679	0,91
1350	0,8276	3,2E-04	6	109,680	0,91
1400	0,8530	3,7E-04	6	109,491	0,91
1450	0,8860	3,2E-04	6	109,684	0,91
1500	0,9066	3,5E-04	6	109,687	0,91
1550	0,9103	4,0E-04	6	109,689	0,95
1600	0,6688	3,9E-04	6	109,690	0,96

Table2. Spectral Responsivity of DGT10 detector

Wavelength / nm	Spectral Responsivity A/W	STD A/W	Num of measurements /n	Temperature /Ohm	Combined relative standard uncertainty (k=1) /%
900	0,3956	3,1E-04	6	109,655	0,92
950	0,4580	2,8E-04	6	109,653	0,92
1000	0,5186	3,2E-04	6	109,649	0,92
1050	0,5691	1,5E-04	6	109,648	0,91
1100	0,6153	1,4E-04	6	109,645	0,91
1150	0,6648	1,3E-04	6	109,643	0,91
1200	0,7121	1,3E-04	6	109,642	0,91
1250	0,7553	1,4E-04	6	109,640	0,91
1300	0,7961	1,7E-04	6	109,639	0,91
1350	0,8346	3,8E-04	6	109,638	0,91
1400	0,8634	5,2E-04	6	109,637	0,92
1450	0,9000	6,3E-04	6	109,636	0,92
1500	0,9239	9,7E-04	6	109,636	0,92
1550	0,9274	1,3E-03	6	109,636	1,04
1600	0,6771	1,1E-03	6	109,637	1,07

Table3. Spectral Responsivity of DGT11 detector

Wavelength / nm	Spectral Responsivity A/W	STD A/W	Num of measurements /n	Temperature /Ohm	Combined relative standard uncertainty (k=1) /%
900	0,3979	8,4E-04	6	109,767	0,96
950	0,4549	8,3E-04	6	109,768	0,95
1000	0,5099	5,1E-04	6	109,773	0,92
1050	0,5550	5,0E-04	6	109,773	0,92
1100	0,5957	5,6E-04	6	109,778	0,92
1150	0,6405	5,5E-04	6	109,779	0,92
1200	0,6829	5,7E-04	6	109,784	0,92
1250	0,7221	6,2E-04	6	109,784	0,92
1300	0,7608	6,4E-04	6	109,786	0,92
1350	0,7997	8,3E-04	6	109,789	0,92
1400	0,8327	8,8E-04	6	109,795	0,92
1450	0,8714	6,3E-04	6	109,795	0,92
1500	0,9001	1,1E-03	6	109,800	0,93
1550	0,9123	8,8E-04	6	109,801	0,99
1600	0,6751	1,1E-03	6	109,804	1,08

7. Uncertainty of Measurements

Combined standard uncertainties given in the Table 3 - Table 5 were obtained by using standard deviations given in these tables and the uncertainty components given in the Table 4. Each uncertainty components in Table 4 were multiplied by the responsivity values in the Table 3 - Table 5 to get the effect of these uncertainty components on responsivity. Then after evaluating the combine uncertainty the relative combined uncertainty values were obtained by dividing it to the responsivity values.

7.1 Uncertainty Components for Spectral Responsivity Measurements

Uncertainty due to Reference Detector: Reference detector is Ge detector which was calibrated against Electrically Calibrated Pyroelectric Radiometer (ECPR). The ECPR was calibrated against silicon photodiode based trap detector which is traceable to cryogenic radiometer.

Uncertainty due to Interpolation and Extrapolation: Silicon photodiode based trap detector was calibrated at 488 nm, 515 nm and 633 nm laser wavelengths. Then between these wavelengths scale was obtained by interpolation. The ECPR was calibrated against trap detector at 1064 nm laser wavelength and the scale was extrapolated using the reflectance values of ECPR sensor.

Uncertainty due to Uniformity: Uniformity of reference detector was obtained by scanning the detector active area with a 1 mm laser beam diameter.

Uncertainty due to Linearity: Reference detector optical response was measured at various power levels at single laser wavelengths and its linearity was evaluated.

Uncertainty due to Amplifier: The uncertainty used in the for the amplifier was taken from the calibration certificate

Uncertainty due to Multimeter: The uncertainty used in the for the multimeter was taken from the calibration certificate

Uncertainty due to Bandwidth: The reference detector response was measured at different bandwidths and related uncertainty was evaluated.

Uncertainty due to Wavelength: The reference detector response was measured at a specific wavelength interval using monochromator. Then monochromater was scanned by changing initial wavelengths by amount of monochromator wavelength uncertainty. Using these values uncertainty due to wavelengths was evaluated.

Uncertainty due to Stray Light: Using some filters effect of stray light of monochromator was evaluated.

Uncertainty due to Temperature: Reference detector response to incident light was recorded at different room temperature levels and the effect on the results was evaluated.

Table 4. Uncertainty Budget for the Spectral Responsivity of DGT09 detector

Source Of Uncertainty	Unit	Wavelength nm														
		900	950	1000	1050	1100	1150	1200	1250	1300	1350	1400	1450	1500	1550	1600
Standard Deviation	**A/W**	4,7E-04	2,7E-04	3,3E-04	3,0E-04	3,2E-04	2,6E-04	2,6E-04	2,5E-04	2,9E-04	3,2E-04	3,7E-04	3,2E-04	3,5E-04	4,0E-04	3,9E-04
Primary Reference	**A/W**	2,4E-03	2,7E-03	3,0E-03	3,3E-03	3,5E-03	3,7E-03	4,0E-03	4,2E-03	4,4E-03	4,6E-03	4,7E-03	4,9E-03	5,0E-03	5,0E-03	3,7E-03
Interpolation/ Extrapolation	**A/W**	6,9E-04	7,8E-04	8,7E-04	9,4E-04	1,0E-03	1,1E-03	1,1E-03	1,2E-03	1,3E-03	1,3E-03	1,4E-03	1,4E-03	1,4E-03	1,4E-03	1,1E-03
Uniformity	**A/W**	3,5E-04	3,9E-04	4,4E-04	4,7E-04	5,0E-04	5,4E-04	5,7E-04	6,0E-04	6,3E-04	6,6E-04	6,8E-04	7,0E-04	7,2E-04	7,2E-04	5,3E-04
Linearity	**A/W**	6,9E-05	7,8E-05	8,7E-05	9,4E-05	1,0E-04	1,1E-04	1,1E-04	1,2E-04	1,3E-04	1,3E-04	1,4E-04	1,4E-04	1,4E-04	1,4E-04	1,1E-04
Polarization	**A/W**	1,4E-04	1,6E-04	1,7E-04	1,9E-04	2,0E-04	2,1E-04	2,3E-04	2,4E-04	2,5E-04	2,6E-04	2,7E-04	2,8E-04	2,9E-04	2,9E-04	2,1E-04
Repeatability	**A/W**	5,8E-04	4,7E-04	5,5E-04	5,6E-04	6,0E-04	5,9E-04	6,3E-04	6,5E-04	6,9E-04	7,3E-04	7,7E-04	7,7E-04	8,0E-04	2,5E-03	2,0E-03
Amplifier	**A/W**	2,6E-04	2,9E-04	3,3E-04	3,5E-04	3,8E-04	4,0E-04	4,3E-04	4,5E-04	4,7E-04	4,9E-04	5,1E-04	5,3E-04	5,4E-04	5,4E-04	4,0E-04
Voltmeter	**A/W**	8,6E-05	9,8E-05	1,1E-04	1,2E-04	1,3E-04	1,3E-04	1,4E-04	1,5E-04	1,6E-04	1,6E-04	1,7E-04	1,8E-04	1,8E-04	1,8E-04	1,3E-04
Bandwidth	**A/W**	6,9E-04	7,8E-04	8,7E-04	9,4E-04	1,0E-03	1,1E-03	1,1E-03	1,2E-03	1,3E-03	1,3E-03	1,4E-03	1,4E-03	1,4E-03	1,4E-03	1,1E-03
Wavelength	**A/W**	1,2E-04	1,3E-04	1,5E-04	1,6E-04	1,7E-04	1,8E-04	1,9E-04	2,0E-04	2,1E-04	2,2E-04	2,3E-04	2,4E-04	2,4E-04	2,5E-04	1,8E-04
Stray Light	**A/W**	3,5E-05	3,9E-05	4,4E-05	4,7E-05	5,0E-05	5,4E-05	5,7E-05	6,0E-05	6,3E-05	6,6E-05	6,8E-05	7,0E-05	7,2E-05	7,2E-05	5,3E-05
Beam Size	**A/W**	1,7E-03	1,9E-03	2,1E-03	2,3E-03	2,4E-03	2,6E-03	2,8E-03	2,9E-03	3,1E-03	3,2E-03	3,3E-03	3,4E-03	3,5E-03	3,5E-03	2,6E-03
Temperature	**A/W**	2,4E-03	2,7E-03	3,1E-03	3,3E-03	3,5E-03	3,8E-03	4,0E-03	4,2E-03	4,4E-03	4,6E-03	4,7E-03	4,9E-03	5,0E-03	5,1E-03	3,7E-03
Combined Uncertainty (k=1)	**A/W**	4,0E-03	4,5E-03	5,0E-03	5,4E-03	5,8E-03	6,2E-03	6,5E-03	6,9E-03	7,2E-03	7,6E-03	7,8E-03	8,1E-03	8,3E-03	8,6E-03	6,4E-03
Expanded Uncertainty (k=2)	**A/W**	8,1E-03	9,0E-03	1,0E-02	1,1E-02	1,2E-02	1,2E-02	1,3E-02	1,4E-02	1,4E-02	1,5E-02	1,6E-02	1,6E-02	1,7E-02	1,7E-02	1,3E-02
Relative Combined Uncertainty (k=1)	**%**	0,92	0,91	0,92	0,91	0,91	0,91	0,91	0,91	0,91	0,91	0,91	0,91	0,91	0,95	0,96
Relative Expanded Uncertainty (k=2)	**%**	1,85	1,83	1,83	1,83	1,83	1,83	1,82	1,82	1,83	1,83	1,83	1,82	1,83	1,90	1,91

Table 5. Uncertainty Budget for the Spectral Responsivity of DGT10 detector

Source Of Uncertainty	Unit	Wavelength (nm)														
		900	950	1000	1050	1100	1150	1200	1250	1300	1350	1400	1450	1500	1550	1600
Standard Deviation	**A/W**	3,1E-04	2,8E-04	3,2E-04	1,5E-04	1,4E-04	1,3E-04	1,3E-04	1,4E-04	1,7E-04	3,8E-04	5,2E-04	6,3E-04	9,7E-04	1,3E-03	1,1E-03
Primary Reference	**A/W**	2,2E-03	2,5E-03	2,9E-03	3,1E-03	3,4E-03	3,7E-03	3,9E-03	4,2E-03	4,4E-03	4,6E-03	4,8E-03	5,0E-03	5,1E-03	5,1E-03	3,7E-03
Interpolation/ Extrapolation	**A/W**	6,3E-04	7,3E-04	8,2E-04	9,0E-04	9,8E-04	1,1E-03	1,1E-03	1,2E-03	1,3E-03	1,3E-03	1,4E-03	1,4E-03	1,5E-03	1,5E-03	1,1E-03
Uniformity	**A/W**	3,1E-04	3,6E-04	4,1E-04	4,5E-04	4,9E-04	5,3E-04	5,7E-04	6,0E-04	6,3E-04	6,6E-04	6,9E-04	7,1E-04	7,3E-04	7,4E-04	5,4E-04
Linearity	**A/W**	6,3E-05	7,3E-05	8,2E-05	9,0E-05	9,8E-05	1,1E-04	1,1E-04	1,2E-04	1,3E-04	1,3E-04	1,4E-04	1,4E-04	1,5E-04	1,5E-04	1,1E-04
Polarization	**A/W**	1,3E-04	1,5E-04	1,6E-04	1,8E-04	2,0E-04	2,1E-04	2,3E-04	2,4E-04	2,5E-04	2,6E-04	2,7E-04	2,9E-04	2,9E-04	2,9E-04	2,1E-04
Repeatability	**A/W**	4,4E-04	4,6E-04	5,2E-04	4,7E-04	5,1E-04	5,4E-04	5,8E-04	6,2E-04	6,5E-04	7,6E-04	8,6E-04	9,5E-04	1,2E-03	4,5E-03	3,7E-03
Amplifier	**A/W**	2,4E-04	2,7E-04	3,1E-04	3,4E-04	3,7E-04	4,0E-04	4,2E-04	4,5E-04	4,7E-04	5,0E-04	5,1E-04	5,4E-04	5,5E-04	5,5E-04	4,0E-04
Voltmeter	**A/W**	7,8E-05	9,1E-05	1,0E-04	1,1E-04	1,2E-04	1,3E-04	1,4E-04	1,5E-04	1,6E-04	1,7E-04	1,7E-04	1,8E-04	1,8E-04	1,8E-04	1,3E-04
Bandwidth	**A/W**	6,3E-04	7,3E-04	8,2E-04	9,0E-04	9,8E-04	1,1E-03	1,1E-03	1,2E-03	1,3E-03	1,3E-03	1,4E-03	1,4E-03	1,5E-03	1,5E-03	1,1E-03
Wavelength Dependency	**A/W**	1,1E-04	1,2E-04	1,4E-04	1,5E-04	1,7E-04	1,8E-04	1,9E-04	2,0E-04	2,1E-04	2,3E-04	2,3E-04	2,4E-04	2,5E-04	2,5E-04	1,8E-04
Stray Light	**A/W**	3,1E-05	3,6E-05	4,1E-05	4,5E-05	4,9E-05	5,3E-05	5,7E-05	6,0E-05	6,3E-05	6,6E-05	6,9E-05	7,1E-05	7,3E-05	7,4E-05	5,4E-05
Beam Size	**A/W**	1,5E-03	1,8E-03	2,0E-03	2,2E-03	2,4E-03	2,6E-03	2,7E-03	2,9E-03	3,1E-03	3,2E-03	3,3E-03	3,5E-03	3,6E-03	3,6E-03	2,6E-03
Temperature	**A/W**	2,2E-03	2,5E-03	2,9E-03	3,2E-03	3,4E-03	3,7E-03	4,0E-03	4,2E-03	4,4E-03	4,6E-03	4,8E-03	5,0E-03	5,1E-03	5,2E-03	3,8E-03
Combined Uncertainty (k=1)	**A/W**	3,6E-03	4,2E-03	4,7E-03	5,2E-03	5,6E-03	6,1E-03	6,5E-03	6,9E-03	7,3E-03	7,6E-03	7,9E-03	8,2E-03	8,5E-03	9,6E-03	7,2E-03
Expanded Uncertainty (k=2)	**A/W**	7,3E-03	8,4E-03	9,5E-03	1,0E-02	1,1E-02	1,2E-02	1,3E-02	1,4E-02	1,5E-02	1,5E-02	1,6E-02	1,6E-02	1,7E-02	1,9E-02	1,4E-02
Relative Combined Uncertainty (k=1)	**%**	0,92	0,92	0,92	0,91	0,91	0,91	0,91	0,91	0,91	0,91	0,92	0,92	0,92	1,04	1,07
Relative Expanded Uncertainty (k=2)	**%**	1,84	1,83	1,83	1,82	1,82	1,82	1,82	1,82	1,82	1,83	1,83	1,83	1,85	2,08	2,14

Table 6. Uncertainty Budget for the Spectral Responsivity of DGT11 detector

Source Of Uncertainty	Unit	Wavelength nm														
		900	950	1000	1050	1100	1150	1200	1250	1300	1350	1400	1450	1500	1550	1600
Standard Deviation	**A/W**	8,4E-04	8,3E-04	5,1E-04	5,0E-04	5,6E-04	5,5E-04	5,7E-04	6,2E-04	6,4E-04	8,3E-04	8,8E-04	6,3E-04	1,1E-03	8,8E-04	1,1E-03
Primary Reference	**A/W**	2,2E-03	2,5E-03	2,8E-03	3,1E-03	3,3E-03	3,5E-03	3,8E-03	4,0E-03	4,2E-03	4,4E-03	4,6E-03	4,8E-03	5,0E-03	5,0E-03	3,7E-03
Interpolation/ Extrapolation	**A/W**	6,3E-04	7,2E-04	8,1E-04	8,8E-04	9,5E-04	1,0E-03	1,1E-03	1,1E-03	1,2E-03	1,3E-03	1,3E-03	1,4E-03	1,4E-03	1,4E-03	1,1E-03
Uniformity	**A/W**	3,2E-04	3,6E-04	4,0E-04	4,4E-04	4,7E-04	5,1E-04	5,4E-04	5,7E-04	6,0E-04	6,3E-04	6,6E-04	6,9E-04	7,1E-04	7,2E-04	5,4E-04
Linearity	**A/W**	6,3E-05	7,2E-05	8,1E-05	8,8E-05	9,5E-05	1,0E-04	1,1E-04	1,1E-04	1,2E-04	1,3E-04	1,3E-04	1,4E-04	1,4E-04	1,4E-04	1,1E-04
Polarization	**A/W**	1,3E-04	1,4E-04	1,6E-04	1,8E-04	1,9E-04	2,0E-04	2,2E-04	2,3E-04	2,4E-04	2,5E-04	2,6E-04	2,8E-04	2,9E-04	2,9E-04	2,1E-04
Repeatability	**A/W**	9,0E-04	9,1E-04	6,5E-04	6,6E-04	7,3E-04	7,5E-04	7,9E-04	8,4E-04	8,8E-04	1,0E-03	1,1E-03	9,3E-04	1,3E-03	3,4E-03	3,8E-03
Amplifier	**A/W**	2,4E-04	2,7E-04	3,0E-04	3,3E-04	3,5E-04	3,8E-04	4,1E-04	4,3E-04	4,5E-04	4,8E-04	5,0E-04	5,2E-04	5,4E-04	5,4E-04	4,0E-04
Voltmeter	**A/W**	7,9E-05	9,0E-05	1,0E-04	1,1E-04	1,2E-04	1,3E-04	1,4E-04	1,4E-04	1,5E-04	1,6E-04	1,7E-04	1,7E-04	1,8E-04	1,8E-04	1,3E-04
Bandwidth	**A/W**	6,3E-04	7,2E-04	8,1E-04	8,8E-04	9,5E-04	1,0E-03	1,1E-03	1,1E-03	1,2E-03	1,3E-03	1,3E-03	1,4E-03	1,4E-03	1,4E-03	1,1E-03
Wavelength Dependency	**A/W**	1,1E-04	1,2E-04	1,4E-04	1,5E-04	1,6E-04	1,7E-04	1,8E-04	1,9E-04	2,1E-04	2,2E-04	2,2E-04	2,4E-04	2,4E-04	2,5E-04	1,8E-04
Stray Light	**A/W**	3,2E-05	3,6E-05	4,0E-05	4,4E-05	4,7E-05	5,1E-05	5,4E-05	5,7E-05	6,0E-05	6,3E-05	6,6E-05	6,9E-05	7,1E-05	7,2E-05	5,4E-05
Beam Size	**A/W**	1,5E-03	1,8E-03	2,0E-03	2,1E-03	2,3E-03	2,5E-03	2,6E-03	2,8E-03	2,9E-03	3,1E-03	3,2E-03	3,4E-03	3,5E-03	3,5E-03	2,6E-03
Temperature	**A/W**	2,2E-03	2,5E-03	2,8E-03	3,1E-03	3,3E-03	3,6E-03	3,8E-03	4,0E-03	4,2E-03	4,4E-03	4,6E-03	4,8E-03	5,0E-03	5,1E-03	3,8E-03
Combined Uncertainty (k=1)	**A/W**	3,8E-03	4,3E-03	4,7E-03	5,1E-03	5,5E-03	5,9E-03	6,3E-03	6,6E-03	7,0E-03	7,4E-03	7,7E-03	8,0E-03	8,3E-03	9,0E-03	7,3E-03
Expanded Uncertainty (k=2)	**A/W**	7,6E-03	8,6E-03	9,4E-03	1,0E-02	1,1E-02	1,2E-02	1,3E-02	1,3E-02	1,4E-02	1,5E-02	1,5E-02	1,6E-02	1,7E-02	1,8E-02	1,5E-02
Relative Combined Uncertainty (k=1)	**%**	0,96	0,95	0,92	0,92	0,92	0,92	0,92	0,92	0,92	0,92	0,92	0,92	0,93	0,99	1,08
Relative Expanded Uncertainty (k=2)	**%**	1,92	1,89	1,84	1,84	1,84	1,84	1,84	1,84	1,84	1,85	1,85	1,83	1,85	1,97	2,16